UNIVERSITÀ
DEGLI STUDI
DI PADOVA

Sede Amministrativa: Università degli Studi di Padova

Dipartimento di Biologia

SCUOLA DI DOTTORATO DI RICERCA IN BIOSCIENZE E BIOTECNOLOGIE

INDIRIZZO: BIOTECNOLOGIE

CICLO XXVII

SUPEROXIDE RADICAL DISMUTATION AS PROTECTIVE MECHANISM TO HAMPER THE PROGRESSION OF PARKINSON'S DISEASE

Direttore della Scuola : Ch.mo Prof. Giuseppe Zanotti

Coordinatore d'indirizzo: Ch.mo Prof. Fiorella Lo Schiavo

Supervisore: Ch.mo Prof. Mariano Beltramini

Co-Supervisore: Dr. Marco Bisaglia

Dottoranda: Roberta Filograna

Table of contents

Abstract

Parkinson's disease (PD) is a degenerative neurological syndrome characterized by the preferential loss of dopaminergic (DAergic) neurons in the *Substantia Nigra pars compacta*. PD is still incurable and conventional therapies treat only symptoms to improve the quality of life. Therefore, there is a impelling need to find out new therapeutic strategies that not only provide symptomatic relief but also halt or reverse the neuronal damage hampering PD progression. Even though the pathogenesis of this disorder remains poorly understood, oxidative stress has been identified as one of the major contributors for the nigral loss in both sporadic and genetic forms of the disease. In particular, the selective vulnerability of DAergic neurons to oxidative stress might be ascribed to dopamine (DA) metabolism, which occurs in the cytosol and represents in itself a relevant pathway for superoxide radicals production. The main hypothesis of this thesis is that the inhibition of reactive oxygen species (ROS) overproduction might delay, block or prevent the degenerative process that occurs in PD patients. In this scenario, our project was addressed to study *in vitro* and *in vivo* the potential protective role of the superoxide dismutase (SOD) enzymes and SOD mimetic compounds against oxidative injury, related to PD, adopting two experimental paradigms. We focused on SODs because they exert a crucial function in cellular antioxidant defense, promoting the elimination of superoxide anion.

The first experimental paradigm was represented by the herbicide paraquat (PQ) whose mechanism of action relies on the production of oxidative stress and it is epidemiologically linked to sporadic PD. The second one, which has been used to model a familial form of PD, was based on PINK1 deficiency. Indeed, *PINK1* gene mutations have been identified as cause of recessive early-onset parkinsonism. This gene encodes for a serine/threonine kinase that is involved in the mitochondrial quality control and in the regulation of cellular oxidative status.

To evaluate whether SODs might have a protective activity against PQ toxicity or PINK1 deficiency, the cytosolic and mitochondrial SODs, respectively SOD1 and SOD2, were overexpressed in the human neuroblastoma SH-SY5Y cells

and in *Drosophila melanogaster*. In cells and flies, the overexpression of the mitochondrial isoform rescued acute PQ toxicity. The selective effect observed seems to be associated to an intrinsic mechanism of acute treatment, which strongly compromise mitochondria, increasing ROS in these organelles and promoting their fragmentation. On the contrary, in flies the cytosolic isoform ameliorated motor dysfunctions induced by a chronic PQ exposure, even when SOD1 was overexpressed exclusively into the DAergic neurons. These observations indicate that the cytosolic compartment is particularly affected by chronic PQ treatment suggesting that other oxidative processes in the cytosol of DAergic cells, such as DA metabolism, might amplify PQ-induced oxidative stress making them particularly vulnerable. In SH-SY5Y cells, PINK1 deficiency resulted in mitochondrial fragmentation. Even in this case, SODs appeared protective rescuing the phenotype. However, while SOD1 overexpression slightly reduced these mitochondrial alterations, SOD2 seemed to reverse mitochondrial fragmentation allowing the maintenance of a healthy mitochondrial network. In flies, loss of PINK1 induced a severe motor impairment, which was rescued only by the overexpression of the cytosolic isoform suggesting that the protein might be involved in other pathways that are not strictly correlated with mitochondrial functioning.

Once the beneficial activity of SODs has been demonstrated, we then investigated the therapeutic potential use of a SOD-mimetic compound, M40403. We found that the molecule was able to protect cells and flies against the oxidative damage induced by both acute and chronic PQ exposure. In addition, the SOD mimetic was effective also in PINK1 deficient cells and flies reducing, respectively, mitochondrial fragmentation and locomotor defects. Finally, M40403 administration in SOD1 and SOD2 deficient flies partially replaced the loss of both isoforms suggesting that it can act at cytosolic and mitochondrial level.

Overall, these findings demonstrate that specific SOD-mimetic compounds can be efficacious in reducing oxidative stress and should be further explored as therapeutic agents to hamper the progression of PD.

In parallel, we developed a second research line which was aimed to the characterization of two human neuroblastoma cell lines in order to identify, between them, the most reliable cellular model for PD studies.

Cellular models are largely used to study *in vitro* the molecular mechanisms underlying DAergic degeneration in PD. Although their use presents several advantages, cell lines do not always recapitulate morphological and neurochemical properties of DAergic neuronal cells. Considering the relevance of DA metabolism in the pathogenesis of PD, the DAergic phenotype is an important requirement. Human neuroblastoma cell lines are commonly used as models in PD research, although they are undifferentiated, do not exhibit markers of mature neurons and appear able to synthetize different neurotransmitter, in particular the catecholamines DA and noradrenaline (NA). For this reason, we studied the ability of three different agents, phorbol ester 12-O-tetradecanoylphorbol-13-acetate (TPA), retinoic acid (RA) and staurosporine to drive neuronal differentiation toward a DAergic phenotype in SH-SY5Y and BE(2)-M17 cells. The first cell line is largely adopted and studied, even though the phenotype acquired upon differentiation is still a debated issue. In contrast, the second one is poorly characterized and might represent a valid alternative cellular system. In this thesis, we first investigated the acquisition of neuronal-like features in terms of growth inhibition, cell morphology and neuronal markers expression. Our results indicated that staurosporine and RA were the most efficient treatments to inhibit cell growth, respectively in SH-SY5Y and BE(2)-M17. Furthermore, in both cell lines, RA and staurosporine promoted the formation a complex network of neuritic extensions and the expression of mature neuronal markers. To evaluate whether the differentiation promotes a DAergic or NAergic phenotype in these cell lines, we analyzed the expression profile of the major genes involved in DA and NA metabolism and the intracellular content of these neurotransmitters. In SH-SY5Y cells, RA and TPA induced the down-regulation of DA- and NA-related genes as well as a decrease of neurotransmitter amounts compared to undifferentiated cells, indicating the loss of the catecholaminergic phenotype. On the contrary, staurosporine treatment resulted in the up-regulation of all these genes and an increase of NA content, enhancing the NAergic phenotype.

Surprisingly, in BE(2)-M17, DA and NA levels detected in undifferentiated cells were considerably more elevated than in SH-SY5Y which suggests that these cells presents a more pronounced catecholaminergic phenotype. The latter was not affected by TPA and RA treatments, which did not substantially alter gene expression and the amount of neurotransmitters. In contrast, staurosporine promoted the up-regulation of the genes involved in metabolism of DA and NA and an increase of their intracellular amounts, indicating a relevant enhancement of the observed phenotype.

These results indicate that the BE(2)-M17 cell line emerges as a new experimental model with a catecholaminergic phenotype that differs substantially from those of SH-SY5Y cells, suggesting different fields of application for the two cell lines.

Riassunto

La malattia di Parkinson è una sindrome neurologica degenerativa, caratterizzata dalla perdita preferenziale dei neuroni dopaminergici della *Substantia Nigra pars compacta.* Questa patologia è attualmente incurabile e le terapie convenzionali agiscono esclusivamente sui sintomi migliorando la qualità della vita. Pertanto, è necessario identificare nuove strategie terapeutiche che non solo forniscano un efficacie trattamento della sintomatologia ma agiscano anche ritardando i danni neuronali e arrestando la progressione della malattia. Sebbene l'eziologia è tuttora sconosciuta, lo stress ossidativo sembra svolgere un ruolo chiave nella degenerazione dopaminergica sia nella forme sporadiche che familiari della patologia. In particolare, la selettiva vulnerabilità di tali neuroni allo stress ossidativo potrebbe essere associata al metabolismo della dopamina (DA), evento molecolare citosolico responsabile, esso stesso, della sovrapproduzione di specie reattive dell'ossigeno (ROS) L'ipotesi principale alla base di questa tesi è che l'inibizione della produzione di ROS possa ritardare, arrestare o prevenire il processo neurodegenerativo che si verifica nei pazienti affetti dal morbo di Parkinson. In questo scenario, il nostro progetto si propone di studiare *in vitro* e *in vivo* il potenziale ruolo protettivo delle superossido dismutasi (SOD) e di composti che ne mimano l'attività (SOD mimetici) contro i danni ossidativi, correlati a tale patologia, utilizzando due diversi paradigmi sperimentali. La scelta di studiare questi enzimi è legata alla loro funzione cellulare antiossidante, cruciale nel promuovere l'eliminazione dell'anione superossido, radicale capostipite nella produzione a valle di specie molto più tossiche e reattive.

In questo studio, il primo paradigma utilizzato è l'erbicida paraquat (PQ), il cui meccanismo di tossicità si basa sulla produzione di stress ossidativo. L'esposizione cronica a tale molecola è stata correlata epidemiologicamente all'insorgenza delle forme sporadiche di Parkinson. Il secondo modello adottato si basa sulla deficienza della chinasi PINK1, responsabile di una forma familiare della malattia. Infatti, mutazioni a carico del gene *PINK1* sono state identificate come causa di parkinsonismo giovanile precoce. Questa proteina sembra svolgere un ruolo chiave nel *mitochondrial quality control* e nella regolazione dello stress ossidativo.

Al fine di studiare la potenziale azione protettiva delle SOD contro la tossicità esercitata dal PQ o indotta dall'assenza di PINK1, l'isoforma citosolica e quella mitocondriale, rispettivamente SOD1 e SOD2, sono state sovraespresse nelle cellule di neuroblastoma umano SH-SY5Y e in *Drosophila melanogaster*. *In vitro* e *in vivo*, esclusivamente la sovraespressione dell'isoforma mitocondriale ha evidenziato un effetto protettivo contro l'esposizione acuta al PQ. La selettività osservata potrebbe essere associata ad un meccanismo di tossicità intrinseco dell'erbicida che, ad elevate dosi, comprometterebbe fortemente i mitocondri, aumentando la produzione di ROS in questi organelli e promuovendone la frammentazione. Al contrario, in *Drososphila*, l'enzima citosolico SOD1 è in grado di migliorare le performance motorie, alterate dall'esposizione cronica al PQ. Tale effetto è stato rilevato anche quando la sovraespressione era indotta esclusivamente a livello dei neuroni dopaminergici. Le nostre osservazioni indicano che in tali condizioni il compartimento citosolico potrebbe essere particolarmente compromesso, suggerendo che nei neuroni dopaminergici il citosol possa essere la sede di altri meccanismi ossidativi, tra i quali il metabolismo della DA, in grado di amplificare o esacerbare lo stress ossidativo indotto dal PQ, rendendo tali cellule particolarmente vulnerabili. In cellule SH-SY5Y, la deficienza di PINK1 ha causato un fenotipo mitocondriale caratterizzato dalla frammentazione del network di questi organelli. Anche in questo caso, le SOD hanno svolto una funzione protettiva contrastando la frammentazione mitocondriale osservata. Tuttavia, mentre la sovraespressione della SOD1 ha ridotto solo parzialmente il danno, la SOD2 è apparsa in grado di garantire il mantenimento di un corretto network mitocondriale. In *Drosophila*, la perdita di PINK1 promuove una severa disabilità motoria, la quale può essere migliorata dall' attività dell'isoforma citosolica SOD1, suggerendo che PINK1 possa essere coinvolta in altri processi molecolari non strettamente correlati col mantenimento del funzionamento mitocondriale.

Dimostrata l'azione protettiva delle SOD, abbiamo deciso di studiare il potenziale utilizzo terapeutico del SOD mimetico M40403. I risultati delle nostre analisi hanno evidenziato che tale molecola svolga un'attività antiossidante, *in vitro* e *in vivo*, proteggendo dal danno ossidativo indotto dal trattamento acuto e cronico con

l'erbicida PQ. Inoltre, il composto M40403 è stato testato in modelli cellullari e animali privi di PINKI1 nei quali ha migliorato, rispettivamente, il fenotipo mitocondriale e i difetti nell'apparato locomotore. Infine la somministrazione di questo SOD mimetico in linee di *Drosophila* deficienti per SOD1 o SOD2, ha rivelato che la molecola possa sopperire parzialmente all'assenza di ciascun enzima, supportando l'ipotesi che possa agire sia a livello citosolico che mitocondriale.

Complessivamente, i dati ottenuti finora hanno dimostrato che l'utilizzo di specifici composti SOD mimetici, in particolare M40403, possa essere efficacie nel contrastare danni ossidativi. Questi composti dovrebbero essere ulteriormente studiati al fine di identificare un possibile agente terapeutico per la malattia di Parkinson.

Parallelamente al progetto appena descritto, ci siamo focalizzati su un seconda linea di ricerca volta alla caratterizzazione dei due linee di neuroblastoma umano al fine di definire quali, tra queste, rappresenti il modello cellulare più attendibile per lo studio della malattia di Parkinson.

I modelli cellulari sono largamente utilizzati nello studio *in vitro* dei meccanismi molecolari alla base della degenerazione dei neuroni dopaminergici. Nonostante il loro utilizzo presenti grandi vantaggi, queste linee cellulari non sempre ricapitolano le proprietà morfologiche e neurochimiche dei suddetti neuroni. Pertanto, considerando il ruolo del metabolismo della DA nell'eziologia del morbo di Parkinson, l'acquisizione del fenotipo dopaminergico risulta essere un requisito importante. In particolare, le linee cellulari di neuroblastoma sono spesso usate come modello, nonostante siano proliferanti, non esprimano *markers* caratteristici dei neuroni maturi e siano in grado di sintetizzare diversi neurotrasmettitori, in particolare le catecolamine DA e noradrenalina (NA). Per queste ragioni, abbiamo studiato l'abilità di tre differenti agenti, il 12-O-tetradecanoilforbolo-13-acetato (TPA), l'acido retinoico (RA) e la staurosporina, nel guidare il differenziamento delle cellule SH-SY5Y e BE(2)-M17 verso un fenotipo dopaminergico. La prima di queste linee cellulari è ampiamente utilizzata e studiata, nonostante il fenotipo acuisito dopo il differenziamento sia ancora un argomento dibattuto. Al contrario, la

seconda è stata finora poco caratterizzata e potrebbe rappresentare un valido sistema cellulare alternativo.

In questa tesi, al fine di valutare l'acquisizione delle caratteristiche neuronali, abbiamo inizialmente analizzato l'effetto indotto dai tre agenti sull' inibizione della crescita, morfologia cellulare e espressione di *markers* neuronali. I nostri risultati hanno dimostrato che il trattamento con staurosporina e RA siano i più efficienti nell'arrestare la proliferazione cellulare rispettivamente nelle cellule SH-SY5Y e BE(2)-M17. Inoltre, in entrambe le linee, RA e staurosporina promuovono la formazione di un compresso network di ramificazioni neuritiche e l'espressione di specifici *markers* neuronali citoscheletrici. Per studiare l'effetto del differenziamento nell'acquisizione di un fenotipo dopaminergico o noradrenergico nei due modelli cellulari, abbiamo valutato il profilo di espressione dei geni principalmente coinvolti nella sintesi di entrambi i neurotrasmettitori e i loro contenuto intracellulare. In cellule SH-SY5Y, il trattamento con RA e TPA è risultato in grado di promuovere non solo la *down-regolazione* dei geni analizzati ma anche una consistente riduzione del contenuto di DA e NA, suggerendo la perdita del fenotipo catecolaminergico. Al contrario, la staurosporina ha evidenziato la capacità di *up-regolare* l'espressione genica degli enzimi coinvolti nella sintesi dei due neurotrasmettitori e di incrementare il contenuto di NA, amplificando il fenotipo noradrenergico di questo modello. Nella linea cellulare BE(2)-M17, i livelli di DA and NA rilevati prima del differenziamento risultano essere considerevolmente elevati rispetto a quelli misurati nelle SH-SY5Y, evidenziando che la prima abbia un fenotipo catecolaminergico molto più pronunciato della seconda. Quest'ultimo non viene sostanzialmente alterato dai trattamenti con TPA e RA, mentre il differenziamento con staurosporina è nuovamente in grado di *up-regolare* il profilo di espressione analizzato e di promuovere un'ulteriore sintesi di DA e NA, determinando l'acquisizione di un fenotipo ulteriormente marcato.

Concludendo, i risultati di questo studio indicano che la linea BE(2)-M17 possa essere un modello sperimentale alternativo con proprietà neurochimiche differenti dalle SH-SY5Y, suggerendo l'applicazione delle due line cellulari in differenti campi di ricerca.

Chapter 1

Introduction

1.1 Parkinson's disease

Parkinson's disease (PD) is a degenerative neurological syndrome characterized by the selective death of dopaminergic (DAergic) neurons in the midbrain area known as *Substantia Nigra pars compacta* (*SNpc*). These neuronal cells project their axons at striatal level controlling, ultimately, voluntary movements. The neuronal degeneration results in a dopamine (DA) depletion and in the loss of DAergic transmission which manifests with motor symptoms including resting tremor, rigidity, bradykinesia (slowness of movement) and postural instability. However, the neurodegenerative event also affects cholinergic, serotoninergic and noradrenergic pathways explaining other non-motor clinical manifestations present in most patients, such as cognitive impairment, olfactory deficits, sleep disturbance, depression and constipation (Poewe, 2008). The second pathological hallmark of PD is the presence of intracytoplasmic proteinaceous inclusions observed in neuronal cell body and processes, known respectively as Lewy bodies (LBs) and Lewy neurites (LNs). The major component of LBs and LNs is α-synuclein (α-syn), a small pre-synaptic nerve terminal protein mainly expressed in the neocortex, hippocampus, substantia nigra (SN), thalamus and cerebellum (George, 2002).

Currently, the etiopathogenesis of PD is still not clearly understood. In most cases, patients present a sporadic or idiopathic form, which is considered a multifactorial disease with variable contributions of genetic susceptibility and environmental factors (Pilsl & Winklhofer, 2012). About 5-10% of cases can be classified as familial forms, caused by genetic inheritance. As sporadic and genetic forms share often most of the clinical, pathological and biochemical features, the understanding of the molecular mechanisms underlying the familial forms could allow to identify the principal pathways involved also in sporadic PD (Lesage & Brice, 2012). Actually, studies on families with Mendelian inheritance evidenced protein aggregation, ubiquitin-proteasome system (UPS) impairment, mitochondrial dysfunction as crucial players in the onset or progression of the motor disorder. Each of these molecular pathways, through different mechanisms, might be responsible for reactive oxygen species (ROS) overproduction and the consequent oxidative stress

has been identified as one of the major contributors for the nigral loss or dysfunction (Kumar et al, 2012).

PD is also defined as an age-related (dependent) disorder; in fact the prevalence of PD escalates steeply with age (de Rijk et al, 1997)and because of higher life expectancy, the incidence of PD is expected to increase dramatically worldwide (Dorsey et al, 2007). Aging could be considered the main risk factor for the etiology of this syndrome. The progressive decline of normal cellular processes that occurs with aging could be responsible for a vulnerable state able to exacerbate the cellular demise which characterizes PD (Collier et al, 2011). In the 1950s, "the free radical theory of aging" postulated a deep and strong correlation between ROS overproduction and aging. According to this theory, in aerobic organism the most relevant determinant of life span was associated to cellular damage to biological macromolecules via free radicals production (Harman, 1956). Two decades later, mitochondria were recognized as the main source and target of these reactive molecules (Harman, 1972). Actually, ROS are by-product of aerobic respiration and in particular of oxidative phosphorylation (OXPHOS) that occurs at mitochondrial level. Even though this theory was considered valid for several decades, many alternative theories have been proposed since the discovery that free radicals can not only cause molecular damage to cells, but also serve as signals acting as modulators of physiological processes (Jin, 2010). Particularly relevant is the modern or modified free radical theory based on the concept that ROS signaling and homeostasis is probably the most important enzyme/gene pathway responsible for the development of cell senescence. Therefore, aging might be caused by a disruption of the whole signaling network involving ROS (Afanas'ev, 2010; Vina et al, 2013). In this scenario, neuronal cells are also considered hypersensitive to ROS-induced damage because of: a) their massive oxygen consumption associated with an high energy demand (Wang & Michaelis, 2010), b) their low regenerative capacity due to their post mitotic nature and c) their high level of unsaturated fatty acids which are hot spot for oxidative processes (Uttara et al, 2009). These facts might explain the vulnerability of neuronal tissues to chronic and degenerative disease, including PD.

1.2 Oxidative stress

Oxidative stress is a condition associated with an excessive bioavailability of ROS as a consequence of a redox imbalance between their production and detoxification through antioxidant systems (Kregel & Zhang, 2007). ROS include both free radicals, such as superoxide anion ($O_2^{\bullet -}$), hydroxyl radical ($OH^{\bullet -}$), and other non radical molecules, like hydrogen peroxide (H_2O_2) (Andersen, 2004). These species can either be generated exogenously or produced intracellularly from several different sources. Cytosolic enzyme systems contributing to oxidative stress include the family of NADPH oxidases, a superoxide-generating system, which was first identified in the neutrophil. However, several evidence suggest that the majority of intracellular ROS production is derived from the mitochondria. The production of mitochondrial superoxide radicals occurs primarily at two discrete points in the ETC, at level of complex I and complex III . Once the $O_2^{\bullet -}$ is generated, it could lead to the formation of other ROS, such as H_2O_2 and $OH^{\bullet -}$. The latter can be the result of the reduction of H_2O_2 in the presence of endogenous iron by means of the Fenton reaction. In addition, it could arise from electron exchange between $O_2^{\bullet -}$ and H_2O_2 via the Harber-Weiss reaction. Furthermore, when both $O_2^{\bullet -}$ with NO are synthesized within cell, they will combine spontaneously to form peroxynitrite ($ONOO^{\bullet -}$), which is highly reactive nitrogen species (RNS) (Finkel & Holbrook, 2000). In physiological condition, ROS homeostasis is guaranteed by a complex antioxidant system (see Paragraph 1.4.1). However, if this scavenging system is overwhelmed, ROS biovailability increases. ROS and the derived RNS can interact with many cellular components including nucleic acids, proteins and lipids causing cell injury leading to a pathological state (Valko et al, 2007).

1.2.1 Evidence of oxidative stress in PD patients

The link between oxidative stress and degeneration of DAergic neurons has been highlighted through *post-mortem* examinations of PD brains. In the analyzed tissues, a strong evidence of oxidative damage was found in lipids, proteins and nucleic acids. Unsaturated lipids are susceptible to oxidative modifications at the level of their carbon-carbon double bonds. As consequence, ROS can induce lipid peroxidation in cell membranes through the generation of a radical chain reaction which leads to the production of 4- hydroxyl 2,3-nonenal and malondialdehyde. Both these markers have been observed in DAergic cells of PD brains (Dexter et al, 1989; Yoritaka et al, 1996). Additionally, the same kind of analyses revealed that patients presented an increase of the common product of nucleic acids oxidation, 8-hydroxyguanosine, at level of nigral neurons (Zhang et al, 1999). Different investigations also identified the presence of an high content of tyrosine nitration (Good et al, 1998) and protein carbonylation (Alam et al, 1997; Floor & Wetzel, 1998) in PD brains. These modifications are hallmarks of oxidative protein damage induced respectively by nitric peroxide and other reactive species.

Alterations of the antioxidant defense can also be considered as an indirect evidence of ROS accumulation. Actually, the earliest biochemical indicator of an impairment of the antioxidant system and a consequent nigral degeneration is a depletion of glutathione (GSH) depletion observed in SN and corpus striatum of PD patients (Sofic et al, 1992). The role of GSH is fundamental for cell physiology , indeed, this molecule is the most abundant non protein thiol in mammalian cells, which acts as reducing agent, antioxidant, and free-radical scavenger (Mardones et al, 2012).

In conclusion, the overall reported data support the concept that oxidative stress contributes to neurodegeneration of DAergic cells. As previously mentioned, oxidative stress is intimately interconnected to several key pathways correlated to neurodegeneration (Jenner, 2003). Most of them are directly involved in genetic forms of the disease; while, others might be responsible for the vulnerability of DAergic neurons. Each molecular mechanism will be discuss in details in the next sections.

1.2.2 Mitochondrial dysfunction

Mitochondrial dysfunction includes the impairment of a wide spectrum of normal functions which affects the activity of respiratory chain complexes, ROS and ATP production, calcium regulation, mitochondrial membrane potential maintenance and mitochondrial dynamics and clearance (Gandhi & Abramov, 2012). Most processes are connected and interdependent; consequently, their impairment might be concomitant.

Several observations support the involvement of mitochondria in the pathogenesis of PD. The first evidence was the discovery that an intravenously injection of 1-methyl-4-phenyl-1,2,3,6-tetrahydropyridine (MPTP) resulted in a severe parkinsonian–like phenotype (Langston et al, 1983). This compound has been demonstrated to be selectively toxic to DAergic neurons. In the brain, MPTP is first converted in its metabolite, MPP^+, by monoamine oxidase B (MAO-B); afterwards, MPP^+ is actively transported by the dopamine transporter (DAT) within DAergic neurons, where it blocks mitochondrial complex I activity (Javitch et al, 1985). Complex I is located in the inner mitochondrial membrane and it is a part of the respiratory electron transport chain (ETC) which catalyzes electron transfer from NADH to ubiquinone. It is considered the main source of radical production, but it is also a preferential target of oxidants and radicals leading to its inhibition or inactivation (Navarro & Boveris, 2009). Further investigations confirmed the pathological role of this complex, whose defects have been reported in PD patients (Parker et al, 1989). In addition, *post-mortem* examinations revealed an high prevalence of somatic mitochondrial DNA deletions in SN of PD brains (Bender et al, 2006).

Mitochondrial genome encodes for 13 subunits of OXPHOS complexes; therefore, mitochondrial DNA deletions are likely to impact on cellular bioenergetics. The effects associated with a decline of mitochondrial respiration are a deficit of ATP levels, an increase of ROS production and a concomitant opening of the permeability transition pore (PTP), which results in a consequent depolarization of mitochondrial membrane potential. The latter event is followed by the release into

the cytosol of cytotoxic apoptotic proteins, such as cytochrome c, leading to DAergic cell death.

Another line of evidence for mitochondrial dysfunction, related to vulnerability of nigral neurons, came from the identification, in autosomal recessive forms of PD, of mutations in genes encoding for the proteins Parkin, PINK1 and DJ-1 which are all involved in mitochondrial functions. PINK1 and Parkin have a role in the mitochondrial quality control, while DJ-1 seems to be a mitochondrial redox sensor. Their function and role will be analyzed further on.

1.2.3 Neuroinflammation and reactive microgliosis

In recent years, chronic inflammation has been identified as a prominent player in PD where it may contribute to the nigrostriatal pathway degeneration promoting the progression of the disease (Tansey & Goldberg, 2010). *Post-mortem* analyses supported this idea. The first observation came from the identification of a large numbers of reactive microglial cells, hallmark of an ongoing neuroinflammatory process, in PD patients (McGeer et al, 1988).

Microglia are the resident macrophages of central nervous system,considered as the prime component of immunological defense in this organ. Resting microglial cells display a ramified morphology with highly dynamic branching processes which are necessary to extend their surveillance in the surrounding neuronal environment.

Microglial activation is mediated by pattern recognition receptors (PPR) on the cell surface, engaged by pathogen-associated molecular patterns (PAMPs) which are bacterial- or viral-derived molecules, such as lipopolysaccharide (LPS) (Beraud et al, 2013). Once PPRs recognize their specific ligand, a signal transduction cascade leads to morphological changes, cell proliferation, migration to the site of damage and antigen presentation. Thus, these cells assume an *amoeboid* shape and a phagocytic activity. To perform the acquired antimicrobial function, microglial cells induce the production and release of pro-inflammatory cytokines, such as tumor necrosis factor α (TNF-α) and interleukin-1β (IL-1β). In addition, they express enzymes, involved in the inflammatory response mediated by oxidative stress such as

inducible nitric oxide synthase (iNOS), cyclooxygenase 2 (COX2) and NADPH oxidase, which generate RNS and ROS. The latter process, known as respiratory burst, is crucial to induce detrimental damage in pathogens. In PD patients, several markers of activated microglia have been reported. Pro-inflammatory modulators, including TNF-α, IL-1β and interferon-γ (IFN-γ), were constitutively overexpressed in brains, serum and cerebrospinal fluid (CSF) (Blum-Degen et al, 1995; Dobbs et al, 1999; Mogi et al, 1994; Mogi et al, 2007). In addition, other investigations showed an increment of COX2 and iNOS levels in SN (Knott et al, 2000).

While mild microglial activation has a physiological and protective effects, chronic inflammation may damage and kill the surrounding neural cells. Under pathological condition, microglial PPR recognize danger-associated molecular patterns (DAMPs) which originate from multiple sources, including injured and dying neurons. Therefore, in response to neuronal damage microglia become overactivated releasing the same multitude of immunomodulatory molecules, that generally characterized inflammation. In these circumstances, cytokines, RNS and ROS might have a severe cytotoxic effect, inducing more widespread damage to neighbouring neurons, which in turn might release other pathological stimuli and toxins amplifying the degenerative process (Block et al, 2007). Even though the initial insult has ceased, this overactivated state persists because of a positive feedback from damaged DAergic neurons, leading a self propelling vicious cycle, known as reactive microgliosis. Among the different substances released by dying neurons, α-syn, neuromelanin (NM) and matrix metalloproteinase-3 (MMP-3) have been identified as microglial activators (Fig.1.1) (Collins et al, 2012).

As mentioned before, α-syn is the main component of LBs and LNs; this fibrillar protein is also correlated to genetic and sporadic form of PD. I*n vivo* and *in vitro* studies showed that α-syn may activate microglia altering the expression levels of subset of PPR, namely toll-like receptors and increasing the proinflammatory molecules and oxidative stress (Beraud et al, 2011; Su et al, 2008).

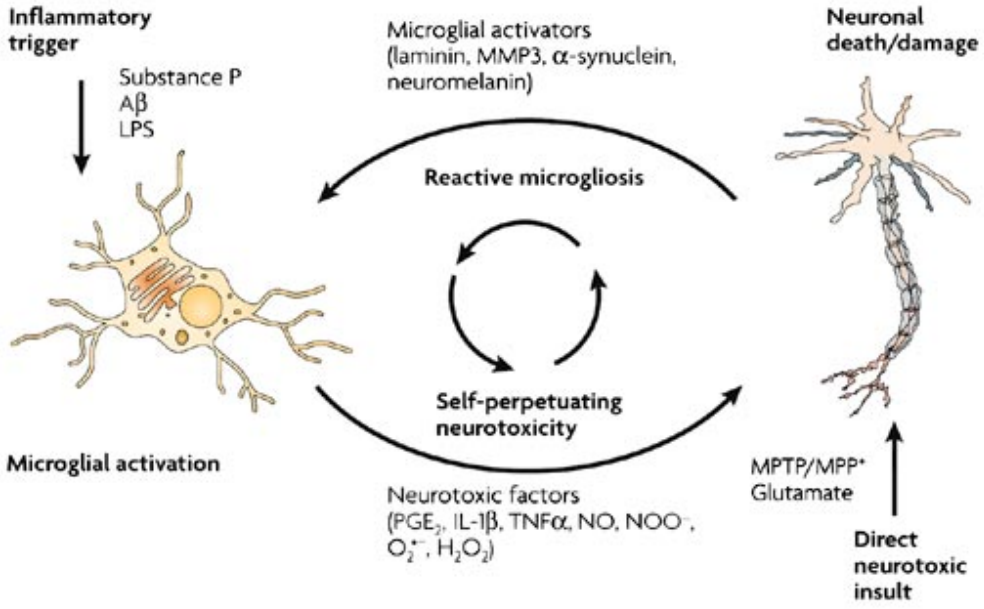

Fig. 1.1. Proposed mechanism for reactive microgliosis that might drive the progression of DAergic cell death in PD patients. After a cell injury, nigral neurons may release specific substances (e.g. MMP-3, α-syn and neuromelanin) able to activate microglia, generating a self propelling vicious cycle responsible for PD progression (Block et al, 2007).

1.2.4 UPS impairment

In physiological condition, the balance between protein synthesis and degradation is tightly regulated. The UPS is one of the two cellular machineries responsible for protein degradation. Therefore, its failure or impairment can cause accumulation of unfolded and/or damaged proteins, which is a common hallmark of neurodegenerative diseases, including PD. UPS utilizes ubiquitinated polypeptide chains as signals for selective degradation. Ubiquitin-protein ligation requires three enzymes which catalyze sequential reactions. First, the carboxyl end of ubiquitin is activated in an ATP-dependent process by the ubiquitin-activating enzymes, E1. Then, activated ubiquitin is transferred to ubiquitin-conjugating enzymes, E2. Finally, it is ligated to lysine residues of protein substrates by ubiquitin protein ligases, E3. Polyubiquitinated proteins are generally degraded by the 26S proteasome in short fragments, that can be recycled. Afterwards, polyubiquitin chains are disassembled by ubiquitin carboxy-terminal hydrolases (UCHL1) to produce

monomeric ubiquitin molecules that can be recycled (Fig.1.2) (McNaught et al, 2001).

The involvement of UPS in PD pathogenesis was supported by the discovery that *Parkin* and *UCH-L1*, genes associated with familial forms of PD, encode for proteins directly involved in ubiquitination or in ubiquitin-recycling processes. In addition, further works reported a significant reduction in the proteasome enzymatic activity in SN in sporadic PD patients (Fig.1.2) (McNaught et al, 2003; McNaught & Jenner, 2001).

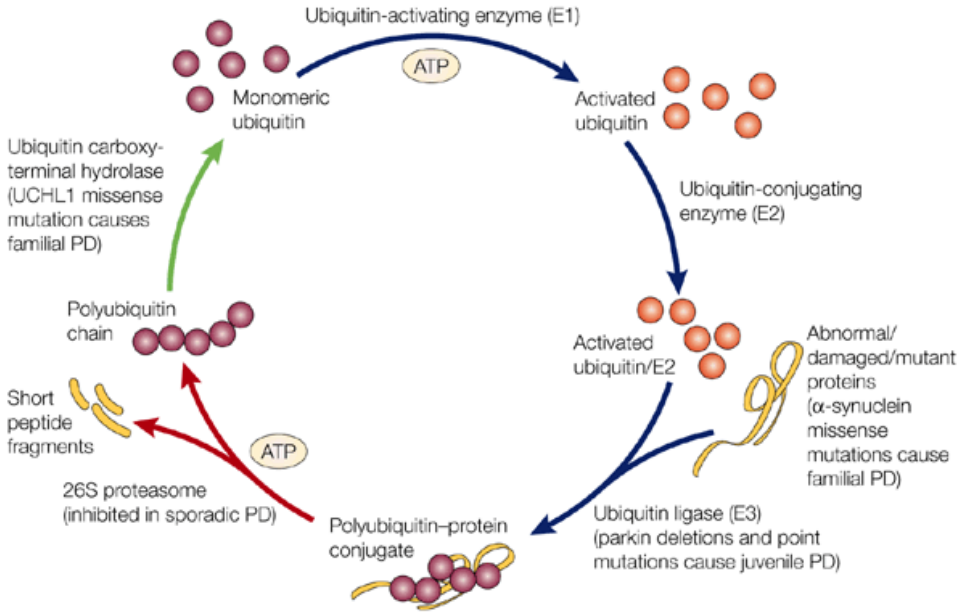

Fig.1.2. Degradation of protein mediated by UPS; some of its components are strongly involved in sporadic and familial forms of PD. The cycle represent the degradation of an abnormal/damaged or mutant protein (eg α-syn). The process requires the labelling of this protein with polyubiquitin chain, catalyzed by three different enzymes, afterwards the target protein is degraded by proteasome and the polyunquitin chains are recycled. Different components involved in this mechanism are affected in sporadic and genetic form of PD (details are presents in the figure) (McNaught et al, 2001).

In agreement with these findings, immunocytochemical analyses revealed the accumulation of ubiquitinated proteins and UPS components within LBs (Ii et al, 1997). Furthermore, *in vitro* and *in vivo* studies strongly supported the link between UPS impairment and DAergic degeneration. For example, in fetal rat ventral mesencephalic cultures the inhibition of proteasomal function leads to the

degeneration and the formation of α-syn and ubiquitin-positive inclusions (McNaught et al, 2002). Systemic injections of proteasome inhibitors in adult rats induced behavioral, pathological, and neurochemical features of PD, including motor symptoms, DAergic cell death and DA depletion (McNaught et al, 2004).

UPS failure might be involved in ROS overproduction exacerbating protein aggregation and degenerative events (Domingues et al, 2008). In fact, it has been reported that the selective proteasome inhibitor lactacystin, reduced loss of viability and increased oxidative damage at the level of proteins, DNA and lipids in NT-2 and SK-N-MC cell lines (Lee et al, 2001). However, it is possible that oxidative stress, in turn, may contribute to UPS impairment: oxidized proteins could be not properly recognized by UPS leading to their intracellular accumulation that could induce proteasomal inhibition. Shamoto-Nagai and colleagues have shown that after a treatment with the complex I inhibitor rotenone, human neuroblastoma SH-SY5Y cells exhibited a reduced proteasomal activity through the production of oxidatively modified proteins, including oxidative modification of the proteasome itself (Shamoto-Nagai et al, 2003). Overall, these data suggest that protein degradation and oxidative species generation may be strongly correlated.

1.2.5 Iron accumulation

Iron is an essential element for living organism. It is involved as cofactor in several reactions; in particular, in the central nervous system it plays a crucial role in myelination, neurotransmitter synthesis and oxidative metabolism, including OXPHOS, nitric oxide metabolism and oxygen transport. Iron homeostasis is strictly regulated at the level of its uptake, export and storage. Under pathological conditions, the dysregulation of these mechanisms might induce iron accumulation, that is a common feature of several neurodegenerative disorders (Benarroch, 2009). In PD patients, a significant iron accumulation was observed in the SN using different experimental procedures [see (Friedman et al, 2009)]. In the brain, the highest content of iron is bound to ferritin, a protein largely expressed in glial cells (Weinreb et al, 2013). At the level of the nigrostriatal system, large amounts of Fe^{3+} ions are also sequestered in subcellular organelles, known as NM granules (Zecca et

al, 2004). However, as consequence of its accumulation, iron may saturate iron-chelating sites on NM, leading to an increase of the active redox state ions (Fe^{2+}) which then get released from NM owing to weak affinity (Bharath et al, 2002). Thus, the reactive free iron pool can trigger oxidative stress *via* Fenton reaction generating the hydroxyl radical, which is responsible for cellular damage. Additionally, it has been suggested that iron accumulation could promote α-syn fibrillation (Uversky et al, 2001) and have an involvement in UPS impairment (Li et al, 2012).

1.2.6 DA metabolism

None of the molecular pathway previously described provides an explanation for the preferential degeneration of DAergic neurons, that characterizes PD.

The most probable mechanism that could clarify the selectivity of this phenomenon could be the presence of DA and its metabolism itself (Hastings & Zigmond, 1997). This neurotransmitter is a reactive molecule potentially toxic for the cell if it is not properly stored (Bisaglia et al, 2013). DA is synthesized in the cytoplasm by tyrosine hydroxylase (TH), which catalyzes the hydroxylation of tyrosine to L-DOPA, and aromatic amino acid decarboxylase (AADC), that converts L-DOPA in DA. After its synthesis, more than 90% of cytosolic DA is immediately transferred into synaptic vesicles by the vesicular monoamine transporter 2 (VMAT2); about 10% escapes sequestration and is metabolized (Eisenhofer et al, 2004). Therefore, the storage may be considered the pivotal step in the regulation of DA in the cytosol, where the neutral pH makes it unstable and prone to oxidation through several pathways (Graham, 1978). Among them, two are the mechanisms considered the main contributors for reactive and toxic species production. First, monoamine oxidase (MAO) can transform DA in the corresponding aldehyde (DOPAL), which is a substrate for aldehyde dehydrogenase (ALDH) to produce the dihydroxyphenylacetic acid (DOPAC). The secondary product of MAO reaction is H_2O_2, which in turn can undergo a Fenton chemistry with transition metals such as iron to form the hydroxyl radical. Alternatively, the catechol ring of DA can undergo oxidation to form ROS and DA-derived quinones (DAQ) (Berman & Hastings, 1999). As described above, ROS can extend their toxicity on cellular components,

lipid, nucleic acid and proteins, causing cell death. In addition, DAQ may react with cellular nucleophiles, such as DNA and sulfhydryl groups on cysteinyl residues of proteins (Tse et al, 1976).

We recently described all the possible pathogenic molecular pathways in which DAQ could be involved [see (Bisaglia et al, 2014)]. For instance, there are evidences of DAQ-DNA adducts formation *in vitro*, suggesting that this event could promote DNA mutations *in vivo*. These modifications could impact on mitochondrial DNA, which encodes 7 of 49 proteins in Complex I of the ETC, driving the Complex I deficiency observed in PD patients (Zahid et al, 2011). Moreover, the mitochondrial impairment has been also associated to a direct action of quinone on the opening of mitochondrial PTP. The consequent depolarization of the transmembrane potential induces the release of small solutes and proteins, osmotic swelling and a loss of oxidative phosphorylation (Berman & Hastings, 1999). However, DAQ can preferentially react with proteins, in particular with their cysteine residues. These covalent modifications result in loss of protein function with potentially deleterious effects on cell viability. Several studies reported α-syn, Parkin and DJ-1, three proteins involved in the familial forms of PD, as targets of DAQ (Girotto et al, 2012; LaVoie et al, 2005; LoPachin & Saubermann, 1990). Furthermore, DAQ are the fundamental building block of NM, which forms from an excess of cytosolic dopamine not accumulated into the synaptic vesicles (Sulzer et al, 2000). Physiologically, NM is located in NM granules. Under pathological condition, neuronal death might result in NM release in the extracellular space, where it can induce reactive microgliosis by microglia activation (see Paragraph 2.3) (Zecca et al, 2006).

1.2.7 Calcium regulation

In addition to DA metabolism, recent studies suggest that calcium (Ca^{2+}) regulation might be considered another element responsible for the specific susceptibility of DAergic degeneration in PD (Guzman et al, 2010). Calcium plays a central role in cell physiology controlling several processes such as signal transduction, gene expression, muscle contraction, cell death as well as

neurotransmitter release in excitable cells. Intracellular concentration of calcium is rigorously regulated through the balance between: its active extrusion to the extracellular space, mediated by Ca^{2+}-ATPase pump and Na^{+}/Ca^{2+} exchanger; its sequestration and compartmentalization into cellular organelles, such as mitochondria and endoplasmic reticulum; and its influx inside the cells or release from endoplasmic reticulum through calcium channels (Orrenius et al, 2003). The hypothesis of a possible involvement of calcium regulation in PD came from the observation that the SN neurons present peculiar neurophysiological properties. They are autonomously active because they continuously generate low frequency action potentials in the absence of synaptic input (Surmeier, 2007) to sustain DA release. This pacemaking activity derives from the presence of voltage-sensitive L-type calcium (Ca_v) channels. In particular, DAergic neurons present a pore-forming $Ca_v1.3$ subtype. These channels seem to be more expressed in SNpc DAergic neurons than in their neighboring ventral tegmental area (VTA) neuronal cells (Guzman et al, 2009). Because of the pacemaking activity of $Ca_v1.3$ channels, the magnitude of the Ca^{2+} influx is consistent. To maintain the non toxic intracellular level, calcium must be extruded through ATP dependent processes with an high metabolic cost (Surmeier et al, 2011). This energy demand requires an intensive oxidative phosphorylation which increase ROS generation. Recently, Guzman and colleagues confirmed the link between oxidative stress and calcium regulation. Actually, they observed that during autonomous pacemaking, exclusively in SN DAergic neurons the engagement of $Ca_v1.3$ channels and the consequent calcium influx generated mitochondrial ROS overproduction. In agreement with these data, they also found that DJ-1 deletion amplified this oxidant condition because of its involvement in antioxidant defense (Guzman et al, 2010). In conclusion, the peculiar physiological properties of DAergic neuronal cells might increase their vulnerability to oxidative insults.

Overall, the molecular mechanisms previously described can all contribute to the oxidative stress, which can be considered the main player in the degeneration of nigrostriatal neurons, observed in PD patients (Fig.1.3).

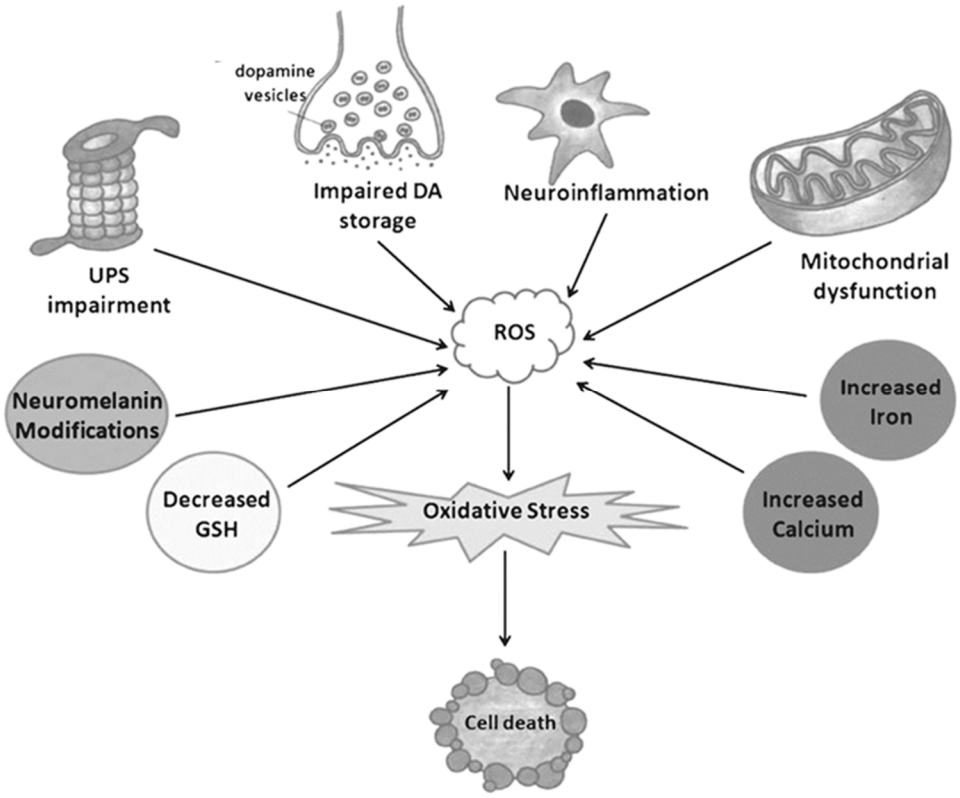

Fig.1.3. Molecular mechanisms involved in ROS overproduction and the consequent oxidative stress, which drives DAergic degeneration in PD [adapted from (Dias et al, 2013)].

1.3. Familial and sporadic forms of PD

Increasing evidence suggest that PD is an heterogeneous disorder with a wide range of clinical symptoms and signs (Perfeito et al, 2012). Some of the molecular pathways discussed above have been identified studying the familial forms of PD. Even though mendelian mutations are rarely the cause of PD, they could allow to define the complex scenario of events involved also in the pathogenesis of idiopathic PD. The genetic contribution to PD development has been established during the past two decades with the identification of 18 PD-related gene loci, named as PARK (Thenganatt & Jankovic, 2014). Meanwhile, the involvement of environmental toxins in the etiology of this motor syndrome came from epidemiological studies. Recently, an exhaustive summary of the state of knowledge has been published, highlighting that prolonged exposure to pesticides might be a risk factor for PD (Kamel, 2013). In the next sections, familial and sporadic forms of PD will be further discussed.

1.3.1 Familial forms

Among the 18 PARK loci, identified through human genetic studies, seven genes have been recognized as cause of monogenic PD (Fujioka & Wszolek, 2012). They present either autosomal dominant or recessive mode of inheritance with different and overlapping phenotypes. The autosomal dominant genes include *SNCA*, *LRRK2, VSP35* and *EIF4G1;* however, only the first two have been deeply studied, whereas the others have recently discovered and only partially investigated.

The *SNCA* gene encodes for α-syn. The physiological function of this protein remains unknown; however, its localization at presynaptic terminals and its association with synaptic vesicles suggest an involvement in the regulation of neurotransmitter release, synaptic function and neuronal plasticity (Lashuel et al, 2013). In particular, the amphipathic α-helical domain in the N-terminal region might drive the interaction with membranes (Perfeito et al, 2012). This small protein is particularly prone to aggregate because of its highly amiloidogenic domain NAC which is essential to form oligomers and insoluble fibers (Giasson et al, 2001). As described in Section 1.2, α-syn, that represents the main component of LBs, can

contribute to PD pathogenesis through several pathways including UPS impairment, iron accumulation, chronic inflammation and DA metabolism.

Mutations in *leucine-rich repeat kinase 2* (*LRRK2*) represent the most common cause of genetic PD. This gene encodes for a large protein (approximately 285 kDa) with two enzymatic activities mediated by two distinct domains, a GTPase and a kinase domain. So far, the precise LRRK2 function has not been identified. Nevertheless, the wide distribution of this protein and its association to various intracellular membranes and vesicular structures, including endosomes, lysosomes, mitochondrial outer membrane, Golgi complex and endoplasmic reticulum, support an involvement in multiple pathways, such as regulation of autophagy, microtubule dynamics, and mitochondrial function (Esteves et al, 2014).

Recessive inheritance is linked to mutations in *Parkin, PINK1, DJ-1* which are causative of early onset PD. Clinically, these forms differ from the classical PD not only for the juvenile manifestation but also for the slow disease progression, the excellent response to the most common used drug, L-DOPA, and the minimal cognitive decline (Bonifati, 2012). Furthermore, at pathological level, the presence of LBs in recessive PD patients is still controversial. First *post-mortem* examinations reported the absence of protein inclusions (Yokochi, 1997), while in further studies LB pathology has been observed in patients with pathogenic *PINK1* and *Parkin* mutations (Farrer et al, 2001; Samaranch et al, 2010). The roles and functions of DJ-1, Parkin and PINK1 will be examined in details in the following sections because of their involvement in maintaining mitochondrial homeostasis and their neuroprotective properties against oxidative damage. Recently, mutations in other genes, such as *ATP13A2, FBXO7, PLA2G6*, have been associated to atypical recessive inherited juvenile disorders, with different clinical manifestations in addition to parkinsonism (Bonifati, 2014).

1.3.1.1 DJ-1

Mutations in *DJ-1* were identified as responsible for a monogenic autosomal recessive parkinsonism (Bonifati et al, 2003). *DJ-1*encodes for a protein of 189 amino acids, that form dimers. DJ-1 is an evolutionarily ancient protein: homologs were found both in prokaryotes and eukaryotes. In particular, some residues are extremely conserved, including one of the three cysteines, the C106. This residue has been identified as highly sensitive to oxidative stress (Kinumi et al, 2004). Even though the biochemical function of DJ-1 is still unclear, its involvement in the antioxidant defenses represents the most plausible hypothesis. Indeed, *DJ-1 knock down* cells presented an increased sensitivity to oxidant insults (Taira et al, 2004). In contrast, the overexpression of DJ-1 in human neuroblastoma cells resulted in an increase of tolerance to rotenone and H_2O_2 exposure, correlated to a significant reduction of ROS (Lev et al, 2008). *In vivo* analyses confirmed the neuroprotective role of this protein against oxidative injury. Actually, *Drosophila DJ-1* mutants were selectively sensitive to ROS-generating environmental toxins, such as rotenone and paraquat. (Meulener et al, 2005). In addition, DJ-1 deficient flies presented locomotor defects and this phenotype was strongly exacerbated after the treatment with an oxidant insult (Park et al, 2005). In agreement with this line of evidence, DJ-1 deficient mice showed striatal denervation after MPTP administration (Kim et al, 2005).

At least three hypothesis have been proposed to explain the molecular mechanism driving DJ-1 activity against oxidative stress. First, it has been suggested that DJ-1 controls the formation of the complex between MAP3 kinase apoptosis signaling regulating kinase 1 (ASK1) and tioredoxin (Trx1). Under basal condition, Trx1 acts on ASK1, which is a potent apoptotic molecule, inhibiting its activity. Upon oxidative stress, Trx1 dissociates from ASK1, inducing its activation. The proposed model suggests that DJ-1 modulates the stability of this complex: DJ-1 suppresses ASK1 activity and prevents the dissociation of ASK1/Trx1 complex (Im et al, 2010). The second mechanism is based on the idea that DJ-1 could have a direct interaction with the cytosolic antioxidant enzyme superoxide dismutase 1 (SOD1) in a copper-dependent mode. Actually, it has been demonstrated that DJ-1

was able to bind copper and to transfer it to SOD1 by acting as a metallochaperone, DJ-1 might regulate the activation of the cytosolic antioxidant enzyme (Girotto et al, 2014). Finally, recent works support an alternative hypothesis which relies on an another possible role of DJ-1 in regulating mitochondrial homeostasis and dynamics. The loss of this protein in several cell lines induced an aberrant mitochondrial morphology (Irrcher et al, 2010) and an accumulation of damaged organelles (Krebiehl et al, 2010). Accordingly, it has been proposed that DJ-1 might act controlling mitochondrial function and autophagy in parallel to the PINK1/Parkin mitochondrial quality control pathway (Thomas et al, 2011) (see 1.3.1.4).

1.3.1.2 Parkin

More than 10 years ago, Kitada *et al.* discovered that "loss of function" mutations in *PARK2* gene, which encodes for Parkin protein, cause autosomal recessive juvenile parkinsonism (Kitada et al, 1998). Mutations in this gene account for about half of recessive PD cases. Parkin is 465 amino acid protein and contains a N-terminal ubiquitin-like domain followed by four zinc fingers domains. Parkin is involved in protein ubiquitination acting as an E3 ubiquitin ligase and targeting substrates prone to degradation through the UPS system (Shimura et al, 2000). Therefore, it has been first hypothesized that Parkin loss of function resulted in the accumulation of toxic substrates leading to DAergic degeneration. However, more recent investigations suggest that this protein acts in a wide range of pathways regulating different cellular processes which are only partially related to degradative events (Winklhofer, 2014). In particular, increasing evidence demonstrated the involvement of Parkin in mitochondrial maintenance.

Flies lacking the *Parkin* gene present a severe phenotype: they are semi-viable and exhibit reduced longevity, motor deficits, male sterility and DAergic neuron degeneration (Greene et al, 2003; Whitworth et al, 2005). The locomotor impairment is due to apoptotic cell death in muscles which seems to be the late consequence of the loss of mitochondrial integrity (Greene et al, 2003). Interestingly, *Drosophila Parkin* mutants are characterized by an alteration in oxidative stress response (Park et al, 2009) and an increased sensitivity to oxygen radical injury

(Pesah et al, 2004). In line with these results, *Parkin* null mice presented a reduction in synaptic excitability in nigrostriatal neurons which is not associated with the degeneration of this cell population (Goldberg et al, 2003). In addition, in the same animal model it has been observed an increase of oxidative stress, a reduction in respiratory capacity of striatal mitochondria which is consistent with a decreased abundance of several subunits of ETC complexes I and IV (Palacino et al, 2004). However, the absence of a PD-phenotype and DAergic degeneration in mouse models suggests the presence of a compensatory mechanism (Dawson et al, 2010), even though such a mechanism has not been identified yet. In agreement with the aforementioned observations, *in vitro* studies support the mitochondrial antioxidant properties of this protein (Machida et al, 2005; Rothfuss et al, 2009). In conclusion, the common denominator for all these models is that Parkin deficiency affects mitochondrial morphology, the ETC complexes and ATP levels (Costa et al, 2013).

The molecular mechanisms in which Parkin is involved are only partially defined. They include mitochondrial biogenesis, mitophagy, mitochondrial transport, fusion and fission (Fig.1.4) (Gaweda-Walerych & Zekanowski, 2013). All of these processes are highly interconnected and regulate the maintenance of a healthy mitochondrial network. As far as mitochondrial biogenesis is concerned, it has been shown that Parkin might regulate mitochondrial biogenesis through a physical interaction with the mitochondrial transcription factor A (TFAM), the main regulator of mitochondrial transcription and replication (Kuroda et al, 2006). Actually, Parkin overexpression in cell cultures increased mitochondrial mass and mtDNA replication (Rothfuss et al, 2009). In contrast, the silencing of the endogenous protein decreased the mitochondrial transcription (Langston et al, 1983). As the other cellular pathways are mostly regulated in association with PINK1, they will be discussed further on.

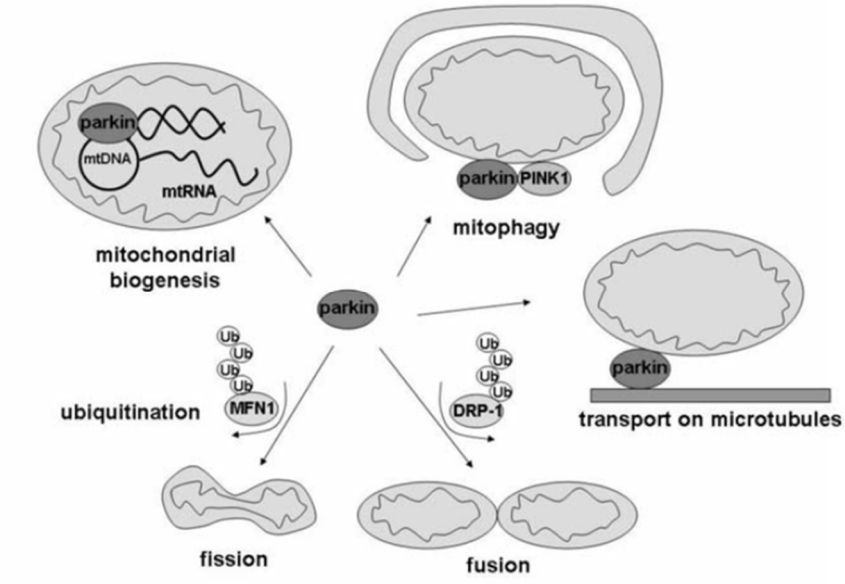

Fig.1.4. Parkin involvement in several processes that regulate mitochondrial functioning Mfn1: mitofusin1; Drp-1: dynamin-related GTPase, Ub: ubiquitin. (Gaweda-Walerych & Zekanowski, 2013).

1.3.1.3 PINK1

PINK1 gene mutations have been identified as cause of the second most common form of early onset parkinsonism (Valente et al, 2004). *PINK1* encodes for an ubiquitously expressed serine/threonine kinase, which contains in the N-terminus a high-confidence mitochondrial targeting sequence (Silvestri et al, 2005). Several pathogenic mutations, insertions and deletions affect the kinase domain leading to the dysfunction of its catalytic activity (Beilina et al, 2005). PINK1 exists in different forms: PINK1 full-length (FL), of approximately 63 kDa and at least other two shorter forms of 52 kDa and 45 kDa, resulting from proteolytic processing of FL.

The subcellular localization of FL and its isoforms is still debated. However, the most accepted point of view suggests that the protein is distributed both at mitochondrial and cytosolic level (Beilina et al, 2005; Silvestri et al, 2005). In particular, it has been shown that, following mitochondrial import, PINK1 precursor is cleaved by mitochondrial proteases and at least a portion of the processed products may be released into the cytosolic compartment (Lin & Kang, 2008). The main controversial issue remains the sub mitochondrial localization. Actually, some studies reported that PINK1 is mainly situated in the outer mitochondrial membrane

(OMM) with the kinase domain facing the cytosol where PINK1-substrated might be found (Zhou et al, 2008). In contrast, other works showed that PINK1 is localized at the level of inner mitochondrial membrane (IMM) and the catalytic domain is exposed in the intermembrane space (Silvestri et al, 2005).

To define the role and function of PINK1 several animal models have been generated. Three independent studies demonstrated that *Drosophila* PINK1 deficient flies exhibited loss of dopaminergic neurons, mobility abnormalities, reduced life span, mitochondrial defects, reduced ATP levels (Clark et al, 2006; Park et al, 2006; Yang et al, 2006)and an increased sensitivity to multiple stresses including oxidative insults (Clark et al, 2006). These observations were not completely confirmed in *PINK1* -/- mice. Indeed, although these animals presented a clear impairment of mitochondrial functions, such as ATP-generation and respiration (Gispert et al, 2009), they manifested a mild phenotype presenting a slight reduction of weight and motor performance not associated with degeneration of nigrostriatal neurons or alteration in DA levels and receptors (Kitada et al, 2007). The real discovery came from genetic analyses with Parkin. The striking similarity in phenotypes between *PINK1* and *Parkin* mutant animals indicated that they may act in a common pathway. In agreement with this hypothesis, it was found that *PINK1/Parkin* double *knock out* flies did not exacerbated the phenotype of either *Parkin* or *PINK1* single *knock out* (Clark et al, 2006; Park et al, 2006). Furthermore, it has been demonstrated that Parkin overexpression in *PINK1* null flies was able to ameliorate mutant phenotypes; but conversely PINK1 overexpression did not influence the *Parkin* mutants phenotype (Clark et al, 2006; Park et al, 2006; Yang et al, 2006). The link between PINK1 and Parkin was further confirmed in human cell culture; in fact, PINK1 deficiency was rescued by the enhancement of Parkin expression (Exner et al, 2007). Overall, these aforementioned findings strongly support that Parkin acts downstream of PINK1 in controlling mitochondrial integrity (Clark et al, 2006; Park et al, 2006).

1.3.1.4 Parkin/PINK1 pathway regulates mitochondrial quality control

Mitochondria produce the highest amount of cellular energy through the OXPHOS complexes. To maintain the functionality of these organelles, cells have developed a strict system of surveillance, referred to as mitochondrial quality control. In physiological conditions, an healthy pool of mitochondria is guaranteed through several pathways that control mitophagy and mitochondrial dynamics, biogenesis and motility. The first line of defense within these organelles occurs at molecular level and it is mediated by chaperones and proteases which act on protein folding and degradation (Rugarli & Langer, 2012).

The subsequent level of defense that might be engaged is the organellar quality control system based on a balance between fusion, fission and degradation (mitophagy) (Lehmann & Martins, 2013). As described in the previous sections, *PINK1* and *Parkin* mutations impact on mitochondrial functioning and integrity, but the mechanism underlying this control is still not completely elucidated. So far, it has been demonstrated that, in mammalian cells, Parkin is selectively recruited from the cytosol to dysfunctional mitochondria which present low membrane potential, promoting the degradation of these impaired organelles (Narendra et al, 2008). Further investigations reported that after mitochondrial depolarization, PINK1 accumulates on OMM of dysfunctional organelles; this stabilization becomes the signal for Parkin recruitment and activation. The ubiquitin ligase activity of this protein on OMM components allows the remodeling of depolarized mitochondrial surface, leading to mitophagy (Matsuda et al, 2010; Narendra et al, 2010). This model is also conserved in *Drosophila* (Ziviani et al, 2010) confirming that PINK1 acts upstream Parkin. However, it is still unclear how PINK1 recruits Parkin on damaged mitochondria. Some authors reported that PINK1 can phosphorylate Parkin directly at a highly conserved residue, the serine 65 (Kondapalli et al, 2012; Shiba-Fukushima et al, 2012). Nevertheless, this modification does not seem to be sufficient for the full activation of ubiquitin-ligase activity of this protein. Actually, abolishing Parkin phosphorylation on serine 65 did not completely inhibit its PINK1-dependent activation (Kane et al, 2014). Recently, three different groups identified a new PINK1 substrate, that might be considered the missing link in this pathway.

Using biochemical and proteomic approaches, they demonstrated that PINK1 phosphorylates ubiquitin at a serine amino-acid residue (serine 65) and this modified ubiquitin, in turn, induces Parkin activity leading to mitophagy (Fig.1.5) (Kane et al, 2014; Kazlauskaite et al, 2014; Koyano et al, 2014).

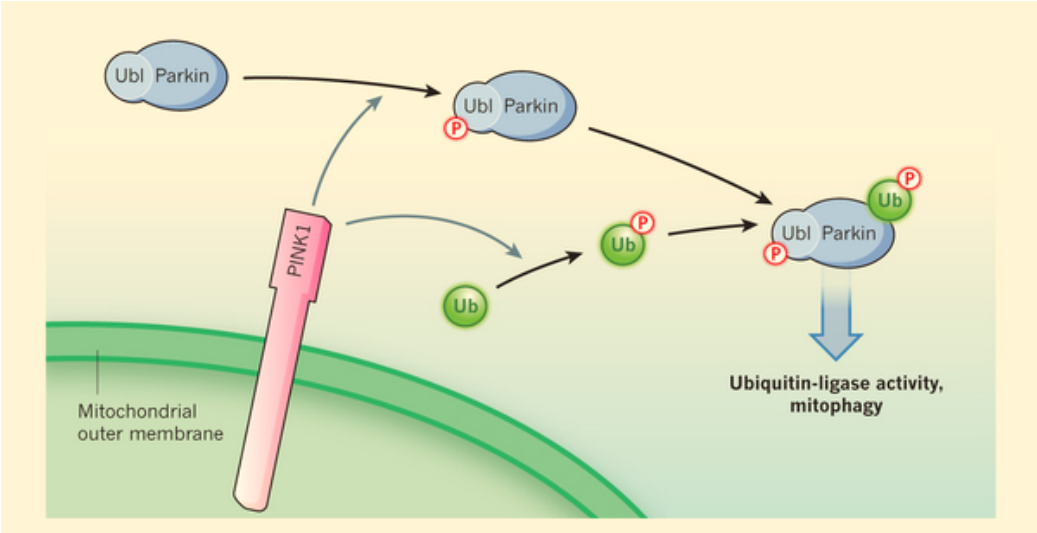

Fig.1.5. PINK1/Parkin pathway involved in mitochondrial quality control. Pink1 accumulates on the OMM of dysfunctional mitochondria anchoring with its kinase domain facing the cytoplasm. PINK1 phoshorilates Parkin but also the ubiquitin (Ub) protein itself. Phosphorylated ubiquitin directly binds to Parkin which becomes activated leading to disposal of the damaged mitochondria through mitophagy (Abeliovich, 2014)

Even though recent researches have partially clarified one PINK1/Parkin molecular pathway, many other aspects correlated to the two proteins need to be elucidated. In fact, PINK1 and Parkin are also involved in mitochondrial dynamics. Mitochondria form a dynamic interconnected network undergoing continuous fission and fusion processes (Fig.1.4). Fusion allows damaged mitochondria to mix their contents with healthy organelles as a mechanism of complementation. Fission is necessary to generate new mitochondria, but it also contributes to remove the mitochondria with insufficient complementation. Three GTPases are involved in fusion: the Mitofusin1 (Mfn1) and Mitofusin2 (Mfn2) and the dynamin-related protein OPA1, while the machinery that control fission is manly based on the dynamin-related GTPase Drp1 [see (Scorrano, 2013)]. Given that *Drosophila Parkin*

and *PINK1* mutants exhibited an alteration in mitochondrial morphology (Clark et al, 2006; Greene et al, 2003), many efforts have been produced to understand if and how PINK1 and Parkin regulate the mitochondrial network. Therefore, the effects of altering the gene expression of the main component of fusion/fission machinery in *Drosophila PINK1* and *Parkin* mutant flies have been explored. *Drp1* loss-of-function mutations were largely lethal in these mutants. In contrast, their phenotypes were strongly rescued promoting mitochondrial fission through Drp1 overexpression as well as reducing fusion through *OPA1* and *Mfn2* loss-of-function mutations (Poole et al, 2008). Furthermore, it has been observed that in *Drosophila,* PINK1 or Parkin deficiency causes an increase in Mfn levels and an hyperfused mitochondrial network (Ziviani et al, 2010). However, the mitochondrial phenotypes observed in mammalian model lacking PINK1 and Parkin is significantly different. Actually, neuroblastoma and primary mouse neurons presented mitochondrial fragmentation (Lutz et al, 2009). These discrepant phenotypes might be explained through a compensatory event: the early event of fragmentation is then followed by a rapid up-regulation of fusion. This should facilitate dilution of dysfunctional mitochondria, but should not favor elimination of damaged mitochondria through mitophagy. Thus, the mitochondrial hyperfusion event might have several deleterious effects in the long term (Pilsl & Winklhofer, 2012). At molecular level, the link between mitochondrial dynamics and PINK1/Parkin may be Mfn, which was identified as Parkin substrate (Fig.1.6). Actually, it has been reported that its ubiquitination mediated by Parkin prevents re-fusion of damaged mitochondria promoting their degradation by autophagic machinery (Ziviani et al, 2010; Ziviani & Whitworth, 2010). Thus, a potential model by which PINK1 and Parkin promote mitochondrial fragmentation and turnover can be postulated: i) upon Parkin recruitment to damaged organelles, it ubiquitinates the mitochondrial fusion-promoting factor Mfn; ii) this event tags Mfn for degradation, abolishing its fusion-promoting activity; iii) refusion of these mitochondria is prevented and they can be segregated for subsequent autophagy (Poole et al, 2010) (Fig.1.6).

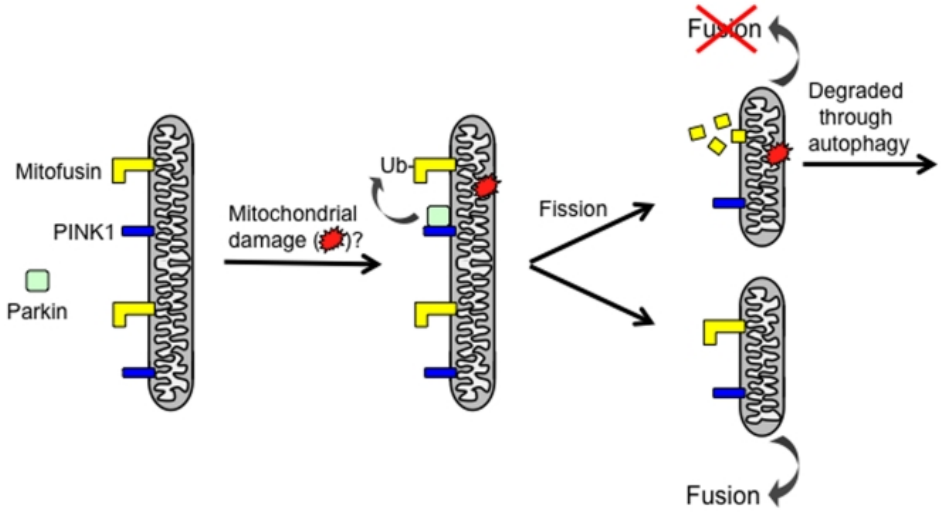

Fig.1.6.Proposed function of PINK1 and Parkin in regulating the segregation of damaged mitochondria. This model postulates that upon Parkin recruitment to damaged portions of the mitochondrial reticulum, it ubiquitinates (Ub) the mitochondrial fusion-promoting factor Mfn thus tagging it for degradation, or otherwise inactivating its fusion-promoting activity (Poole et al, 2010).

Another level of mitochondrial quality control system is also regulated through mitochondrial transport along microtubules mediated by motor proteins, kynesins and dynesins. This event requires the presence of a motor/adaptor complex which is composed by the OMM GTPase Miro and its cytosolic adapter Milton. The hypothesis is that PINK1 and Parkin might impact on mitochondrial transport interacting directly with this complex and regulating trafficking and motility (Fig. 1.4). Accordingly, it has been observed that PINK1 immunoprecipitated with Miro and Milton (Weihofen et al, 2009). Moreover, Wang *et al.* showed that upon mitochondrial depolarization PINK1 can accumulate on OMM and phosphorylates Miro to trigger its degradation through a Parkin-dependent pathway. Thus, the proposed mechanism considers that damaged mitochondria might be stopped in their tracks leading to an initial quarantining step prior to their clearance or a mechanism to spatially restrict their deleterious effects (Wang et al, 2011) (Fig.1.7).

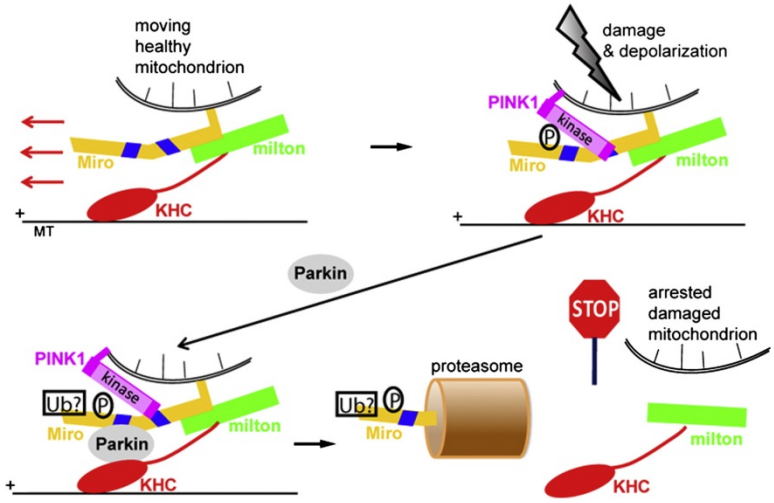

Fig.1.7. Proposed mechanism used by PINK1 and Parkin to control mitochondrial motility. According to this model, PINK1 and Parkin, participate in this regulation by arresting mitochondrial movement. PINK1 phosphorylates Miro, a component of the primary motor/adaptor complex that anchors kinesin to the mitochondrial surface. The phosphorylation of Miro activates proteasomal degradation of Miro in a Parkin-dependent manner. Removal of Miro from the mitochondrion also detaches kinesin from its surface. By preventing mitochondrial movement, the PINK1 and Parkin may quarantine damaged mitochondria prior to their clearance (Wang et al, 2011).

1.3.2 Sporadic forms

The most common form of parkinsonism is the idiopathic or sporadic PD, whose causes are still unknown. As for other human diseases, the environment crucially contributes to the pathogenesis of this motor disorder. However, it is most likely that the sporadic forms are the result of the interaction between environmental stressors and genetic predisposition associated to the aging. To discover and identify the environmental risk factors, several epidemiological studies have been carried out over the past decades. Thus, drinking well water, rural living, farming, and exposure to agricultural chemicals and industrial metals have been classified as negative regulators and potential risk factors for PD onset (Priyadarshi et al, 2001). In contrast, some substances such as cigarettes and coffee consumption have been correlated with a decreased incidence of PD (Pan-Montojo & Reichmann, 2014), even though the mechanism underlying such protection is still unclear. Among the different epidemiological researches, the most consistent results have been obtained

with works focused on pesticides. In 2013, a wide meta analysis based on 104 studies concluded that the prolonged exposure to pesticides is a risk factor for PD (Pezzoli & Cereda, 2013). Pesticides are often not strictly selective for the target species and they might extend their toxicity to other species, including humans. These compounds are responsible for acute and long term health effects due to their ability to alter a variety of physiological functions.

To date, several pesticides have been studied for their possible involvement in PD pathogenesis, including rotenone, maneb and paraquat (PQ). Among them, PQ is the only one that has been significantly associated with PD (Kamel, 2013). As a consequence, this environmental toxicant might be a reliable experimental paradigm to generate *in vitro* or *in vivo* models that recapitulate some of the hallmarks of PD.

1.3.2.1 Paraquat

PQ is a widely used herbicide because of its low cost and rapid action. It is a highly reactive quaternary nitrogen compound which acts on weed and grass control. Recently, European nations and the United States have banned or restricted its use; however, it is still extensively utilized in other less developed countries (Drechsel & Patel, 2008). In humans, acute PQ poisoning mostly induces lung and kidney lesions, while chronic exposure might impact on DAergic neurons. In all these tissues, the mechanism of toxicity is the same: PQ generates massive oxidative stress through its redox cycling within cells (Fig.1.8). Owing to a low redox potential, the PQ dication (PQ^{2+}) is easily reduced to form a radical by a single electron from intracellular enzymes. In presence of molecular oxygen (O_2), the reduced monocation PQ ($\cdot PQ^{+}$) is re-oxidized with the concomitant formation of superoxide anion, which initiates a radical chain reaction leading to cellular damage (Moran et al, 2010). Several enzymes involved in a wide range of cellular processes are capable of initiating this redox cycling and they have been identified in microsomal, plasma membrane, and cytosolic components. They include NADPH oxidase, nitric-oxide synthase and NADPH-cytochrome c reductase (Castello et al, 2007). Different evidences support the hypothesis that, although the involvement of the aforementioned compartments, mitochondria might be the major site for PQ-induced ROS production (Cocheme &

Murphy, 2008). Nevertheless, the mechanism underlying mitochondrial ROS production is still not completely clear. Some studies reported that PQ^{2+} is internalized across the mitochondrial inner membrane, through a mechanism dependent on mitochondrial membrane potential. Once in the matrix, PQ might be reduced generating oxidative stress within this organelle. The proposed mechanism requires the activity of respiratory chain complexes, in particular complex I and III of ETC (Castello et al, 2007; Cocheme & Murphy, 2008).

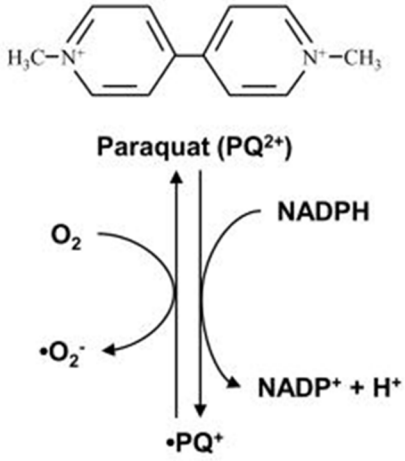

Fig.1.8. PQ redox cycling [adapted from (Franco et al, 2010)].

To act on the nigrostriatal system, PQ must be transported across the blood-brain barrier (BBB) and then taken up by DAergic neuronal cells. Being a charged molecule, PQ can penetrate into the brain only through a specific carrier, presumably a neutral amino acid transporter such as the *system L carrier* (LAT-1), which normally transports the amino acids L-valine and L-phenylalanine (Shimizu et al, 2001). Initially, the structural similarity with MPTP suggested the hypothesis that both the toxicants might have the same mechanism of toxicity. Thus, PQ was commonly believed to be transported into DAergic neurons by DAT and to inhibit complex I (Franco et al, 2010). However, Richardson *et al*. reported that the neurotoxic effects of PQ do not depend on the DAT-mediated transport and that, even if mitochondria might be considered the preferential site for PQ reduction, the herbicide is not a complex I inhibitor (Richardson et al, 2005). These observations

suggested that the preferential vulnerability of DAergic neurons to PQ is not related to a selective transport mechanism into cells and complex I inhibition, while it is most likely to be associated with their susceptibility to oxidative damage due, for example, to the pro-oxidant properties of dopamine (Kang et al, 2009). As an alternative or complementary hypothesis, it has been observed that PQ induces DAergic neurotoxicity through a molecular pathway related to inflammatory response. In mice and in cell cultures, exposure to this herbicide caused neurotoxicity and oxidative stress that is dependent to the respiratory burst generated by microglial activation and induction of NADPH oxidase (Purisai et al, 2007; Wu et al, 2005). Thus, microglial activation and inflammation might be additional events that enhance PQ toxicity.

Overall, these studies confirmed that PQ might increase ROS production through different mechanisms. When, cells cannot compensate for radical overproduction of and the consequent oxidative stress, they can undergo apoptosis or necrosis. Actually, it has been reported that PQ treatment determines DAergic neuronal cell death through the activation of an apoptotic cascade (Peng et al, 2004), that involves mainly the intrinsic mitochondrial pathway (Yang & Tiffany-Castiglioni, 2008).

Because of its ability to generate ROS as well as cell death, PQ is also frequently utilized as experimental paradigm to generate animal models. In mice systemic injections of PQ caused motor defects and the progressive death of DAergic neurons (Brooks et al, 1999) that was not correlated with a decrease in the amount of striatal DA (McCormack et al, 2002). The discrepancy between neurodegeneration and lack of significant dopamine loss was considered an effect of a compensatory mechanisms by which surviving neurons might be capable of restoring neurotransmitter tissue levels. Additionally, the observed phenomenon seems to be selective and specific on the nigrostriatal system. In fact, the number of GABAergic cells in SN *pars reticulata* was not affected by the treatment (McCormack et al, 2002).

In conclusion, the molecular mechanisms involved in PQ neurotoxicity and its involvement in sporadic forms of PD are mostly due to its ability to generate oxidative stress through a redox cycling within cells. PQ administration, as experimental paradigm, allows to develop models for Parkinsonian neurodegeneration that replicate most of the pathological and phenotypic features of this motor disorder.

1.4 Treatments of PD

PD is still an incurable disorder and the available therapies only treat the symptoms improving the quality of life. The most common pharmacological approach is based on DA replacement, in particular on the use of the DA precursor, L-DOPA, which, is able to cross the BBB while the neurotransmitter itself is not. However, chronic administration of L-DOPA is associated with a gradual decline of clinical efficiency and the development of side effects such as dyskinesia (Heumann et al, 2014).

To overcome these limitations,. other classes of drugs have been developed that can be used in addition to L-DOPA enhancing the dopaminergic tone. These include DA agonists, which act directly on the dopamine receptor; monoamine oxidase-B (MAO-B) inhibitors, which increase synaptic DA levels blocking central dopamine oxidative metabolism; and catechol-O-methyltransferase (COMT) inhibitors, which increase bioavailability of L-DOPA inhibiting its peripheral metabolism (Olanow & Schapira, 2013). When PD patients experienced a decrease in the effects of medical therapy over time, surgical therapies are often applied and deep brain stimulation (DBS) is the most frequently performed (Coune et al, 2012). In DBS, an electrode is surgically implanted in the subthalamic nucleus, globus thalamus or ventral intermediate nucleus, providing continuous high frequency electrical stimulation attempting to overwhelm the loss of dopamine signaling in the striatum (Beitz, 2014). Even though this therapy has some beneficial effects against motor symptoms, the sensory motor side effects of stimulation are limiting factors for efficiency of the technique (Benabid, 2003).

Other experimental therapies could offer new hopes for the future. These include gene and cell replacement. To date, five gene therapy trials have been developed with the use of adeno-associated virus (AAV) or lentivirus vector platforms. In the first clinical study, an AAV-vector to express glutamic acid decarboxylase (GAD) was delivered to the subthalamic nucleus. In PD, striatal DA depletion leads to a decrease in the inhibitory control exerted by the external segment of the globus pallidus on the subthalamic nucleus. The subsequent lack of inhibition of the subthalamic nucleus affects the output of the basal ganglia circuitry causing impairments in motor functions. GAD enzyme catalyzes the synthesis of γ-aminobutyric acid, the major inhibitory neurotransmitter in the central nervous system, potentially providing the lost inhibitory control in the basal ganglion motor system, thus restoring appropriate transynaptic balance. Another approach has attempted to improve the ability to synthesize DA using different strategies. The first strategy is based on the expression of the major L-DOPA-converting enzyme AADC in the *putamen* that can be used to increase the efficacy of pharmacological therapy. The second one relies on the delivery of three transgenes, TH, AADC and guanosine 5′-triphosphate cyclohydrolase1 (the rate–limiting enzyme that synthesizes the essential TH co–factor) from a single vector cassette to induce ectopic DA synthesis from tyrosine. Finally, two gene therapy approaches have employed the expression and secretion of neurotrophic factors, glial-derived neurotrophic factor (GDNF) or neurturin (NRTN). Thus rather than directly modulating neuronal activity, they confer trophic support to the dopamine pathway trying to restore its function [see (Bartus et al, 2014)]. To date, these clinical trials did not demonstrate sufficiently robust or consistent benefits to patients, compared to that achieved by placebo controls (Bartus et al, 2014) .

Cell replacement has been suggested as a great potential therapeutic strategy in PD (Loewenbruck & Storch, 2011). Although transplantation of dopamine fetal cells in the striatum of advanced PD patients provided disappointing results (Evans et al, 2012; Olanow et al, 2003) in the future, cell therapies might come back with the use of the appropriate cell source such as stem cells. Actually, current and future studies are attempting to overcome the main obstacle for the clinical application of

stem cell in PD therapy by finding the ideal candidate for cell replacement, among adult, embryonic or induced-pluripotent (iPS) stem cells (Kim & de Vellis, 2009).

In conclusion, so far none of the aforementioned therapies provides more benefits then L-DOPA and all of them present their own set of side effects. Therefore, it is still necessary to find out new therapeutic strategies that not only provide symptomatic benefits without motor complications, but also delay or reverse PD progression (Olanow & Schapira, 2013).

1.4.1 ROS homeostasis and antioxidant defense

As widely discussed, ROS overproduction might trigger and/or amplify the process of neuronal cell death in PD. Hence, it is a clear consequence that the inhibition of this event could block or delay neuronal degeneration. However, to date treatment based on antioxidants showed very disappointing results (Bjelakovic et al, 2012).

To understand the possible limitations of the therapies based on blocking ROS production, it is necessary to thoroughly consider the physiological role of these reactive species. Increasing evidence support that these molecule are involved in maintaining cell homeostasis and in cell signaling (Finkel, 2011). Several studies have shown that oxidants act as cellular messenger regulating cell proliferation, cell death (either apoptosis or necrosis), gene expression and metabolic response (Gemma et al, 2007). Additionally, it has been recently observed that ROS signaling is required for the normal regulation of autophagy (Scherz-Shouval & Elazar, 2011). As mentioned in the Section 1.1, the current theory of aging does not imply that radicals always cause damage (as in the original one) but it is based on the idea that aging is caused by a disruption of the whole signaling network involving ROS. According to this “modified” hypothesis, the indiscriminate reduction of reactive species could alter essential signaling events and this could explain the discouraging outcomes observed with antioxidant treatments in clinical trials.

In physiological condition, to counteract oxidative stress, cells have an intrinsic system, based on a complex network of antioxidant molecules. This

defensive system does not act entirely removing oxidants but, rather, by maintaining a tight homeostatic control of ROS. Endogenous antioxidants include low molecular weight molecules such as GSH, present in millimolar concentrations within cells, as well as a wide array of protein antioxidants with specific subcellular localizations and chemical reactivities (Finkel, 2011) (Fig.1.9).

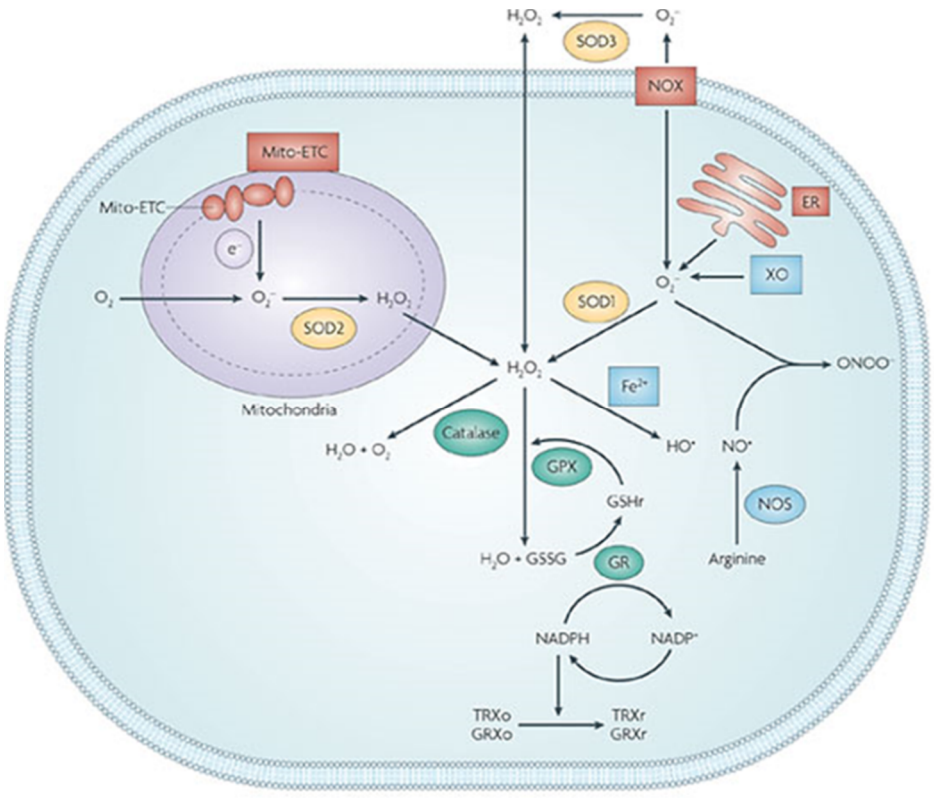

Fig.1.9. Catalytic antioxidant systems. To maintain the proper redox balance, cells developed a system of components that can be divided into two major groups, enzymatic and nonenzymatic. Major ROS-scavenging enzymes; SOD superoxide dismutase (SOD1, SOD2, SOD3) catalase; GPX, glutathione peroxidase; GR, glutathione reductase;GRXo, glutaredoxin (oxidized); GRXr, glutaredoxin (reduced); GSHr, glutathione (reduced); GSSG, glutathione (oxidized); TRXo, thioredoxin (oxidized); TRXr, thioredoxin (reduced); XO, xanthine oxidase (Trachootham et al, 2009).

Among them, superoxide dismutases (SODs) catalyze the disproportionation of superoxide to H_2O_2 and O_2. H_2O_2, generated in this reaction, can be further converted to water and O_2 by the action of catalase in the peroxisomes and through glutathione peroxidases (GPx) in the cytosol and mitochondria (Young & Woodside,

2001). The activity of GPx is dependent on the constant availability of reduced glutathione, which is, in turn, strictly regulated by glutathione reductase (GR). Actually, GR is responsible for the regeneration of GSH from oxidized glutathione (GSSG). In the next section, SOD enzymes will be analyzed more in details.

1.4.2 Superoxide dismutases (SODs)

SODs are considered the first line of defense against ROS, because of their ability to scavenge the $O_2^{\bullet -}$, which is the primary radical responsible for the downstream generation of more toxic ROS. They promote the elimination of superoxide anion radicals derived from both extracellular stimuli, such as ionizing radiation and oxidative insults, and intracellular sources, such as mitochondrial ETC (Miao & St Clair, 2009).

In mammals, three different isoforms have been identified and characterized. Even though, they exert a similar functions, these enzymes differ in chromosome localization, protein structure, metal cofactor requirement and cellular compartmentalization (Miao & St Clair, 2009).

In humans, SOD1 is encoded by a nuclear gene located on chromosome 21q22 (Levanon et al, 1985). This protein is an ubiquitous copper (Cu), zinc (Zn) protein, that resides mainly at cytosolic level, although it has been found also in the nucleus (Gertz et al, 2012), peroxisomes (Islinger et al, 2009) and mitochondrial intermembrane space (Kawamata & Manfredi, 2010). The functional unit of SOD1 is a homodimer, composed of two relatively small subunits of 154 amino acids that folds into a β-barrel formed by 8 antiparallel β-strands arranged in a Greek-key motif (Fig1.10). The copper ion directly participates in the catalytic reaction; while zinc has a structural role for the active site folding but is not necessary for enzymatic activity (Kawamata & Manfredi, 2010). In addition, the protein presents a highly conserved intramolecular disulfide bridge required for the stabilization of matured SOD1 (Furukawa et al, 2004). Therefore, SOD1 maturation into the functional enzyme requires three posttranslational modifications: copper and zinc insertion, disulfide bond formation, and dimerization, all of which contribute significantly to

SOD1 stability. Copper insertion and oxygen-dependent disulfide bridge formation are facilitated by the copper chaperone for SOD1 (CCS) (Furukawa et al, 2004).

The relevance of this enzyme in the antioxidant defense is supported by the discovery that more than one hundred mutations in the *SOD1* gene are causative for familial forms of amyotrophic lateral sclerosis, a neurodegenerative disease (Saccon et al, 2013).

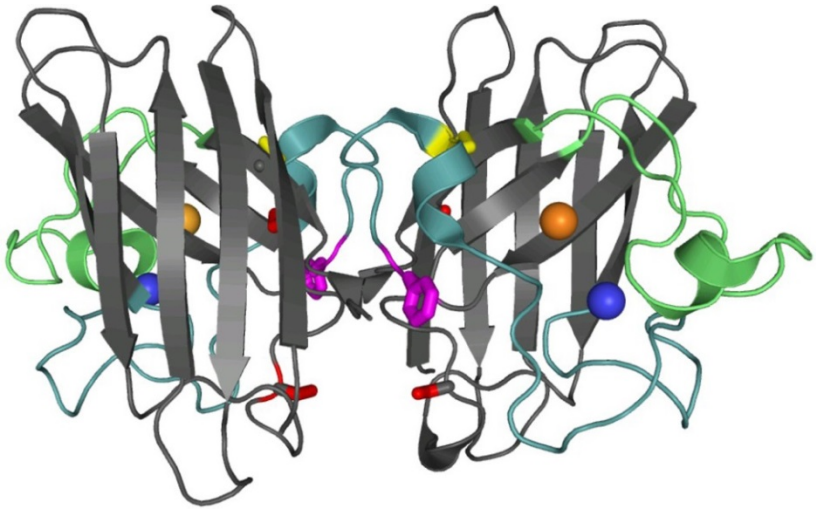

Fig.1.10. Crystal structure and topology of SOD1. SOD1 is a dimeric β-sandwich protein consisting of eight anti-parallel β-strands.. Each monomeric subunit also contains a Zn (blue sphere) and Cu ion (orange sphere), as well as an intramolecular disulfide bond (yellow). The electrostatic loop is depicted in green, while the Zn-binding loop is depicted in cyan (Kayatekin et al, 2012).

The human SOD2 is encoded by a gene located on chromosome 6q25 (Church et al, 1992). This protein, which contains manganese (Mn) in its active site, is synthesized in the cytosol, and imported into the mitochondrial matrix (Wispe et al, 1989). Human Mn-SOD is assembled into a homotetramer of 22-kDa subunits forming a dimer of dimers that creates two symmetrical four-helix bundles (Borgstahl et al, 1992) (Fig.1.11A). The manganese is bound as a five-coordinate complex with a trigonal bipyramidal geometry. Four ligands are provided by the protein, three histidines and one aspartic acid residue, and the fifth ligand by the solvent (Fig.1.11B). The bound solvent ligand is an hydroxide anion for the oxidized

enzyme and it is considered the acceptor for proton transfer upon manganese reduction (Abreu & Cabelli, 2010). The active-site cavity of SOD2 is characterized by a hydrogen bonded network extending from the aqueous ligand of the metal and comprising the side chains of several residues (Perry et al, 2009).

Because of its localization, this mitochondrial protein acts directly against superoxide radicals produced as a byproduct of OXPHOS. A clear evidence of its central role has been identified through the observation that mice lacking SOD2 were characterized by a severe phenotype with a dilated cardiomyopathy and neonatal lethality (Li et al, 1995). In addition, mutant mice presented a consistent reduction in mitochondrial enzyme activities confirming that Mn-SOD is required for normal biological functions, by maintaining the integrity of mitochondrial proteins or complexes susceptible to direct inactivation by superoxide.

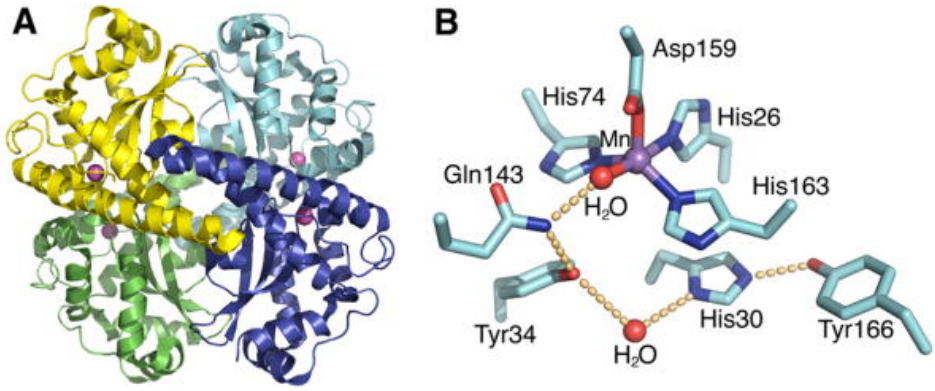

Fig.1.11 Human MnSOD crystal structure. (A) The homotetrameric of structure MnSOD, containing two symmetrical four-helix bundles and four C-terminal α/β domains, is depicted with the four different polypeptide chains, cyan, blue, green and yellow, and active site manganese ions depicted as magenta spheres. **(B)** The MnSOD active site with a hydrogen-bonding scheme. The side chains of the residues involved in the active site, namely, His26, His74, His163, and Asp159, bind the Mn ion, in conjunction with a solvent molecule (Perry et al, 2010).

The human extracellular isoform, SOD3, is encoded by a gene located on chromosome 4p15 (Stern et al, 2003). This enzyme is a homotetrameric Cu- and Zn-containing glycoprotein, with a C-terminal extracellular matrix (ECM)-binding region that binds heparin, other sulphated proteoglycans and collagen (Petersen et al, 2005). The crystal structure revealed that a protein is a tetramer composed of dimers that are similar to the human SOD1 dimers (Antonyuk et al, 2009) (Fig.1.12). While SOD1 and SOD2 are expressed ubiquitously, SOD3 is synthesized in a more limited number of cell types and tissues (Marklund, 1990). The highest levels of this protein have been found in blood vessels, lung, kidney, and uterus, while lower concentrations were present in the eye, skeletal muscle, liver, and brain (Fattman et al, 2003). The physiological function is to prevent cell and tissue damage initiated by extracellularly produced ROS. In addition, EC-SOD is likely to play an important role in mediating nitric oxide-induced signaling events (Fattman et al, 2003).

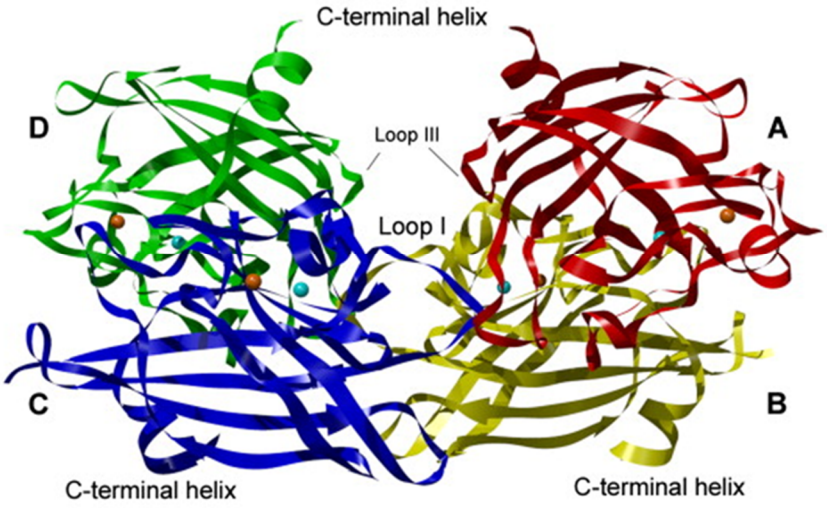

Fig.1.12 Human tetrameric SOD3. The structure shows the four subunits (A, B, C and D) with different colors, the C-terminus, the Cu in cyan and Zn in orange. (Antonyuk et al, 2009).

1.4.3 SOD mimetic compound

Considering the role of oxidative stress in the pathogenesis of PD and the growing knowledge about the protective role that the antioxidant systems plays, many efforts have been directed to develop an efficient antioxidant approach to counteract the oxidative stress-induced neuronal cell death (Navarro-Yepes et al, 2014).

Many endogenous non-enzymatic antioxidant, such as vitamin E, vitamin C, coenzyme Q, have been considered excellent candidate for clinical treatment. In fact, they are cheap, orally bioavailable, safe in large doses, and absorbed and recycled within our bodies (Halliwell et al, 1992). Therefore, the enhancement of antioxidant defenses through dietary supplementation using these compounds should have provided a more reasonable and practical approach to reduce the level of oxidative stress (Finkel & Holbrook, 2000). However, these strategies have been largely unsuccessful. Indeed, a great number of thorough clinical trials have been carried out using several different antioxidants on a wide range of pathologies with little improvement in clinical outcome for the patients [see (Bjelakovic et al, 2012)]. Many other factors and limitations have been proposed to explain the lack of effectiveness of these clinical interventions. For instance, the intrinsic characteristics of the antioxidant studied such as absorption, metabolism, ability to penetrate the BBB and distribution (Navarro-Yepes et al, 2014) as well as the scarce specificity these molecule that could interfere with ROS-dependent cellular signaling (Murphy, 2014). Recently, it has been proposed that a new approach should be based on molecules that react directly with a particular reactive species which contributes to the disease by a specific mechanism, crucial in the pathological process (Murphy, 2014). Since superoxide has been suggested as a critical pathological ROS, because all the very reactive species originate from it. Thus, antioxidants that selectively scavenge superoxide should be therapeutically useful. In agreement with these observations, several preclinical studies supported the potential beneficial effect of SODs in a broad range of disease, including PD. For instance, overexpression of SOD1 in mice has been associated with protection against MPTP toxicity (Przedborski et al, 1992).

In contrast, mice partially deficient for SOD2 showed an increased vulnerability to the same mitochondrial toxin (Andreassen et al, 2001).

The first attempt to use SOD enzymes as drug was achieved through the production of Orgotein, a Cu,Zn- SOD, prepared from bovine tissues, which showed a potent anti-inflammatory activity (Rosner et al, 1980). However, in clinical trials the use of this native enzyme revealed a significant immunogenicity due to the non-human origin of this protein (Muscoli et al, 2003). In addition, because of their large size, these proteins cannot penetrate the BBB, which is a primary requirement of a potential therapeutic agent for PD. In this scenario, the development of synthetic, low molecular weight mimetics of the native enzymes, known as SOD mimetics, could be particularly relevant.

Currently, SOD mimetics can be classified in four different classes: manganese (III) metalloporphyrins (Fig.1.13A), manganese (II)-base complexes (Fig.1.13B), manganese (III) salen complexes (Fig.1.13C) and nitroxides (Fig.1.13D).

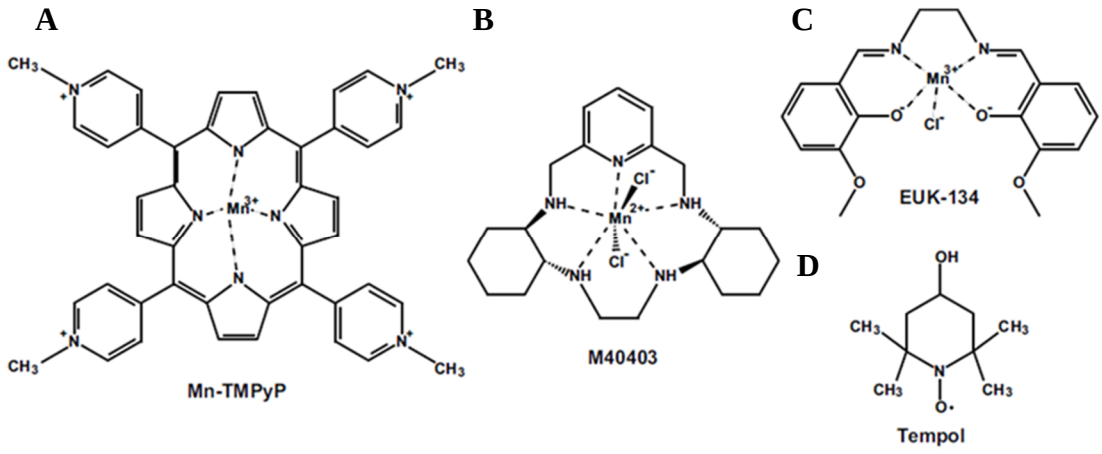

Fig.1.13 Structure of different classes of SOD mimetics. (A) manganese (III) metalloporphyrins (Mn-TMPyP); **(B)** manganese (II)-base complexes (M40403), **(C)** manganese (III) salen complexes (EUK-134) and **(D)** nitroxides (Tempol).

Mn(III) metalloporphyrins have at least four distinct antioxidant properties, acting as scavenger of superoxide (Batinic-Haberle et al, 1998), hydrogen peroxide

(Day et al, 1997), peroxynitrite (Pfeiffer et al, 1998) and lipid-peroxyl (Day et al, 1999). As the native enzyme, the manganese moiety is responsible for superoxide dismutation through the conversion of Mn(III) in Mn(II). The catalase activity could be associated to their ability to also undergo oxidation to Mn(IV) or Mn(V) or Mn(VI) (Salvemini et al, 2002).

Mn(III)–salen complexes have been reported to possess combined superoxide dismutase/catalase mimetic activity (Doctrow et al, 1997). It has been demonstrated that Mn(III)–salen complexes were able to rescue the phenotype of Mn-SOD deficient mice suggesting that these compounds might be also able to enter the mitochondria (Melov et al, 2001). However, the mechanism used by these molecules to detoxify superoxide and hydrogen peroxide is not well defined.

Nitroxides are cell-permeable weak SOD mimetics that react with superoxide very slowly at physiological pH. Actually, their chemistry is based on the nitroxide cycle between the oxidized oxoammonium cation (RNO^+) and the reduced hydroxylamine (RNOH) (Batinic-Haberle et al, 2010). Moreover, nitroxide, (RNO) can be oxidized to RNO^+ with peroxinitrite, which, in turn, rapidly reacts with superoxide regenerating RNO. Thus, the catalytic removal of superoxide may be coupled to the reaction with peroxynitrite (Miriyala et al, 2012).

Overall, the aforementioned classes of compound are SOD mimetics not selective for the superoxide anion. Several studies have been carried out testing their protective effects *in vitro* and *in vivo* [see (Batinic-Haberle et al, 2010; Miriyala et al, 2012; Salvemini et al, 2002)]. Because manganese (II)-base complexes, in particular M40403, are the subject of study in this thesis, they will be discussed in more details.

Manganese (II)-base complexes were discovered and developed using a combination of computer-aided modelling studies (Miriyala et al, 2012) that allowed to generate this new class of agents presenting high SOD activity, high stability, selectivity only for superoxide and *in vivo* efficacy. One of the main property is their catalytic behavior since they remove superoxide anions at a high rate without that the complex itself is consumed (Muscoli et al, 2003). In addition, these SOD mimetics

are highly selective catalysts for superoxide dismutation and they do not react with other biological species.

The unique selectivity of these molecules resides in the nature of the Mn(II) centre of the complex. Actually, the resting oxidation state of the complex is the reduced Mn(II) ion, thus the complex does not react with reducing agents until it is oxidized to Mn(III) by protonated superoxide. Then, the complex is rapidly reduced back to the Mn(II) state by the superoxide anion (Salvemini et al, 2002).

So far, several works reported that M40403 suppresses oxidative stress and inflammation in a variety of *in vitro* and *in vivo* models (Di Napoli & Papa, 2005), for istance in rat model of septic shock (Macarthur et al, 2000), LPS-induced cytokine production by cultured rat alveolar macrophages (Ndengele et al, 2005), inflammatory pain in a carrageenan model of paw edema (Wang et al, 2004), myocardial ischemia–reperfusion injury (Masini et al, 2002), chronic hypoxia-induced pulmonary hypertension (Dennis et al, 2009). Interestingly, the *in vivo* distribution of M40403 supports that it might cross the BBB. Indeed, after 6 hours of injection in rats, the drug was found widely distributed in the body mass, including the brain (Salvemini et al, 1999). Furthermore, results of phase I and phase II clinical trials, performed on approximately 700 subjects/patients using an intravenous formulation of M40403, indicate that it is safe and well-tolerated in humans (Murphy et al, 2008).

To summarize, manganese (II)-base complexes, specially M40403, are small molecules, non-immunogenic and can penetrate cells. They are stable *in vivo* and selective for superoxide. M40403 is also protective in various models of acute and chronic inflammation and seems to be able to cross the BBB. Thus, this SOD mimetic might be an excellent candidate as therapeutic agent to counteract oxidative stress in PD.

1.5 *In vitro* and *in vivo* models for PD studies

To better understand the etiology, pathogenesis and molecular mechanisms underlying DAergic degeneration in PD, several *in vitro* and *in vivo* models have been developed. Cellular models can only provide information on the molecular pathways that are dysfunctional in a disease-mimicking situation (i.e., gene mutations, oxidative stress, neurotoxins exposure, etc.). Nevertheless, they can be particular helpful presenting some interesting advantages. Indeed, they can be human genome-based and easily genetically manipulated, which makes them good candidates not only for exploratory studies on the pathway involved in the disease but also to test the efficacy of disease modifiers. Within the last few years, many efforts have been produced to develop an efficient protocols to differentiate patient-derived fibroblasts or iPS into induced DAergic neurons, that could represent the best *in vitro* model, obtaining a limited success (Auburger et al, 2012). Meanwhile, rodent primary neuronal cultures derived from embryonic central nervous system tissue which retain morphological, neurochemical, and electrophysiological properties of neurons *in situ* (Radio & Mundy, 2008) were largely used as cellular model. However, they present some limitations. Long-term culturing of primary neurons remains the principal disadvantage with cells that cannot be longer propagated. Thus, new cultures must be prepared from nervous system tissue on a regular basis, increasing the genetic variability of the model system across different cultures (Radio & Mundy, 2008). Moreover, the use of rodent cells faces the additional problem of slight but relevant metabolic differences between rodents and humans (Herman, 2002). Alternatively, neuroblastoma cell lines have been also used as *in vitro* models to study neuronal development, neurological disorders, mechanisms of actions and neurotoxicity of compounds affecting the nervous system.

Animal models, both genetic and toxin-based, not only provided invaluable information but also recapitulate many of the phenotypic features of PD allowing to test innovative therapeutic approaches (Le et al, 2014). Model organisms range from yeast, worm, fruit fly, zebrafish, mouse and rat. Even though mammalian models are widely considered as the most powerful approach, their use is costly and time consuming. Furthermore, research using mammalian models is slowed down by the

complexity of the organisms and their genomes, by the long latency of the symptoms and by the difficulty to generate and analyze large cohorts, providing a need for even simpler systems (Debattisti & Scorrano, 2013). In this scenario, the use of non-mammalian models becomes relevant. In particular, *Drosophila melanogaster* is currently considered an attractive and valuable system for studying human neurodegeneration. In the next sections, the main features and properties of human neuroblastoma cell lines and *Drosophila melanogaster* will be presented more in details because of their use as models in this thesis.

1.5.1 *Drosophila melanogaster* as animal model for neurodegeneration

Fruit fly is cheap and easy to handle, it can give rise to a large number of genetically identical progeny and it has a short life span 20522007. In addition, the completion and annotation of genome sequence of *Drosophila* revealed that 77% of genes related to human diseases are conserved in flies 11084932. For instance, the fly genome encodes homologs of *DJ-1*, *PINK1*, *Parkin*, *LRRK2*, human genes linked to familial forms of PD (Hirth, 2010). Furthermore, *Drosophila* shows complex cognitive processes, including learning and memory, and motor behaviors, such as walking, climbing, and flying, which are driven by a sophisticated brain and nervous system. This system consists of about 10^5 neurons, including approximately 200 DAergic cells that are grouped together into six major clusters arranged with bilateral symmetry and a well-defined anatomical location (Whitworth et al, 2006). Genetic perturbations or neurotoxic treatments affecting the number, morphology, or locations of these neurons can be readily recognized.

Several different approaches have been used to model aspects of PD in *Drosophila*, including pharmacological insults (neurotoxin-induced models), the generation of mutant flies as well as the overexpression or *knock down* of familial PD gene homologs (White et al, 2010). The latter strategy is mainly based on the use of GAL4/UAS system which is one the most powerful and versatile tools available in *Drosophila*.

1.6 Aim of the project

The research project of this thesis can be divided in two main topics: the first one is aimed to explore of the potential protective role of SODs and SOD mimetics against oxidative injuries related to Parkinson's disease (PD); the second one relies on the characterization of two human neuroblastoma cell lines in order to identify between them the most suitable cellular model for PD studies.

PD is a degenerative disorder characterized by a progressive loss of DAergic neurons. This motor disease is still incurable and the conventional therapies only treats symptoms. Therefore, it is necessary to develop new therapeutic strategies than not only provide symptomatic relief but also can halt or retard the progression of the disease avoiding further neuronal damage. Increasing evidence demonstrated that oxidative stress is a key player in the etiopathogenesis of both sporadic and familial forms of PD. In this scenario, the function of antioxidant SODs enzymes could be crucial to burden oxidative stress delaying or arresting DAergic degeneration. To test this hypothesis, we investigated, *in vitro* and *in vivo*, whether SODs overexpression or the administration of SOD mimetics ameliorate oxidative injuries induced by the herbicide PQ and/or PINK1 deficiency, used as experimental paradigms related, respectively, to sporadic and familial forms of PD.

In parallel, considering that the DAergic phenotype is an important requirement to study, *in vitro,* the molecular mechanisms involved in PD pathogenesis, we characterized two human neuroblastoma cell lines upon neuronal differentiation. In particular, to develop a reliable model of DAergic neurons, we analyzed the effects of three differentiating agents in their capability to promote the acquisition of a mature neuronal-like phenotype with neurochemical properties of DAergic cells.

Chapter 2

Materials and Methods

2.1 Cell culture -*in vitro* experiments

2.1.1 Reagent stocks

PQ (Sigma): 100 mM in distilled sterile water

SOD mimetics:

- Mn-III-TMPyP (S. Cruz Biotechnology): 4 mM in phosphate buffer (PBS)
- M40403 (synthesized by collaborators from the University of Pavia), 41 mM (20 g/L) in distilled sterile water
- EUK-134 (S. Cruz Biotechnology): 0.5 mM in ethanol for cinetic assays; 100 mM in DMSO for cell viability assessment
- Tempol (Sigma): 1 M in distilled sterile water

CCCP (Sigma): 10 mM in DMSO

Lipofectamine 2000 (Invitrogen)

Fetal bovine serum (FBS-Gibco): heat inactivated at 56°C for 30-60 minutes

Staurosporine (Stauro, Sigma): 40 μM in ethanol

RA (Sigma): 10 mM in DMSO, stored at -°20°C as mono-use aliquots

TPA (Sigma): 40 μM in ethanol

2.1.2 Cell lines

All the cell lines used were maintained in the proper growth medium in a 5% CO_2 humidified incubator at 37°C. The medium was replaced every 3 days and once 80% of confluence was reached, cell cultures were sub-cloned by trypsinization.

Human neuroblastoma SH-SY5Y (IST, Genova, Italy) cells were cultured in a mixture 1:1 of Ham's F12 (F12) and Dulbecco Modified Eagle Medium (DMEM) supplemented with 10% (v/v) FBS.

Human neuroblastoma BE(2)–M17 (ATCC) cells were cultured in in a mixture 1:1 of F12 and DMEM supplemented with 10% FBS.

Human cervical carcinoma HeLa (ECACC) cells were grown in DMEM with 10% FBS.

2.1.3 Neuronal differentiation

Human neuroblastoma cell lines (SH-SY5Y and BE(2)-M17) were chosen because they are widely used as model of DAergic cells. In all of the experiments, the cells were used at early passages (P1-5 after purchase). For cell proliferation analysis, the cells were seeded into 25 cm^2 flasks at a density of 1×10^5 cells. 24 hours after seeding, differentiation was induced by the addition of TPA, RA or staurosporine (STAU) at 15 μM, 10 μM or 10 nM, respectively, for SH-SY5Y and 30 μM, 5 μM or 8 nM, respectively, for BE(2)-M17. Fresh media containing the specific inducing agent were replaced every 2 days. To determine the rate of cell growth, the cells were harvested after 0.05% trypsin treatment and quantified using a hemocytometer. Differences in morphology between proliferative and differentiated cells were evaluated under a phase contrast light microscope (Motic AE2000).

2.1.4 Neuritic outgrowth

To measure the neuritic outgrowth after differentiation, human neuroblastoma cell lines (SH-SY5Y and BE(2)-M17) were seeded on coverslip pre-coated with poly-D-lysine in 24 wells plates. 24 hours after seeding, they were transfected with a vector containing the coding sequence for a GFP, whose expression allow to track the neurite length per single at single cell-level using fluorescence microscopy. The day after transfection, differentiation was induced as described above. After 7 day of treatment, sample were fixed and analyzed. Images were acquired using Leica 5000 B epifluorescence microscope with a magnification of 20X. Neurite length was assessed using ImageJ software.

2.1.5 SOD1 and SOD2 SH-5YSY stable overexpressing cells

To overexpress human SOD1 and SOD2, first full length sequences were amplificated using *Pfu polymerase* (Promega). The forward and reverse primers (Tab.2.1) for amplification contained a *Kozac* sequence, which is recognized by the ribosome as the translational start site (Kozak, 1986), and stop codon. Considering the mitochondrial subcellular localization of SOD2, the mitochondrial translocation sequence was cloned at the N-terminus of the protein. The amplified sequences (SOD1 and SOD2) were separated by agorose gel elettrophoresis, recovered from PCR using PCR Clean-up System (Promega) and cloned into pCR8/GW/TOPO (Invitrogen) (Fig.2.1A).

Gene	**Primer sequence (5'-3')**
Human-SOD1	Fw: ACCATGGCGACGAAGGCCGTGTGCG Rv: TTATTGGGCGATCCCAATTACACC
Human-SOD2	Fw-ACCATGTTGAGCCGGGCAGTGTG Rv-TTACTTTTTGCAAGCCATGTATCTTTC

Tab.2.1. List of primers used for SOD1 and SOD2 amplification.

Each plasmid (entry vector) was used to transform DH5α high competent *E. coli* cells. Bacterial colonies selected using SPECTINOMYCIN antibiotic were used to purify each vector using QIAprep Spin Miniprep Kit (Qiagen). After DNA sequencing, SOD1 or SOD2 fragment which was present into entry vector ,was inserted into the pT-REX-DEST30 final vector (Invitrogen) (Fig.2.4B) for protein expression in mammalian cells using the Gateway technology. Plasmid DNA was then replicated and isolated using NucleoBond® Xtra Midi EF maxi-prep (MACHEREY-NAGEL)

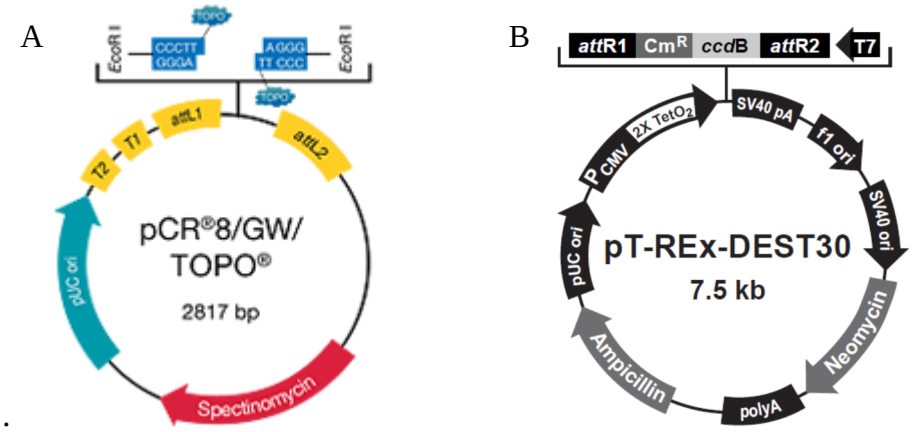

Fig.2.1. Vectors used for human SOD1 and SOD2 overexpression. (A) pCR8/GW/TOPO used as entry vector **(B)** pT-REx-DEST30 used as final vector which contained the Neomycin cassette necessary for selection using G418.

To generate stable cell lines, SH-SY5Y wild-type cells were plated in 6 well plates at 70% of confluence and transfected with 2 µg of final vector using Lipofectomine. To maximize the transfection efficiency DNA:Lipofectamine ratio was kept at 1:4. After 48 hours, 500 µg/ml geneticin (G418, Sigma) was added to the culture for selection. Stably transfected cells were isolated after two weeks in the selection medium. Each isolated clone was expanded and stored at -80°C.

2.1.6 Qualitative assessment of mitochondrial morphology

Assessment of mitochondrial morphology was performed using a mitochondrial fluorescent protein, mt-RFP. The expression vector containing the coding sequence for the mt-RFP was a kind gift from Luca Scorrano (University of Padova, Padova, Italy). Qualitative analysis was done for each cell according to the follow classification. Cells containing a majority of long interconnected mitochondrial networks presented a tubular shape; cells containing a combination of interconnected mitochondrial networks along with some smaller fragmented mitochondria were classified as intermediate; finally cells with a majority of short and multiple punctiform organelle were defined as fragmented.

To this purpose, SH-SY5Y cells were plated on poly-lysine coated coverslips in 24 well plates (10^5 cells per well). After 24 hours, samples were transfected with

0.25 or 0.5 μg of the expression vector containing the coding sequence for the mt-RFP. Lipofectomine were used as transfection agent with the aforementioned DNA:Lipofectamine ratio. After fixation, low resolution images were acquired using epifluorescence using a Leica 5000B with 100X oil objective; while, higher resolution images were acquired through ZEISS LSM700 confocal microscope with 63X oil objective. The data analysis was performed in a blind manner and reported as % of cells with tubular, intermediate or fragmented morphology relative to total cell number.

2.1.7 *PINK1 knock-out* using CRISPR/CAS system

PINK1 gene *knock-out* (KO) has been obtained though *GeneArt® CRISPR Nuclease Vector with CD4 Enrichment Kit* (Lifetchnologies) according to the manufacturer's protocol. This system allowed the expression of the functional components needed for CRISPR/Cas9 genome editing in mammalian cells with the CD4 gene reporter. The latter was used to track transfected cells using anti-CD4 fluorescent antibodies. The CRISPR/CAS system includes three components the *Clustered Regularly Interspaced Short Palindromic Repeats* (CRISPR) associated (Cas) nuclease, Cas9; a target complementary CRISPR RNA (crRNA) and an auxiliary trans-activating crRNA (tracrRNA). In this kit, the crRNA and tracrRNA are expressed together as a guide RNA (gRNA) combining the targeting specificity of the crRNA with the scaffolding/binding ability for Cas9 nuclease of the tracrRNA. Once the gRNA and the Cas9 are expressed in the cell, the genomic target sequence can be permanently disrupted (Fig.2.3). To this purpose, first it was necessary to designed two single-stranded DNA oligonucleotides with suitable overhangs to complement the linearized vector; one encoding the target CRISPR RNA (top) and its complement (bottom). In the procedure, this step is crucial because these oligonucleotides must contain the sequence for the target gene, in this case *PINK1*, required to induce the double break DNA. The optimized length should be 19 or 20 bp. To avoid off-target effects, the sequence should not contain significant homology to other genes. According to these instructions, two pairs of oligonucleotides, namely KO1 and KO2, has been designed (Tab.2.2). Their specificity of the target gene was verified using RGEN tools software (http://www.rgenome.net/cas-offinder/).

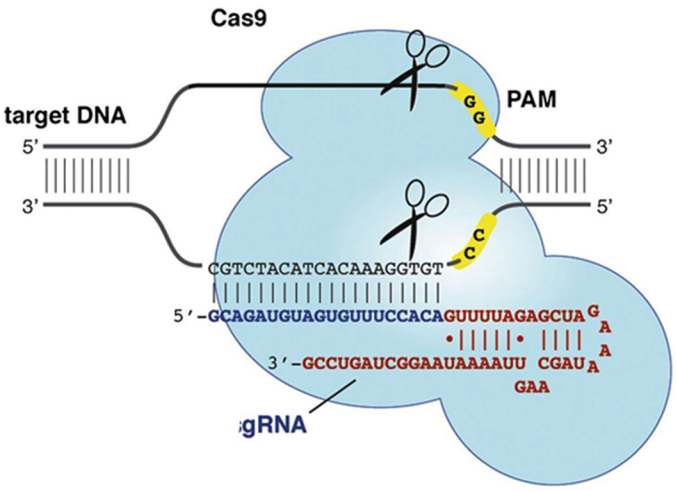

Fig.2.2. CRISPR/CAS mechanism for genome editing. Cas9 assembles with hybrid guide RNAs in human cells and can induce the formation of double-strand DNA breaks (DSBs) at a site complementary to the guide RNA sequence in genomic DNA (Jinek et al, 2013)

Oligonuclotide	**Sequence (5'-3')**
KO1	5'- CGTAATTCACATTGGAGCAGGTTTT-3' top
	5'- CTGCTCCAATGTGAATTACGCGGTG-3' bottom
KO2	5'-CCGCTTCTTCCGCCAGTCGGGTTTT-3' top
	5'-CCGACTGGCGGAAGAAGCGGCGGTG-3' bottom

Tab.2.2. Oligonucleotide sequences, KO1 and KO2, used for *PINK1 knock out* in human cells.

Each pair of oligonucleotide was annealed first incubating samples at 95 °C for 4 minutes in a heat block and then allowing the reaction mixture to cool to 25°C for 5–10 minutes. After annealing, two 100-fold serial dilutions of the double strand (ds) oligonucleotide stock (50 µM) were performed to prepare the final 5 nM ds oligonucleotide working solution. Afterwards, the ligation reaction was set up with the linearized CRISPR Nuclease vector, the oligonucleotide working solution and T4 DNA Ligase. The reaction took place at RT with an incubation of 90 minutes. Once the ligation was completed, DH5α competent E. coli were transformed with the resulting CRISPR nuclease construct. For bacterial transformation, 5 µL of the

ligation reaction (1/4 of the total reaction) were added into a vial of competent cells and mix gently tapping the tube. The vials was maintained on ice for 30 minutes. For heat-shock procedure, cells were incubated for 90 seconds at 42°C and transferred to ice. In each vial, 900 µl SOC medium were added at RT and the culture was incubated for 45 minutes at 37°C. At the end of this incubation, 100 µl of the transformation reaction were spread on a pre-warmed LB agar plate containing 100 µg/mL ampicillin. The plates were incubated overnight at 37°C. For KO1 and KO2 sequences, 3 to 5 ampicillin-resistant colonies were picked and grown overnight in 5 ml LB medium, containing 100 µg/mL ampicillin, at 37°C. Bacteria were then pelleted and plasmidic DNA purification was performed using QIAprep Spin Kit (Qiagen) for mini-prep, following the manufacturer's instructions. Sequencing of the CRISPR nuclease construct was performed using the U6 Forward (supplied with the kit). Once the correct CRISPR nuclease construct was identified, it was used to perform NucleoBond® Xtra Midi EF maxi-prep (MACHEREY-NAGEL). Pure plasmid DNA was transfected in human cells.

LB medium: 0.5% w/v yeast extract, 1% w/v Bacto Triptone, 8.56 mM NaCl, 0.1% NaOH 1N

LB-agar medium: 0.5% w/v yeast extract, 1% w/v Bacto Triptone, 8.56 mM NaCl, 0.1% NaOH 1N, 1.5% w/v agar

SOC medium: 0.5% w/v yeast extract, 2% w/v Bacto Triptone, 8.56 mM NaCl, 2.5 mM KCl, 10 mM MgCl2, 20 mM glucose

To assess the efficiency of *PINK1* gene disruption obtained with each sequence (KO1 and KO2), HeLa cells were used because of their high transfection efficiency (around 80%) that make possible to evaluate *PINK1 knock-out* as reduction of PINK1 protein level. Thus, cells were plated on 6 well plate (10^6 cells per well) and after 24 hours transfected with 2 µg KO1 and KO2 vectors using 8 µl Lipofectomine. The day after transfection, cells were solubilized in lysis buffer and samples were used for western blot analysis. While to evaluate the effect of *PINK1 knock-out* on mitochondrial morphologies, SH-SY5Y cells were seeded on poly-lysine coated coverslips, in 24 well plates (10^5 cells per well) and the day after

seeding were co-transfected with 0.75 μg of KO1 or KO2 vector and with 0.25 μg mt-RFP plasmid using 3 μl of Lipofectomine. The ratio between the two vectors as well as the volume of Lipofectamine was optimized to obtain the best transfection efficiency and the lower cell toxicity. 24 hours after transfection, cells were fixed and stained with Alexa Fluor 488 anti-human CD4 antibody that allowed to label transfected cells. Assessment of mitochondrial morphology was performed as described in the Section 2.1.6

2.1.8 Cell Treatment

2.1.8.1. PQ exposure

In order to evaluate the effect of SODs overexpression or SOD mimetic treatments, SH-5YSY WT and stable cell lines, were exposed to increasing concentration of PQ. All the used doses and the exposure time are reported below:

- For CCK-8 assay: 50-100-250-500 μM of PQ for 24 hours
- For cytofluorimetric analysis: 100-250-500 μM of PQ for 48 hours
- For mitochondrial morphology: 500 μM of PQ for 24 hours
- For ROS production: 500 μM of PQ for 6 and 12 hours.

Because the herbicide presents a great instability losing its activity with freeze-thaw cycles. Stock solutions of 100 mM PQ were prepared and mono-use aliquots were stored at -20°C.

2.1.8.2. SODs mimetics

Considering that the four compounds interfered with the CCK-8 colorimetric assay, their antioxidant activity was tested in rescuing PQ-induced apoptosis through cytofluorimetric measurements. After the determination of the specific activity of SOD mimetics (see Paragraph 2.1.16), the antioxidant properties of each molecule against oxidative injury has been assessed. The concentration of each drug has been established based on their catalytic activity adding in the medium the same number of catalytic units for each molecule. In addition, in a previous work EUK-134 has

been used at 25 μM in the human neuroblastoma SK-N-MC cells showing a protective effect against H_2O_2 (21205220). Therefore, based on these informations, the final concentrations utilized were:

- 150 nM for Mn-TMPyP
- 10 μM for M40403
- 25 μM for EUK-134
- 800 μM for Tempol.

While, for the assessment of mitochondrial morphology protocols described in the Section 2.1.6 and 2.1.8.1 were followed.

2.1.8.3. Carbonyl cyanide m-chlorophenyl hydrazone (CCCP)

In order to evaluate the efficiency of *PINK1* gene disruption with CRISPR/CAS system, the protonophore CCCP (in ethanol, Sigma) was used to induce the mitochondrial depolarization. The dissipation of mitochondrial membrane potential induced through CCCP allow the PINK1 stabilization and accumulation, required to measure the reduction of protein level after gene *knock-out*. Thus, HeLa cells were transfected with PINK1 KO1 and KO2 vectors for 24 hours and were exposed to 10 μM CCCP for 4 hours. Samples were then lysed and used for western blot analysis.

2.1.9 Immunofluorescence

Cells were plated on 15 mm glass coverslips pre-coated with poly-D-lysine in 24 wells plates in 0.5 ml of medium. After treatment, cells were fixed for 30 min at room temperature (RT) with 4% paraformaldehyde (PFA) in phosphate buffered saline (PBS) solution pH 7.4, rinsed three times with PBS, permeabilized with 0.1% Triton X in PBS for 30 min at RT and incubated in blocking solution (5% FBS in PBS) for 30 min. The cells were incubated for 1 hour at RT with primary antibodies (Tab.2.3) diluted in blocking solution.

Primary Antibody	**Host**	**Company**	**Dilution**
Anti-neurofilament	Mouse	Covance	1:1000
Anti-neuronal β-III tubulin	Mouse	Sigma	1:200
Anti- SOD1	Rabbit	Prestige, Sigma	1:500
Anti-SOD2	Rabbit	StressMarq	1:200
Anti-SDHA	Mouse	Santa Cruz	1:200
Alexa Fluor 488 anti-human CD4	Mouse	Biolegend	1.:10

Tab.2.3. List of primary antibodies (host species, company and dilutions) used in immunofluorescence.

After 3 washes in PBS, cells were subsequently incubated with secondary antibody (Tab.2.4) for 1 hour at RT. Nuclei were counterstained using 0.16 µM Hoechst 33258 (Life technologies) for 5 min, and after extensive washing in PBS, the coverslips were mounted with ProLong Gold Antifade (Life Technologies). Low resolution images were acquired using a Leica 5000B epifluorescence microscope, while higher resolution images were acquired through Leica SP5 confocal microscope.

For neuronal differentiation cells were fixed after 4 or 7 days of differentiation. For stable transfected clones, samples were fixed 24 hours after

seeding. For mitochondrial network, cells were fixed after 24 of transfection and 24 of PQ exposure (with or without 10 μM of M40403). For PINK1 gene disruption, samples were fixed 24 hours after transfection. The anti- human CD4 primary antibody used was conjugated with Alexa Fluor 488, therefore the incubation with the secondary antibody was not necessary.

Secondary Antibody	Host	Company	Dilution
Alexa Fluor 488 (green)	Mouse	Life Technologies	1:200
Alexa Fluor 488 (green)	Rabbit	Life Technologies	1:200
Alexa Fluor 568 (red)	Mouse	Life technologies	1.200
Alexa Fluor 568 (red)	Rabbit	Life technologies	1.200

Tab.2.4. List of secondary antibodies (host species, company and dilutions) used in immunofluorescence. 488 and 568 are the two excitation wavelengths used with fluorescence microscopy, which correspond respectively to green and red fluorescence.

2.1.10 mRNA expression levels using quantitative RT-PCR.

Determination of gene expression was performed using semi-quantitative and quantitative real-time PCR (qRT-PCR). Total RNA was extracted from undifferentiated or differentiated cells using TRIzol according to the manufacturer's instructions (Life technologies). Reverse transcription was performed using the ImProm II Reverse Transcription System (Promega) and cDNA was obtained for semi-quantitative or RT-PCR reactions. Semi-quantitative PCR was performed with GoTaq DNA Polymerase (Promega) using the following conditions for amplification: a single denaturation step at 95°C for 5 min followed by 30 cycles of 30 s of denaturation at 95°C, 30 s of annealing at 60°C and 1 min of extension at 72°C. A final extension step at 72°C was applied for 10 min. Amplified DNA was subsequently analyzed by 2.0% agarose gel electrophoresis and the images were acquired by Quantity One software using the Gel Doc XR System (Bio-Rad). For quantitative analysis, qRT- PCR assays were performed in 96-well optical plates with a 7500 real-time PCR system (Applied Biosystems) using the following parameters: 95°C for 10 min, 38 cycles of 20 s at 95°C and 60 s at 60°C, followed by

2 cycles of 15 s at 95°C and 60 s at 60°C. cDNA was amplified using the Power SYBR Green Master Mix (Applied Biosystems) containing 0.2 µM primers. The primer forward (Fw) and reverse (Rv) sequences and expected lengths of the amplified products are listed in Tab.2.5.

Gene	**Primer sequence (5'-3')**	**Product length (bp)**
GAPDH	Fw: ATGAAGGGGTCATTGATGG	138
	Rv: AAGGTGAAGGTCGGAGTCAA	
RPII	Fw: TTGGTGACGACTTGAACTGC	123
	Rv: CCATCTTGTCCACCACCTCT	
TH	Fw: GCCCTACCAAGACCAGACGTA	89
	Rv: CGTGAGGCATAGCTCCTGA	
AADC	Fw: GAAGCCCTGGAGAGAGACAA	121
	Rv: CCTTGTTGCAGATAGGACCG	
VMAT2	Fw: GAAGAGAGAGGCAACGTCA	149
	Rv: CGTCTTCCCCACAAACTCAT	
DβH	Fw: GCCTTCATCCTCACTGGCTA	109
	Rv: TTCTCCCAGTCAGGTGTGTG	
DAT	Fw: TGCAACAACTCCTGGAACAG	113
	Rv: AAGTACTCGGCAGCAGGTGT	

Tab.2.5. List of primers used for semi-quantitative and real time-PCR.

The expression of individual target genes was calculated using the ΔΔCt-method (26). Sample Ct –values were normalized by Ct –values of the housekeeping genes. *Glyceraldehyde 3-phosphate dehydrogenase* (*GAPDH*) was the reference gene used for *AADC* and *DβH* quantification while *RNA polymerase II (RPII)* was the internal control gene for *TH*, *VMAT2* and *DAT*. These two housekeeping genes

were expressed at the same level as target genes. These results were further normalized using undifferentiated cells.

2.1.11 Western blot analysis

For western blot (WB) analysis, cells were harvested, washed with PBS and solubilized in lysis buffer. Cell lysates were centrifuged at 14000×g for 30 minutes. Total protein content was measured using BCA assay (Thermo Scientific). SDS-PAGE was used to separate protein according their size. Samples were prepared boiling for 10 minutes proteins in presence of Laemmli buffer. Equal amount of proteins were loaded and run on acrylamide gel at 90 V for 90 minutes in running buffer. Once proteins were properly separated, they were blotted onto PVDF membranes (Immobilion, Millipore). The membrane was blocked in TTBS plus 5% nonfat dry milk for 1 hour at RT and then incubated with primary antibody diluted in TTBS (Tab.2.6). The PVDF membranes were washed in TTBS and probed with horseradish peroxidase-conjugated secondary antibody diluted in TTBS (Tab.2.6). After TTBS washing, the PVDF membrane was covered with enhanced chemiluminescence advance (ECL, GE Healthcare) and then exposed to an ECL Hyperfilm (GE Healthcare) for a period sufficient to detect the bands. The film was developed and fixed. Densitometry was carried out using ImageJ Software using an housekeeping protein, such as tubulin or glyceraldehyde 3-phosphate dehydrogenase (GAPDH), as loading control.

Lysis buffer: 20 mM Tris-HCl pH 7.5, 150 mM NaCl, 1 mM EDTA, 0.5% Tween 20 or 1% Triton X-100, 2.5 mM sodium pyrophosphate, 1 mM beta-glycerophosphate, 1 mM $NaVO_4$ and protease inhibitor cocktail (Sigma)

Laemmli loading buffer 4X: Tris-HCl 50 mM pH 6.8, SDS 2%, DTT 100 mM, bromophenol blue 0.1%, glycerol 10%

Acrylamide gel:

Stacking gel (4%): acrylamide solution 4%, Tris-HCl 0.125 mM pH6.8, SDS 0.1%, APS 0.1%, TEMED 0.1% (acrylamide solution is constituted by acrylamide: bis acrylamide ratio equal to 29:1)

Resolving gel (13%): acrylamide solution 13%, Tris-HCl 0.375 mM pH 8.8, SDS 0.1%, APS 0.1%, TEMED 0.008%

Transfer buffer: 25 mM Tris-HCl, 192 mM glycine, 10% v/v methanol

TTBS buffer: 50 mM Tris-HCl, 150 mM NaCl, 0.1% v/v Tween

Running buffer: Tris-HCl 25 mM, glycine192 mM, SDS 0.1%, pH 8.3

Primary Antibody	**Host**	**Company**	**Dilution**	**Incubation**
Anti-SOD1	rabbit	Prestige, Sigma	1:10000	1 hour at RT
Anti-SOD2	rabbit	Prestige, Sigma	1:10000	1 hour RT
Anti-PINK1	rabbit	Novus	1.1000	overnight at 4°C
Anti- tubulin	mouse	Sigma	1:5000	1 hour at RT
Anti-GAPDH	mouse	Sigma	1:2000	1 hour at RT
Secondary Antibody	**Host**	**Company**	**Dilution**	**Incubation**
Anti-rabbit	goat	Sigma	1:16000	1 hour at RT
Anti-mouse	goat	Sigma	1:2000	1 hour RT

Tab.2.6. List of primary and secondary antibodies (host species, company and dilution and incubation) used in western blot analysis.

2.1.12 Cell viability assay

Cell viability was measured by colorimetric assay using Cell Counting Kit-8 (CCK-8, Sigma) according to manufacturer's instruction. CCK-8 is a sensitive colorimetric assay based on the use of 2-2-methoxy-4-nitrophenyl-3-4-nitrophenyl-5-2,4-disulfophenyl-2H-tetrazolium (WST-8), which in presence of an electron carrier, 1-Methoxy PMS, is reduced by cellular dehydrogenase to give a yellow-orange formazan dye (Fig.2.3). The latter is an highly dye soluble in the tissue culture media and its amount, generated by the activities of those enzymes in cells, is directly proportional to the number of living cells. Among the different colorimetric kit,

CCK-8 was selected because of its higher detection sensitivity compared to other tetrazolium salts such as MTT, XTT, MTS or WST-1.

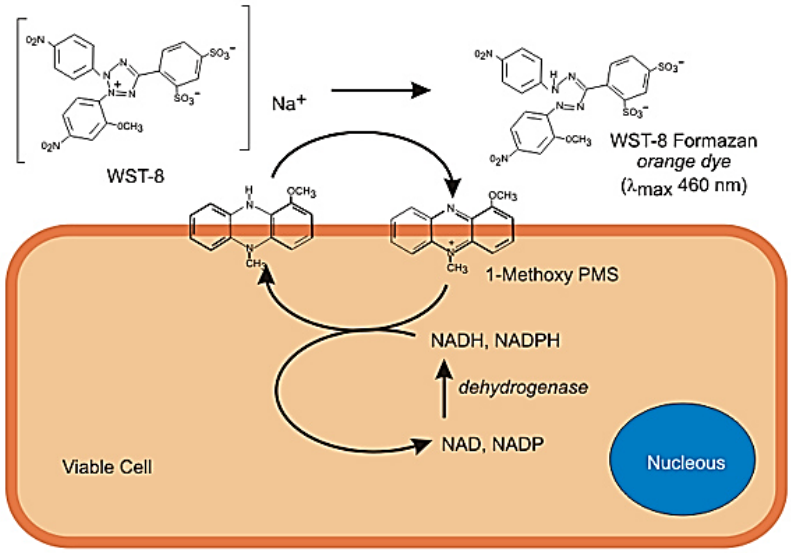

Fig.2.3. CCK-8 assay mechanism. The colorimetric assay is based on the WST-8 tetrazolium salt that in presence of a specific electron carrier, 1-Methoxy PMS, can be reduced in WST-8 formazan dye by the activity of the intracellular dehydrogenases. The formazan salt is an orange highly soluble salt and its formation, related measuring the absorbance at 460 nm, is directly proportional to the number of living cells.

Cell viability of SH-SY5Y WT and transgenic cells was assessed after PQ treatment. Thus, cells were plated on each well of 96-well plates (10^4 cell per well) in phenol red free media. One day after seeding, cells were treated with the herbicide (see Paragraph 2.1.8.1). Then, 10 µl of CCK-8 solution were added to each well and incubated for 4 or 6 hours at 37°C. The absorbance was measured at 460 nm using a plate reader (Victor ^{TM} X3, Perkin Elmer). Each condition was performed in 8 technical replicates for experiment. Cell viability was expressed as % compared to untreated cells (100% of viability). Data were presented as mean ± SEM of at least 3 independent experiments.

2.1.13 Cytofluorimetric analysis for apoptosis detection

In literature, it widely reported that PQ triggers cell death through apoptosis. To detected apoptotic cell death, *Annexin V/PI double staining kit* (BD Pharmigen^{TM}) has been used in cytofluorimetric analyses. Several morphological changes take place during apoptosis. For instance, one of the early events that happens in the apoptotic pathway is the loss of plasma membrane asymmetry. In particular, in apoptotic cells the membrane phospholipid phosphatidylserine (PS) is translocated from the inner to the outer leaflet of the plasma membrane. While, a late event of the programmed-cell death is the loss of membrane integrity and permeability. Therefore, the annexin V/ PI protocol is a commonly used approach for studying these two events. This technique allows to discriminate between apoptotic, necrotic and viable cells using two fluorescent probes. Propidium iodide (PI) is a red-fluorescent nuclear and chromosome counterstain. Since it is not permeant to live cells, it is used to detect necrotic or late apoptotic cells, characterized by the loss of the integrity of the plasma and nuclear membranes. In this case, PI can pass through the membranes, intercalate into nucleic acids, and display its fluorescence. Annexin V is a 35-36 kDa Ca2+ dependent phospholipid-binding protein that has a high affinity for PS, and binds to cells with exposed PS. Annexin V labeled with a fluorescent tag, such as FITC, can be used with flow cytometry to measure this event.

These fluorescent dyes were used to assess PQ-induced apoptosis. Thus, WT and SOD1 and SOD2 overexpressing cells were cultured onto 6 well plates and, after 24 hours of attachment period, were treated with PQ for 48 hours. For analysis, cell were detached from supports with papain protease instead of trypsin. This enzyme was selected because its milder negative effect on cell survival, reducing the apoptotic and necrotic events due to cell detachment. Cells were detached by 3 minutes treatment with papain protease (Worthington), centrifuged at 500 x g for 5 min and resuspended in 500 µl of 1X binding buffer. The cell suspension was transferred to a 5-ml round bottom-tube and 1.5 µl of annexin V-FITC (dilution 1:50) and 2 µl of PI (5 µg/ml) were added and incubated for 8 minutes at RT. Samples

were analyzed by FACSCanto II flow cytometry (BD Bioscience) acquiring 10,000 ungated events

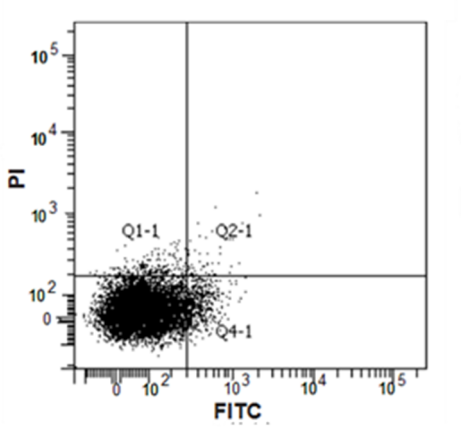

Fig.2.4. Representative dot plot obtained by cytofluorimetric analyses. PI signal was plotted versus Annexin V- FITC. These Plots are cut in four regions corresponding to: viable (PI/FITC -/-; Q3), apoptotic (PI/FITC -/+; Q4), late apoptotic (PI/FITC +/+; Q2) and necrotic (PI/FITC +/-; Q1) cells.

The data generated by flow-cytometry can be plotted in two-dimensional dot plots in which PI is represented versus Annexin V-FICT (Fig.2.4). These Plots are cut in four regions corresponding to:

- viable cells which are negative to both probes (PI/FITC -/-; Q3);
- apoptotic cells which are Annexin positive PI negative (PI/FITC -/+; Q4);
- late apoptotic which are Annnexin and PI positive (PI/FITC +/+; Q2);
- necrotic which are Annexin negative PI positive (PI/FITC +/-; Q1).

Cytofluorimetric data were expressed as % of viable cells (PI/FITC -/-; Q3) compared to untreated cells (100% of viability). Data were mean ± SEM of at least 3 independent experiments.

Binding buffer 10X: 0.1 M Hepes/NaOH pH 7.4, 1.4 M NaCl, 25 mM $CaCl_2$).

2.1.14 Cellular redox state measurement through roGFP2

As described in the Introduction, cells have an elaborate mechanism to maintain redox state within each compartment. An excessive oxidation, due to impaired ROS homeostasis, can alter this state impacting on the cell survival. In the current work, in order to measure ROS overproduction, induced by PQ, genetically encoded redox sensor GFP (roGFP2) has been used. Conventional dyes for redox measurement could present a low specificity or could interact with several oxidant within cells promoting an artificial ROS formation. Among the different approaches to measure ROS production, the most promising tools are genetically encoded redox sensors, which present several advantages. For instance, they allow to detect in *real time* redox state in different live cells or animal tissues, without the permeation and pre-incubation of exogenous probes, and to have a ratiometric quantification of this event, that can be accurately assessed regardless of the absolute levels of probe concentration due to expression or photobleaching (Liu et al, 2012). These indicators are GFP mutants (roGFP), with two surface-exposed cysteine placed at the position 147 and 204 on adjacent β-strands close to the chromophore. Formation of the disulfide bridge between these two residues induces the protonation of the chromophore, which impacts on protein fluorescence excitation spectrum (Fig.2.5). In particular, the oxidation of two cysteines increases the fluorescence intensity at 405 nm with concomitant decrease at 488 nm, while reduction reverses the spectrum (Fig.2.6). The ratio between the fluorescence (collected between 500-530 nm) using the 405 and 488 as excitation wavelengths reports the redox state of the cell. Among the different variants, roGFP2 was selected as probe because it exhibits the largest dynamic range, it is brighter, pH insensitive in physiological condition, and is resistant to photoswitching (Bhaskar et al, 2014). Two different isoforms of this indicator has been used: the first one, namely roGFP2, which is distributed throughout the cell cytosol and the second one, known as mt-roGFP2, which is localized into mitochondria. The use of fluorescent proteins with a distinct localization allowed to quantify the ROS production in the two compartments.

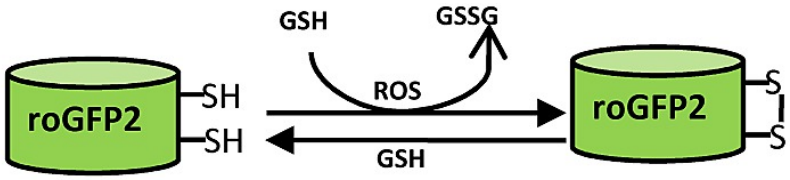

Fig.2.5. roGFP2 mechanism. roGFP2 contains two cysteine residues capable of forming an intramolecular disulfide bond in response to changes in intracellular redox status [adapted from (Bhaskar et al, 2014)]

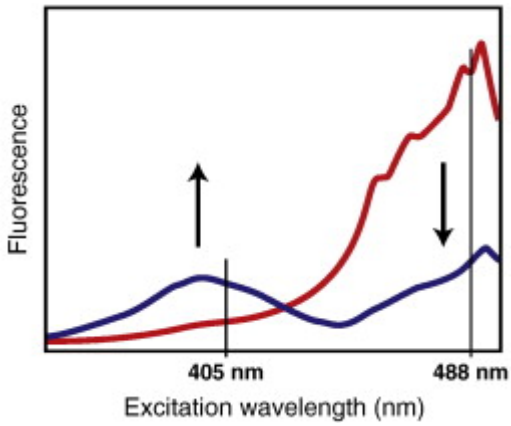

Fig.2.6. Fluorescence excitation spectra of roGFP2. Fully reduced (red line) or fully oxidized (blue line) state. Emission is followed at 500-530 nm (Morgan et al, 2011).

The expression vectors (from Remington's Lab, University of Oregon) containing the sequence for each variants were used to transform DH5α competent E. coli cells. Kanamycin- resistant colonies were isolated and used for plasmid DNA isolation using NucleoBond® Xtra Midi EF maxi-prep (MACHEREY-NAGEL) according to the manufacturer's protocol. The pure vector was used to transfect SH-SY5Y cells. 2x 10^5 cells were plated on poly-lysine pre-coated dishes with glass bottom (µ-Dish 35mm, Ibidi) for live imaging. Two days after seeding, cell were transfected with 0.8 µg of DNA using 3.2 µl Lipofectamine (800 µl total volume) for 24 hours. Thus, cells were exposed to 500 µM PQ for 6 or 12 hours in growing medium without phenol red. After treatment, samples were imaged using Leica SP5 confocal microscope with 63x oil immersion objective. Fluorescence was collected between 500-530 nm using 405 and 488 nm as excitation wavelength. To avoid photobleaching and/or laser-induced oxidation, images were acquired every 2 minutes using a wide pinhole and a fast scanning speed (256 x 256 and 512 x 512

respectively for low and high resolution images). Laser power for each filter was set up using 1 mM H_2O_2 and 4 mM DTT to define the maximum of fluorescence (avoiding saturation) respectively at 405 and 488 mm.

Microscope settings:

- roGFP2: Power 8% 405; 38% 488; smart gain 830 V; smart off:-6.2% pinhole 250 µm
- mt-roGFP2: Power 7% 405; 35% 488; smart gain 830 V; smart off:-6.2% pinhole 364 µm

For each fluorescent probe, the calibration was performed altering the redox state using 1 mM H_2O_2 for 20 minutes and 4 mM dithiothreitol (DTT) for 12 minutes that were respectively necessary to define the extreme oxidizing and reducing conditions and the probe dynamic range (ratio between these two values). Once probes were calibrated, they were used to investigated the effect of PQ exposure. Using the same settings for calibration, different fields of each samples were acquired. Raw images were exported to ImageJ software as RGB TIF for analysis. Each cells in the field was selected as region of interest (ROI) and in turn, each ROI was used to measure mean intensity. Background correction was performed for single ROI. The ratio between values of 405 and 488 images was reported in 0-100% range of oxidized state using extreme oxidizing and reducing values and compared to untreated cells. Therefore, data were expressed as the mean ± SEM, calculated through error propagation.

2.1.15 Quantification of catecholamine levels.

Undifferentiated and differentiated cells were harvested, washed with PBS, and mixed with ice-chilled 0.2 M perchloric acid containing 5 mM EDTA and 5 mM sodium bisulfate (100 µl of solution in every 4x106 cells). Lysates were centrifuged at 7000 g for 20 min at 4°C and the supernatants were collected and stored immediately at -80°C until further analysis. High-performance liquid chromatography (HPLC) (Agilent 1100 Series) coupled with an ESA Coulochem II electrochemical detector was used to measure the concentrations of noradrenaline

(NA) and DA. Separations were achieved on a 150 × 4.6 mm Waters C18 column. The mobile phase consisted of 75 mM NaH2PO4, 1.7 mM 1-octanesulfonic acid, 25 μM EDTA and 10% (v/v) acetonitrile, adjusted to pH 3 with phosphoric acid. The column was maintained at RT and the flow rate was 0.6 ml/min. An analytical cell ESA 5011A was used with the electrochemical potentials set at -150 mV and +220 mV. The working standard solution was prepared in 0.2 M perchloric acid containing 5 mM EDTA and 5 mM sodium bisulfite. Five- to twenty-microliter samples were injected. The peak areas of the external standards were used to quantify the sample peaks. The lower detectable concentrations of DA and NA were of approximately 3 nM when twenty microliters were injected. For each sample used, the protein concentrations were detected using the BCA protein assay kit (Thermo Scientific Pierce), and the DA and NA concentrations were then expressed in nanomoles per gram of proteins.

2.1.16 SOD-mimetic compound activity assays

SOD-mimetic compound activities were determined through the citochrome c assay (McCord, 2001). The reduction rate of cytochrome c by O_2 550 nm utilizing xanthine-xanthine oxidase as a source of superoxide. The reaction mixture consisted in 50 mM K-phosphate, pH 7.8, 0.1 mM EDTA, 50 μM xanthine, 10 μM cytochrome c in the absence (control) or in the presence of different amounts of human SOD1 or SOD-mimetics, in a total volume of 1 ml. After the addition of ~ 3 mU of xanthine oxidase, spectra were acquired every 10 s for a total period of 4 min. Each kinetic was performed in triplicate. Percent inhibition was calculated as follows: % inhibition = [(control rate-sample rate)/control rate] × 100 The values calculated with different amounts of SOD1 or SOD-mimetics (expressed in μmol) have then been fitted by a rectangular hyperbola: y = abx/(1+bx) where “a” represents the maximal percentage of inhibition obtained and “b” indicates the units per μmol of protein.

2.1.17 Statistical Analysis.

Each experiment was performed in triplicate. The data were expressed as the mean ± SEM. Student's t-test or one way ANOVA were used to evaluate statistically significant differences using the GraphPad Prism software.

2.2 *Drosophila melanogaster- in vivo* experiments

2.2.1 Reagent stock

PQ (Sigma): 100 mM in distilled sterile water

SOD mimetics:

- M40403 (synthesized by collaborators from the University of Pavia), 10 mM in distilled sterile water

2.2.2 Fly stocks

Flies were raised on standard yeast-molasses-agar medium at 25°C and 70% relative humidity in 12 hours light/dark cycles. The following strains were obtained from the Bloomington Drosophila Stock Center: UAS-Sod (#33605), UAS-Sod2 (#24494), da-GAL4 (#5460), UAS-Sod-RNAi (#24491), UAS-Sod2-RNAi (#24489). TH-GAL4 was a gift from Serge Birman (CNRS, Paris), while $PINK1^{B9}$mutants were provided by J. Chung (KAIST). A white Dahomey (w,Dah) strain was utilized as wild-type control line (a gift from Linda Partridge, UCL). For all experiments employing GAL4 expression to drive UAS-transgenes, GAL4/+ or $PINK1^{B9}$/+; GAL4/+ were utilized as controls.

2.2.3 Semi-quantitative PCR to assess Sod or Sod2 overexpression

Total RNA was extracted form whole body of 5-10 flies using TRIzol reagent (Life technologies). Afterwards, Reverse transcription and semi-quantitative PCR were performed as described in the Section 2.1.10 using Sod and Sod2 primers (Tab.2.7). Amplified DNA was subsequently analyzed by 2.0% agarose gel

electrophoresis and the images were acquired by Quantity One software using the Gel Doc XR System (Bio-Rad).

Gene	Primer sequence (5'-3')	Product length (bp)
Sod	Fw: GTCGACGAGAATCGTCACCT	187
	Rv: TTGACTTGCTCAGCTCGTGT	
Sod2	Fw: CTGAAGAAGGCCTCGAGTC	222
	Rv: ATAGTAGGCGTGCTCCCAGA	

Tab.2.7. List of primers used for semi-quantitative PCR to evaluate Sod and Sod2 overexpression.

2.2.4 Fly treatment

2.2.4.1 PQ administration

For survival experiments, flies were starved for 4 hours and then kept in vials with filter paper soaked with 5 mM paraquat in 5% sucrose for 4 days .

For locomotion activity, flies were starved for 4 hours and then kept in vials with filter paper soaked with 1 mM paraquat in 5% sucrose for 7 days. The filter paper was replaced every 2 days.

2.2.4.2 M40403

To assess the beneficial effect of M40403 against PQ, treatment was performed in adult flies. Therefore, 200 μM or 1 mM M40403 were added to the filter paper containing PQ and 5% sucrose. SOD mimetic was administered for 4 or 20 days in survival and for 7 days in locomotion performance experiments. While to investigate whether this compound could rescue the strong phenotype of $PINK1^{B9}$, the treatment was performed during the larval development (form mating to eclosion) through the addition of the M40403 directly to the fly food. Therefore, in order to test the thermal stability of this compound, its antioxidant activity against PQ, has been assessed before and after an incubation at 70°C. Once the stability of the SOD mimetic was confirmed, it was added to the medium during the melting process. In this case, considering that it well know that larvae used to eat more than adults, lower

concentrations were tested. To minimize the total amount of drug used, a final volume of 2 ml of medium, containing from 0.1 to 1 mM of M40403, were put on empty tube. After one day, these tubes were used to set up the crosses.

2.2.5 Survival assessment

Groups of 20-25 one- to two-day-old flies were exposed to PQ, in presence or absence of M40403 for 4 days. First, gender sensitivity to PQ was assessed. Then, considering that female were much more resistant to the drug, only male were used in the further experiments. Surviving to the chemical treatment was determined every day for 4 days. Experiments were repeated 4-6 times for control and experimental genotypes, and the mean and SEM were calculated.

Sod or Sod2 RNAi lines presented a reduced lifespan. Therefore, in order to evaluate whether M40043 could replace native enzyme, survival these fly lines was assed. Groups of 20-25 one- to two-day-old male flies were collected and kept in vials with filter paper in presence or absence of M40403. Every 2 days, filter paper was replaced with a fresh one. Surviving was determined every day for a 20 days.

2.2.6 Locomotion Assay

To quantify whether prolonged exposure to PQ could impact on fly motor performance as well as Sods overexpression or SOD mimetic administration could rescue the herbicide toxicity, groups of 20-25 one- to two-day-old flies were exposure to PQ for 7 days. The locomotion assays were performed after 7 days of treatment. The mobility of flies from each treatment group was assessed using a counter-current apparatus in a negative geotaxis climbing assay. Flies were placed in an empty plastic vial (2.5 cm diameter), gently tapped to the bottom, and the number of flies crossing a line at 8 cm height within a time period of 10 s was scored. Each animal was tested 5 times. The number of male flies tested per genotype was $n > 150$.

$PINK1^{B9}$ mutants (male flies) presented a strong phenotype with a reduced life span, sterility, muscle degeneration and motor dysfunction. To investigate whether Sods overexpression or/and M40403 treatment could rescue this phenotype,

motor performance were tested using the aforementioned procedure. Thus, climbing assays were performed with groups of 20-25 one- to two-day-old flies. Climbing index was measured in PINK1^{B9} mutants (PINK1^{B9} /Y; male) and compared with control (PINK1^{B9} /+; female). For each genotypes, more than 150 flies, from two different crosses, were tested.

2.2.7 Statistical analysis.

Data were analyzed using GraphPad Prism 4 software. “t-test”, one-way ANOVA followed by Bonferroni post hoc test or logrank test were used to determine whether groups were statistically different. P values < 0.05 were considered significant.

Chapter 3

Results and Discussion

Antioxidant defense against oxidative injuries

As described in the Introduction, oxidative stress plays a crucial role in the pathogenesis of PD. The main goal of this work is to investigate whether the inhibition or the reduction of ROS overproduction could delay, block or prevent the degeneration of DAergic neurons. To this aim, the role of SODs, the superoxide scavenging enzymes considered the first line of defense against ROS, has been investigated. In particular, the ability of these enzymes and SOD mimetic compounds to counteract oxidative injury, related to sporadic and genetic forms of PD, has been evaluated *in vitro* and *in vivo*.

3.1 Effect of PQ toxicity on cell viability and apoptosis

As discussed in Section 1.3.2.1, chronic exposure to the herbicide PQ has been identified as a risk factor for sporadic forms of PD. Furthermore, with animal models, PQ proved to recapitulate some of the key PD pathological features such as motor impairment, loss of dopaminergic neurons, protein aggregation as well as proteasomal and mitochondrial dysfunction (Castello et al, 2007; Yang et al, 2007).

In literature, it has been demonstrated that PQ affects cell viability through oxidative stress (Chang et al, 2013); however, it is still unclear whether the molecular events that lead to toxicity occur in the cytosol or in mitochondria or in both compartments. In the present study, PQ has been used as experimental paradigm because of its ability to generate superoxide anion and related ROS through its redox cycling within cells. The effect of PQ treatment has been evaluated in human SH-SY5Y neuroblastoma cell line, which was used as model of DAergic neurons. To assess cytotoxicity induced by this herbicide, the viability of cells was measured after 24 hours of treatment with increasing concentration of PQ (50-500 μM) through the colorimetric CCK-8 assay. This technique allows to quantify the activities of intracellular dehydrogenases, which are directly proportional to the number of living cells. Cell viability was found to decrease significantly in a PQ dose dependent manner (Fig.3.1). In agreement with previous works (Yang & Tiffany-Castiglioni, 2007; Yang et al, 2010), in the presence of the highest amount of PQ used (500 μM), the viability was approximately 40% of that of untreated cells.

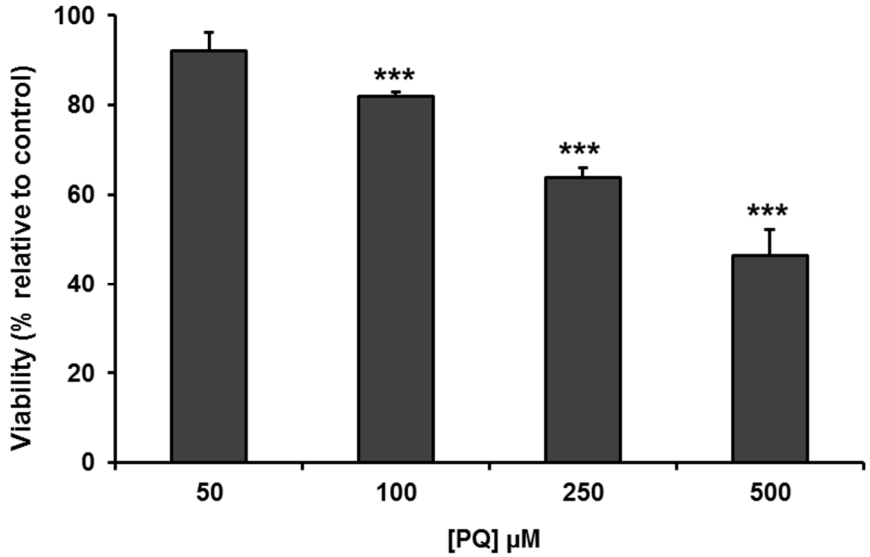

Fig.3.1 PQ treatment impacts on cell viability of SH-SY5Y cells. Cells were treated with increasing concentration of PQ (50-500 µM) for 24 h. Viability was measured by CCK8 colorimetric assay. Histograms indicate the percentage of viable cells after treatment, relative to untreated cells used as control. Data are expressed as mean of at least three independent experiments ± SEM. Statistical significance was determined by t-test comparing treated with untreated cells. (***$p<0.001$).

To further characterize the effect of the exposure to PQ, the capability of this molecule to trigger apoptotic cell death was also assessed. Cytofluorimetric analyses were performed in the presence of red-fluorescent propidium iodide (PI) and recombinant annexin V conjugated to fluorescein (FITC annexin V) in order to discriminate among apoptotic, necrotic and viable cells. PI is a nucleic acid binding dye, which is impermeable to live cells, but stains necrotic and late apoptotic cells. Annexin V is a Ca^{2+} dependent phospholipid-binding protein that has a high affinity for phosphatidylserine, a membrane phospholipid that translocates from the inner to the outer leaflet of the plasma membrane during the early phases of apoptosis. As the events analyzed by cytofluorimetric assay occur in a time period subsequent to the metabolic dysfunctions observed using the colorimetric test, the incubation with PQ was extended to 48 hours. Our analyses clearly indicated that the PQ exposure promoted an increase of apoptotic events (PI/FITC -/+; Q_4) (Fig.3.2A) and a concomitant decrease of viable cells (PI/FITC -/-; Q3), as highlighted in the histogram(Fig.3.2B).

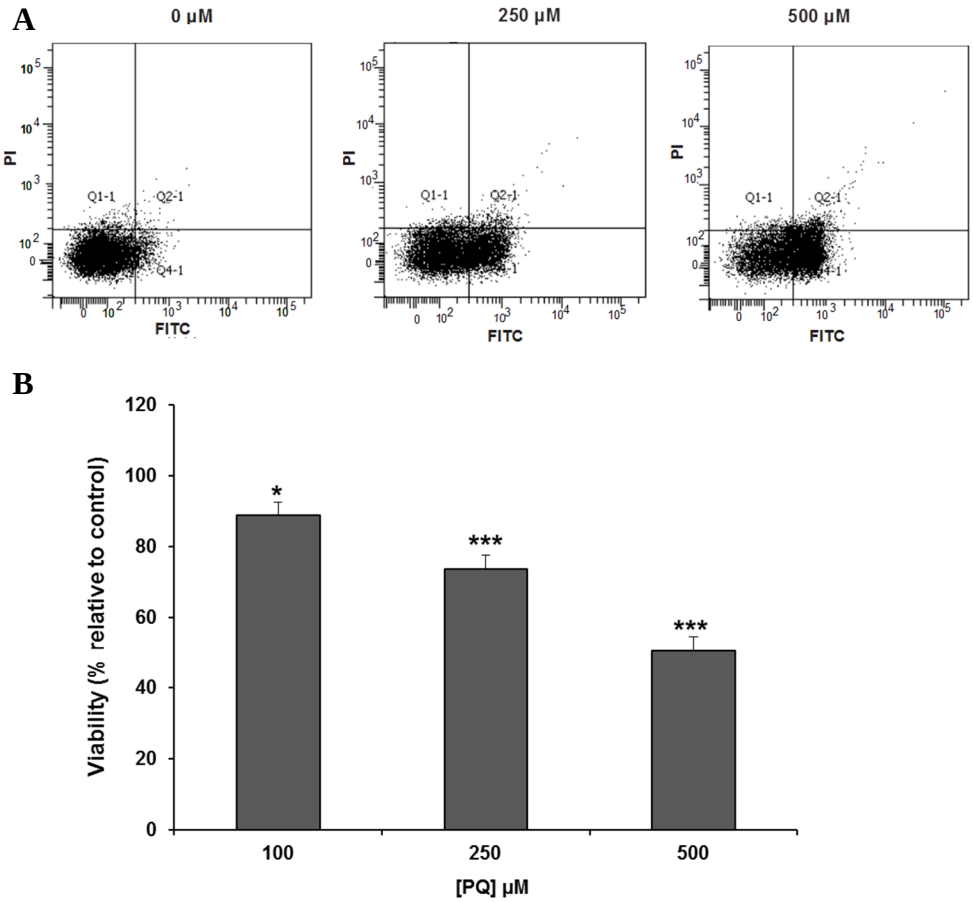

Fig.3.2. PQ induces apoptosis in SH-SY5Y cells. (A) Dot plots corresponding to cytofluorimetric analysis carried out on SH-SY5Y cells treated with increasing amounts of PQ. Before the analysis cells were labelled with propidium iodide (PI) and annexin V-FITC and 10^4 cells were analyzed for each condition tested. The staining pattern resulting from simultaneous use of these dyes made it possible to distinguish viable, apoptotic and necrotic cells. Plots are divided in four regions corresponding to viable (PI/FITC -/-; Q3), apoptotic (PI/FITC -/+; Q4), late apoptotic (PI/FITC +/+; Q2) and necrotic (PI/FITC +/-; Q1) cell populations. **(B)** Data are expressed as mean of at least three different experiments ± SEM. Statistical significance was determined by t-test comparing treated with untreated cells. (*p<0.05, **p<0.01, ***p<0.001).

In agreement with previous studies (Chang et al, 2013; Yang & Tiffany-Castiglioni, 2008), these data showed that the herbicide reduced the viability through the induction of apoptotic pathway. Indeed, it has been previously reported that PQ significantly increased protein levels of p53 and the pro-apoptotic factor Bax, inducing release of cytochrome c from mitochondria. Additionally, the herbicide increased the activities of caspases 9 and 3 suggesting that the mitochondrial intrinsic

pathway associated with p53 might be the main mechanism involved (Yang & Tiffany-Castiglioni, 2008).

3.2 SODs overexpression in SH SY5Y cells

To investigate the potential protective role of the SODs against PQ toxicity, the cytosolic and mitochondrial isoforms, respectively SOD1 and SOD2, were stably overexpressed in SH-SY5Y cells. The stable overexpression was necessary in this cell line because of their low transfection efficiency (about 15% in optimized conditions), unsuitable for the evaluation of any effect of SODs overexpression. Cells were transfected using an expression vector containing the coding sequence for each of these proteins as well as a neomycin resistance cassette used to select and isolate G418-resistant clones that expressed SODs in a stable manner. The expression level of each isoform was assessed by western blot analysis (Fig.3.3A) and quantified through densitometry (Fig.3.3B), normalizing with tubulin as loading control. In the selected colonies, SOD1 was overproduced about 3-5 folds, while the overexpression of SOD2 was about 2-6 times higher than untransfected cells.

A

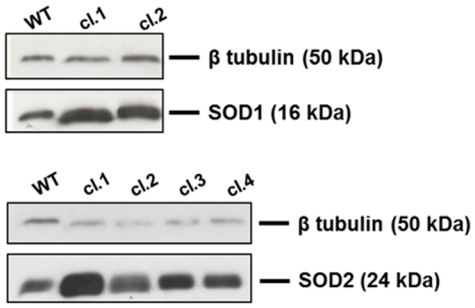

B

	cl. 1	cl.2
SOD1	3.3 ± 0.9	4.6 ± 1.3

	cl. 1	cl.2	cl.3	cl.4
SOD2	5.7 ± 1.3	4.2 ± 0.9	3.1 ± 0.5	2.2 ± 0.4

Fig.3.3 SOD1 and SOD2 overexpression in SH-SY5Y cell line. (A) Western blot analyses and **(B)** densito-metric quantification of SOD1 and SOD2 in stably transfected and untransfected SH-SY5Y cells. The quantification was obtained using Image J software. The β-tubulin signal was used as loading control. Data are expressed as mean of three independent experiments ± SEM.

Each clone was further characterized by immunofluorescence. Representative images for SOD1 clone 2 (SOD1 cl.2) and SOD2 clone 1 (SOD2 cl.1) are reported in Fig.3.4. The distribution of SOD1 (red) and SOD2 (green) fluorescence confirmed

either the overexpression of these enzymes and the isolation of a single population, in which all cells expressed approximately the same protein level (Fig.3.4).

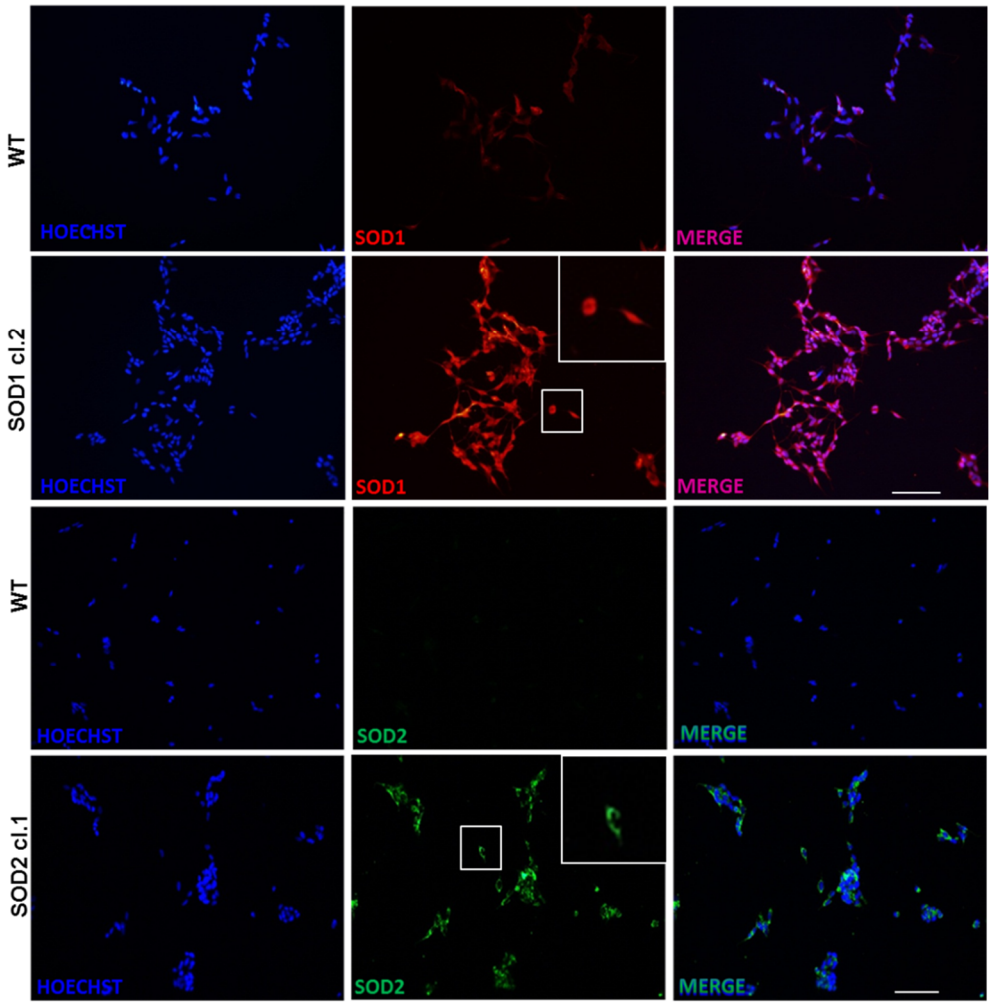

Fig.3.4 SOD1 and SOD2 overexpression and localization in SH-SY5Y cell line. Immunofluorescence microscopy. Red staining revealed that SOD1 was evenly distributed in stably transfected SH-SY5Y and confirmed overexpression compared to untransfected cells. Green staining confirmed the isolation of a unique clone and the increased expression of SOD2 protein in stably transfected SH-SY5Y compared to untransfected cells. Scale bar 100 µm.

Furthermore, the correct localization of overexpressed SOD2 inside the mitochondria has been demonstrated by a co-immunostaining with succinate dehydrogenase A (SDHA, red), an inner mitochondrial membrane protein (Fig.3.5).

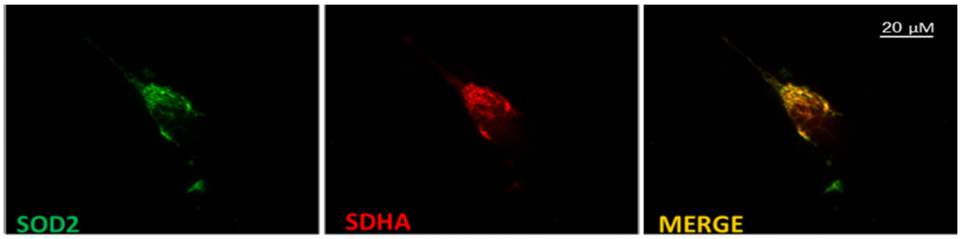

Fig.3.5 Mitochondrial localization of overexpressed SOD2. SOD2 immunoreactivity (green fluorescence) showed excellent overlapping with Succinate dehydrogenase A (red fluorescence), which is located on the inner membrane of the mitochondria, indicating the mitochondrial localization of SOD2. Scale bar 20 µm.

3.3 SOD2 protects SH-SY5Y cells against PQ toxicity

The cell lines generated were used to determine whether an increase in SODs activity protects against oxidative injury induced by PQ. Considering that the insertion of the expression vector in the host genome occurred randomly, we decided to analyze two clones for each protein. Thus, cells were exposed to increasing concentration of PQ (50-500µM) for 24 hours. Then, cell viability was measured by colorimetric assay. Interestingly, the overexpression of these proteins produced very different effects in terms of cell viability. While SOD1 was unable to protect cells from the toxic insult induced by PQ in both the analyzed clones (Fig.3.6A), SOD2 provided an improved survival of cells exposed to PQ at the different concentrations tested (Fig.3.6B). In addition, the resistance of the different Mn-SOD cell colonies to PQ seemed to be correlated to the level of protein overexpression; accordingly, SOD2 was more protective in cl.1 (5.7 fold of overexpression) than cl.3 (3.1 fold).

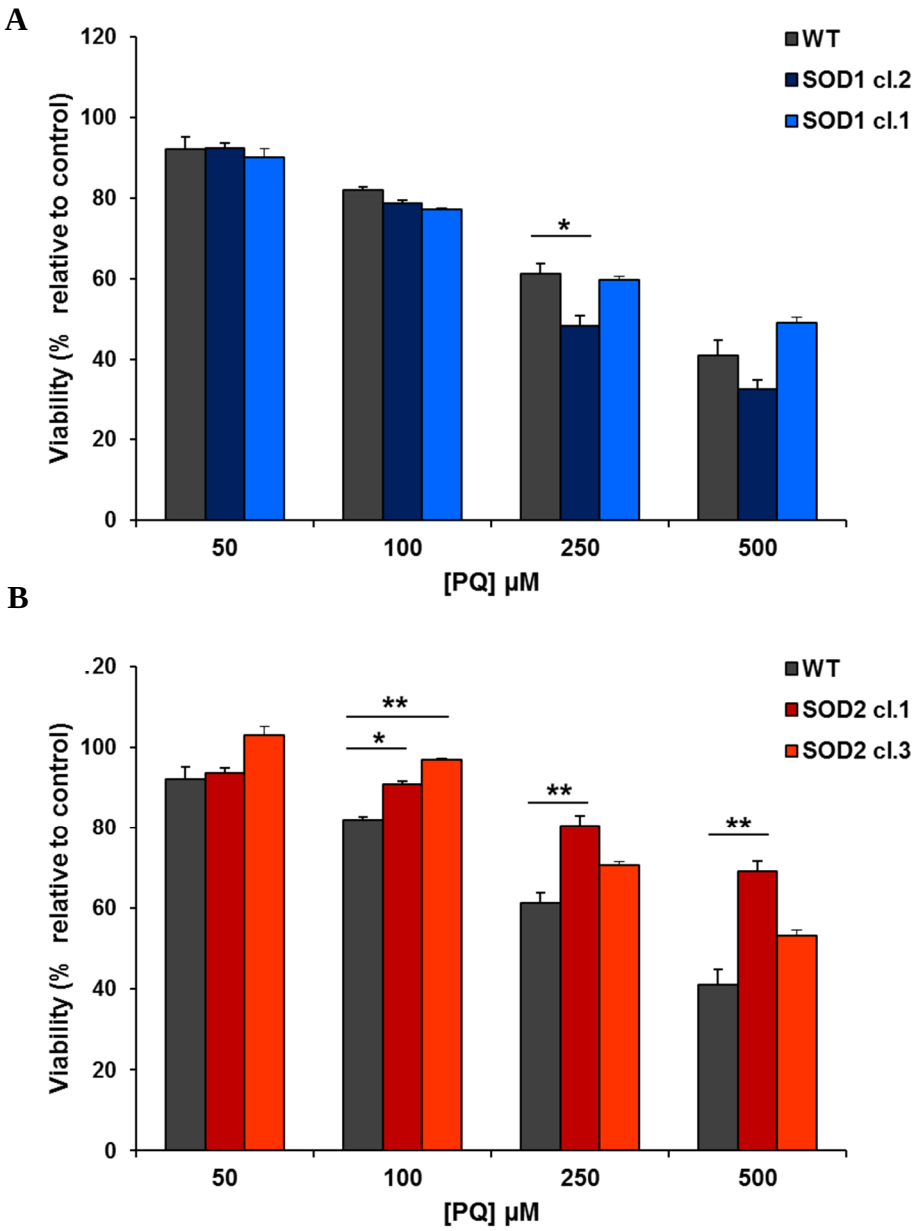

Fig.3.6. SOD2 protects SH-SY5Y cells against PQ toxicity. Cell viability was measured by CCK8 colorimetric assay after 24 hours of PQ treatment. Histograms indicate the percentage of viable cells after treatment, relative to untreated cells used as control. **(A)** Untransfected (WT), SOD1 cl.2 and SOD2 cl.1 **(B)** Untransfected (WT), SOD1 cl.1 and SOD2 cl.3 overexpressing cells were treated with increasing amount of PQ. Data are expressed as mean of at least three different experiments ± SEM. Statistical significance was determined by t-test comparing SOD-overexpressing cells with untransfected cells. (*$p<0.05$, **$p<0.01$).

3.4 Protective role of SOD2 against PQ induced apoptosis

To further investigate the activity of SODs against PQ exposure, cytofluorimetric analyses were performed after 48 hours of treatment. Our previous data on *wild-type* (WT) cells confirmed that PQ toxicity was mediated by apoptotic cell death. As reported in Fig.3.7, dot plots showed that in WT cells apoptotic events increased in the presence of PQ in a dose-dependent manner. A similar degree of apoptosis was also observed with SOD1 overexpression, while in the SOD2 overexpressing cells only at the highest amount of PQ used, apoptotic events were evident. The results of these analyses are summarized in Fig.3.8 and expressed as percentage of viable cells (PI/FITC -/-; Q3). The histogram clearly showed a beneficial activity exerted by SOD2 against the toxicity of this environmental toxin.

Overall, the results obtained with human neuroblastoma SH-SY5Y cell line indicate a selective role of mitochondrial SOD in rescuing cytotoxicity and apoptosis mediated by PQ, supporting the idea that an acute treatment with this herbicide could directly impact on mitochondrial functions leading to their impairment. These observations are in agreement with a recent work published by Rodriguez-Rocha et al. (Rodriguez-Rocha et al, 2013). These authors reported that in SH-SY5Y cells the overexpression of the mitochondrial Mn-SOD but not the cytosolic Cu,Zn-SOD prevented cell death induced by PQ. However, independent evidence suggested the protective effects of the cytosolic isoform, Cu,Zn-SOD, under exposure to the herbicide (Choi et al, 2006). Indeed, it has been found that the fusion protein PEP-1–Cu,Zn-SOD was able to rescue PQ toxicity in primary astrocyte cultures. In addition, when the same fusion protein was injected intraperitoneally in mice, a complete protection against DAergic neuronal cell death was observed (Choi et al, 2006). Thus, whether PQ-induced oxidative stress involves mainly mitochondria or cytosol is still unclear and need to be further investigated.

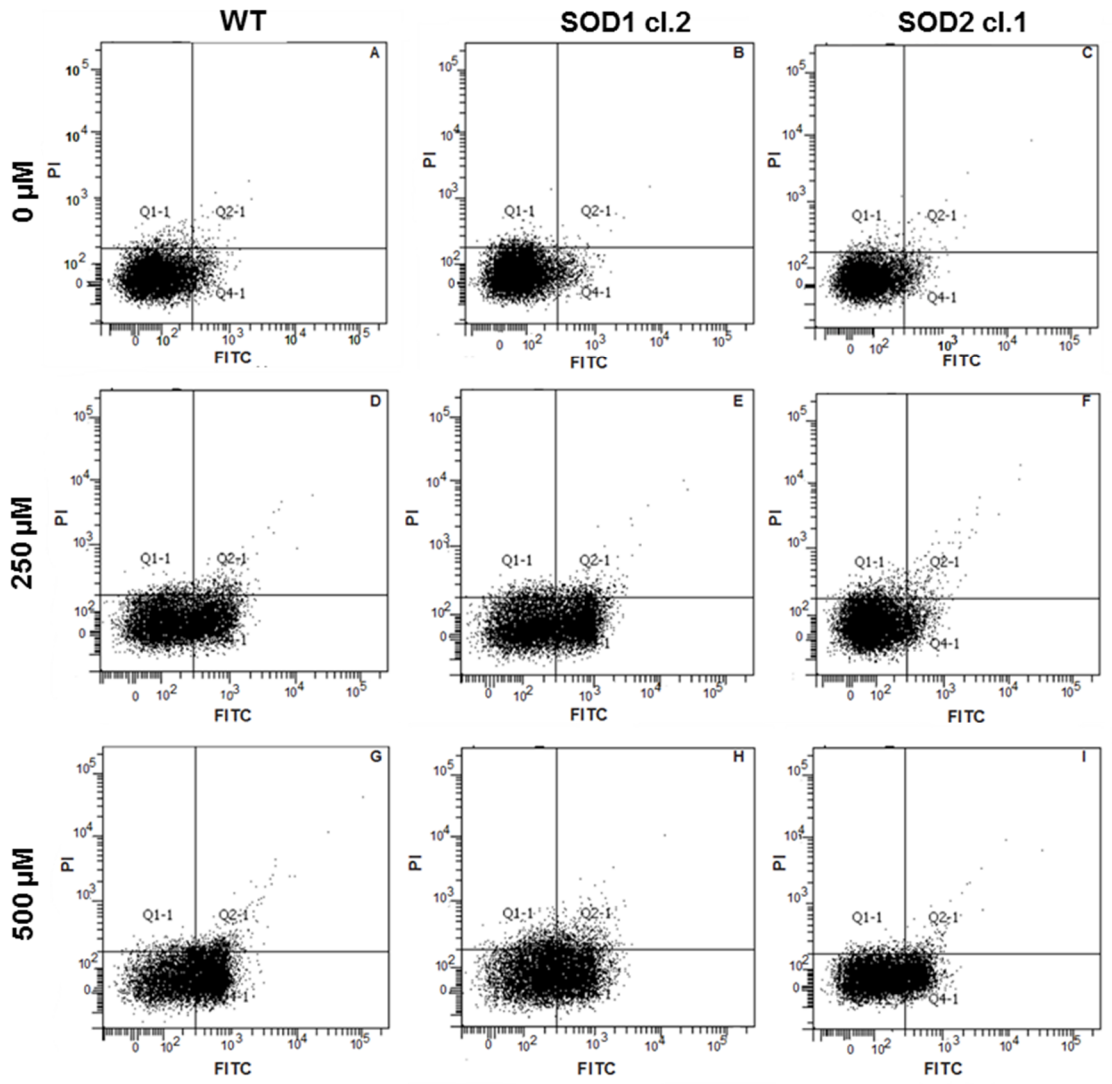

Fig.3.7. SOD2 protects SH-SY5Y cells against PQ toxicity. Dot plots corresponding to cytofluorimetric analysis carried out on untransfected, SOD1- and SOD2- stably transfected cells, treated with increasing amounts of PQ. Before the analysis, cells were labeled with propidium iodide (PI) and annexin V-FITC. The staining pattern resulting from the simultaneous use of these dyes allows to distinguish viable, apoptotic and necrotic cells. Plots are divided in four regions corresponding to viable (PI/FITC -/-; Q3), apoptotic (PI/FITC -/+; Q4), late apoptotic (PI/FITC +/+; Q2) and necrotic (PI/FITC +/-; Q1) cell populations. Untransfected cells and SOD1 overexpressing cells show increase an of apoptosis after the incubation with PQ while in the SOD2 clonal cells only at the highest amount of PQ used, apoptotic events is evident.

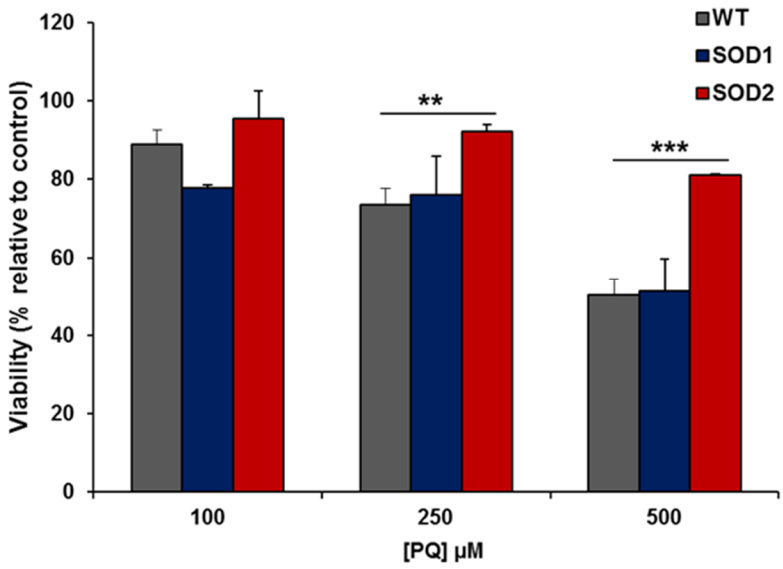

Fig.3.8. SOD2 overexpression protects SH-SY5Y cells against PQ induced apoptosis. Untransfected (WT), SOD1 (cl.2)- and SOD2 (cl.1)-overexpressing cells were treated with increasing amount of PQ. Histograms indicate the percentage of viable cells after treatment, relative to untreated cells used as control. Cell viability was measured by flow cytometry after 48 hours of treatment. Data are expressed as mean of at least three different experiments ± SEM. Statistical significance was determined by t-test comparing SOD-overexpressing cells with untransfected cells. (*$p<0.05$, **$p<0.01$, ***$p<0.001$).

3.5 ROS production induced by PQ

To elucidate the alterations in the oxidative state induced by PQ and to define whether this process involves different cell compartments, the redox sensor roGFP2 has been used. This genetically encoded indicator allows measuring cellular redox status in *real time* regardless of the absolute levels of probe concentration, through ratiometric imaging (Celotto et al, 2012). As other sensors of this category, roGFP2 consists of a GFP mutant in which two surface-exposed cysteine residues are inserted in a position close to the GFP intrinsic chromophore. Depending on the redox state of the cell, disulfide formation occurs between these cysteines thus promoting the protonation of the chromophore with concomitant alteration of the excitation spectrum. In particular, reduced probe presents a predominant peak around 488 nm. Upon oxidation, an increased intensity around 405 nm is observed at the expense of the excitation at 488 nm. Thus, the ratio between the fluorescence emission collected

at 500-530 nm using the two excitation wavelength (405 and 488 nm) permits a ratiometric quantification. In our experiments, two different variants of roGFP2 have been used, the cytosolic roGFP2 and the mitochondrial mt-roGFP2, in order to quantify the ROS production in the two different compartments. For each fluorescent probe, a calibration assay was first performed. The redox state was altered by 1 mM H_2O_2 and4 mM DTT that were added to induce respectively fully oxidizing or fully reducing conditions. The ratio between these two states indicated the dynamic range of each probe. To this aim, cells were seeded on specific dishes for *live* imaging, transfected and then after 24 hours images were acquired. Oxidative and reducing agents were added in *real time* during images acquisition. To avoid photobleaching and/or laser-induced oxidative damages, images were acquired with a confocal microscope every 2 minutes using a wide pinhole and a fast scanning speed as previously suggested (Dooley et al, 2004) (see Section 2.1.14).

As reported in Fig.3.9, in the initial phase, unperturbed cells were in a predominantly reduced state. After the addition of 1 mM H_2O_2, the ratio (405/488) increased over reaching a plateau within few minutes, in agreement with the oxidation effect depending on peroxide. Afterwards, by adding 4 mM DTT the reduced state was restored shifting the fluorescence ratio to its minimum. Thus, the dynamic responsiveness to redox changes of each probe has been evaluated. The data are summarized in Tab.3.1 that reports the values of the fluorescence ratio, upon the two different excitation wavelength (405/488), as recorded in correspondence to 100% of oxidized and reduced states and the consequent dynamic range. Consistent with the theoretical value reported in literature (around 9) (Meyer & Dick, 2010), the dynamic range determined in our work was about 8.

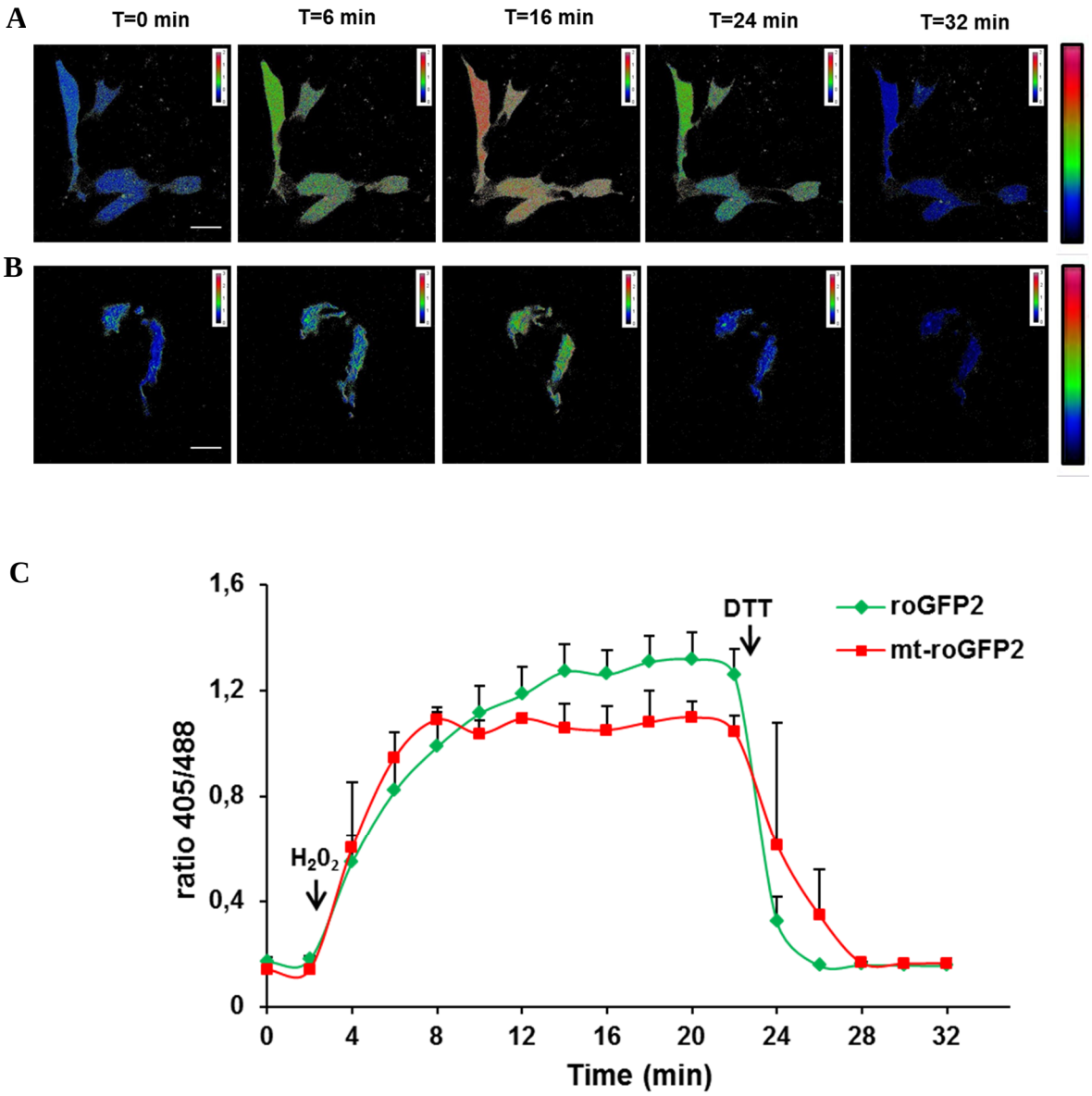

Fig.3.9 Probe calibrations using H_2O_2 and DTT. Cells were transiently trasfected with roGFP2 and mt-roGFP2 and after 24 hours real time quantification of cytosolic and mitochondrial redox changes were measured in response to 1 mM H_20_2 and 4mM DTT. Density map correspond to the ratio between fluorescence collected using 405 and 488 nm as excitation wavelenght. The visualization was obtained using the lut "rainbow" of ImageJ. **(A)** roGFP **(B)** mt-roGFP. **(C)** Representative time course of redox changes monitored by change of fluorescence emission intensity at 500-530 nm upon excitation at 405 nm versus 488 nm of roGFP2 and mt- roGFP2. data are expressed as mean ± SEM of three indipendent experiments.

	100% reduced	100% oxidized	Dynamic range
roGFP2	0.13 ± 0.01	1.17 ± 0.11	8.63 ± 0.86
mt-roGFP2	0.13 ± 0.00	0.97 ± 0.02	8.09 ± 0.80

Tab.3.1. Summary of ratio (405/488) corresponding to 100% reduced and oxidized state and of the dynamic range for each sensor. Dynamic range was calculated as ratio between 100% oxidized and 100% reduced state for each sample. Data are expressed as mean of at least six different experiments ± SEM.

After probe calibration, this technique was used to examine the cell redox status upon PQ exposure. Considering that metabolic dysfunction was observed after 24 hours of exposure (Paragraph 3.1), it is most likely that ROS production is an earlier event. Therefore, cells were seeded, transfected and then treated for 6 and 12 hours with 500 µM PQ. The treatment significantly increased mitochondrial ROS production after both 6 and 12 hours (Fig.3.10). In contrast, PQ was not able to increase the oxidative state in the cytosol.

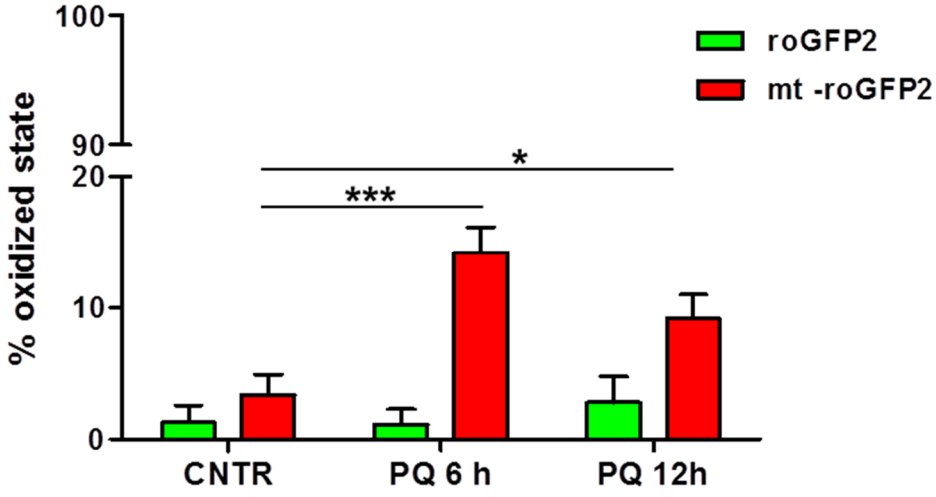

Fig.3.10. Alteration of the cell redox status induced by treatement with 500 µM PQ for 6 and 12 hours. Cells were transiently trasfected with roGFP2 and mt-roGFP2 for 24 hours. Afterwards, they were exposed to PQ for the indicated times. Fluorescence was collected at 500-530 nm using 405 and 488 nm as excitation wavelenght. Fluorescence Ratio (405/488) obtained for each sample was expressed as percent with respect to that observed for the 100% reduced and oxidized state (Tab.3.1). Data are reported as mean ±SEM at least 3 indipendent experiments.. Statistical significance was determined by t-test comparing PQ treated with PQ untreated cells (*$p<0.05$, ***$p<0.001$).

Another group worked on this issue using the same experimental approach, publishing when we were performing our analyses. In this study, the authors showed that, after 24 hours, 500 μM PQ increased exclusively mitochondrial ROS production (Rodriguez-Rocha et al, 2013), coherently with our results.

Taken together, our data strongly suggest that PQ induces apotosis through a ROS-dependent pathway that mainly involved mitochondrial ROS production.

3.6 PQ treatment impacts on mitochondrial morphology

In light of our previous results, we decided to investigate whether PQ affects also the mitochondrial morphology. As mentioned in Section 1.3.1.4, mitochondria form a dynamic interconnected network that continuosly undergo fission and fusion in order to maintain the proper morphology and functioning. Mitochondrial shape depends on the balance between these events which are tightly regulated. Several studies reported that, during apoptotic cell death, mitochondrial morphology changes occur resulting in organelles that are small, round and more numerous (Frank et al, 2001; Jagasia et al, 2005) . This process, known as fragmentation, might be due to the partecipation of fission/fusion machinery components to apoptotic process upstream of caspase activation (Youle & Karbowski, 2005). Recently, different works suggested that ROS production in these organelles could trigger mitochondrial fragmentation probably promoting an enhanced fission that ultimately impacts on mitochondrial network and functions (Pletjushkina et al, 2006; Wu et al, 2011). To analyze whether PQ toxicity affected also the mitochondrial network, SH-SY5Y cells were transiently transfected with a vector containing the coding sequence for the mitochondrial matrix targeted-RFP (mito-RFP) which allowed to monitor the mitochondrial morphological changes through fluorescence microscopy. After transfection, cells were exposed to 500 μM PQ for 24 hours and then fixed before microscopy.

To measure the entity of these changes, mitochondrial morphology was scored as follows: tubular, which is characterized by a long and higher interconnectivity; intermediate that presented a mixture of round and shorter tubular mitochondria and fragmented that was mainly constitued by multiple punctiform

organelles (Fig.3.11A). As shown in Fig.3.11B, untreated cells displayed mitochondria mostly with a tubular shape (more than 80%), while cultures treated with PQ had mitochondria with fragmented and punctiform morphology. These data support the hypothesis that the PQ induces mitochondrial fragmentation by triggering oxidative stress. Coherently with these observations, it has been previously demonstrated that, in *Caenorhabditis elegans*, low concentration of PQ resulted in substantial structural alterations of mitochondrial morphology (Runkel et al, 2013). In addition, it has been shown that, in SH-SY5Y cells, PQ induced a significant alteration of mitochondrial morphology, including swelling, matrix thinning and cristae breakdown/disruption, as well as a mitochondrial membrane depolarization (Rodriguez-Rocha et al, 2013).

Overall, these findings could be explained through the hypothesis that mitochondrial fragmentation precedes mitophagy (Gomes & Scorrano, 2013; Twig et al, 2008). The central idea is that to fit into autophagosome, these organelles have to decrease their normal dimension through fission process. Thus, a low membrane potential or mitochondrial ROS might be the signal used by dysfunctional organelle to drive fission required for triggering mitophagy (Gomes & Scorrano, 2013).

To summarize, our *in vitro* analyses demonstrated that PQ promotes oxidative stress at mitochondrial level, which, in turn, impacts on the morphology of these organelles and, ultimately, on cell viability. These observation might explain the selective protection exerted by SOD2, which resides directly on the site of the damage, hampering PQ toxicity.

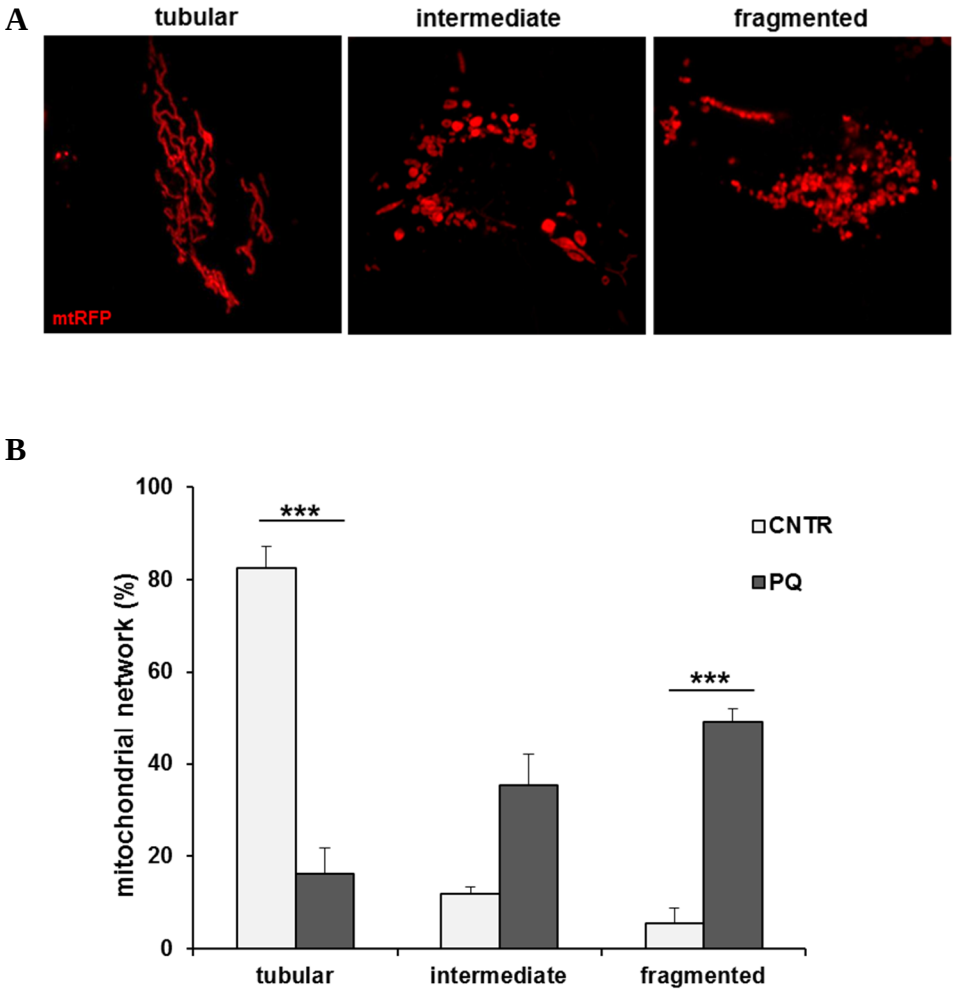

Fig.3.11 PQ affects mitochondrial network leading to fragmentation. SH-SY5Y cells were transfected for 24 hours with mito-RFP, which allowed to visualize the mitochondrial network. Afterwards samples were treated with 500 μM PQ and compared with untreated sample (CNTR). Images were acquired using an epifluorescence microscope (100x objective). **(A)** Mitochondrial network was scored as follows: tubular, long and higher interconnectivity; intermediate, mixture of round and shorter tubular; fragmented multiple punctiform organelles. **(B)** Quantification of the percentage of cells with indicated mitochondrial network. The values represent the percentage of the total number of transfected cells counted (≥50 cells per experiment). The data analysis was performed in a blind manner. Data are expressed as mean ± SEM of 3 independent experiments. Statistical significance was assessed by One way ANOVA with Bonferroni correction (***$p<0.001$).

3.7 Sod-mediated protection against PQ toxicity in *Drosophila*

The findings obtained through SODs overexpression *in vitro*, triggered the investigation of the importance of the protective activity of these enzymes also *in vivo*, using *Drosophila melanogaster* as animal model. Among the well characterized genetic tools that are currently available for functional studies in *Drosophila*, in this work, the UAS/GAL4 system was used to drive the overexpression of the two homologs of SOD1 and SOD2, called Sod and Sod2, respectively. This tool is based on the properties of the yeast GAL4 transcription factor, which activates transcription of its target genes by binding to UAS *cis*-regulatory sites. The two components are carried in separate fly lines: one provides the tissue-specific GAL4 expression, while the responder line carries the coding sequence for the gene of interest under the control of UAS sites. Using this system, the proteins were first expressed ubiquitously via the da-GAL4 driver and the level of overexpression was quantified in terms of mRNA levels through a semi quantitative RT-PCR (Fig.3.12). The young progeny (1-2 day old flies) of these crosses were tested after PQ treatment in term of fly survival.

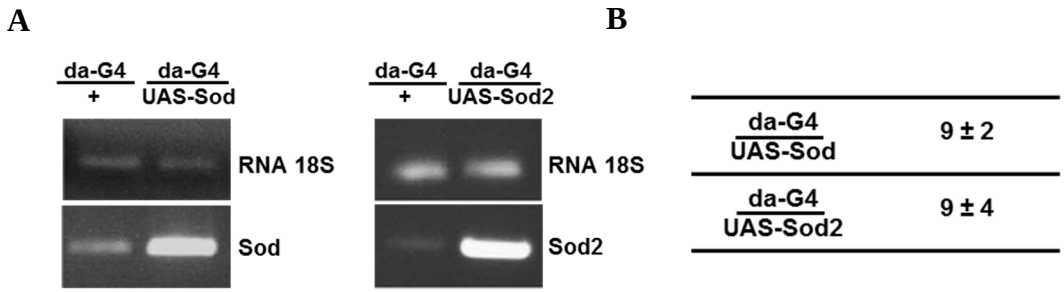

Fig.3.12. Ubiquitous Sod and Sod2 overexpression in flies. (A) Semi-quantitative PCR analysis and **(B)** densitometric quantification of endogenous Sod and Sod2 by Image J software. The da-GAL4/UAS system was used to ubiquitously drive the expression of either Sod or Sod2 in *D. melanogaster* flies. 18S mRNA signal was used as loading control. Data are expressed as mean ± SEM of three experiments.

Initially, PQ toxicity has been investigated in da-Gal4/+ flies, used as control (WT) in order to check whether males and females presented the same response to this treatment. In adult flies, drug was administered through a sucrose-soaked filter paper.

Males and females 1-2 day old were treated with 5 mM PQ for 4 days. In agreement with other reports (Parashar et al, 2008), male flies results to be more sensitive to this herbicide than female flies (Fig.3.13). Thus, all the following experiments were performed evaluating PQ toxicity only in males.

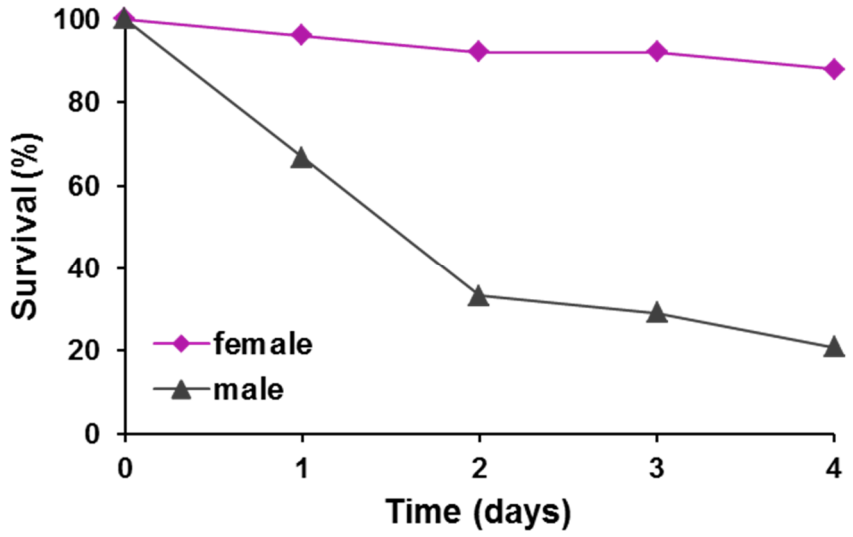

Fig.3.13. Male flies are more sensitive to PQ exposure than females. Flies 1-2 days old were treated with 5mM of PQ for 4 days. The survival was assessed in a single experiment with more than 100 males and females.

The effects of Sods overexpression on male flies survival was studied under the same treatment with PQ. As reported in Fig.3.14, approximately 30% of WT flies died after 1 day and more than 70% after 4 days of treatment. The over-expression of Sod did not provide any protection, as the fly survival was not statistically different from that of control flies. This result is in agreement with a previous works in which the over-expression of Cu,Zn-Sod in several fly lines did not improve their ability to withstand experimental oxidative damage induced by PQ (Orr & Sohal, 1993; Seto et al, 1990). In contrast, more than 60% of flies were still alive even after 4 days of treatment (Fig.3.14) suggesting that the overexpression of mitochondrial isoform made the flies more resistant to PQ toxicity, in agreement with the results described above with SH-SY5Y cells. Coherently with our results, it has been previously reported that flies with Sod2 null mutation as well as RNA interference silencing

were hypersensitive to oxidative stress induced by PQ (Duttaroy et al, 2003; Kirby et al, 2002). These results suggest that the damage induced by an acute PQ exposure (5 mM) is likely to compromise the organismal integrity much more extensively at the mitochondrial level than the cytosol being. This hypothesis could explain why only Sod2 over-expression resulted in rescue. Accordingly, a recent study showed that acute PQ dose caused a significant oxidative stress and mitochondrial dysfunction among flies *in vivo*. In particular, it has been demonstrated that the herbicide was responsible of a significant reduction in the activity of ETC complexes as well as enzymes involved in citric acid cycle (Hosamani, 2013).

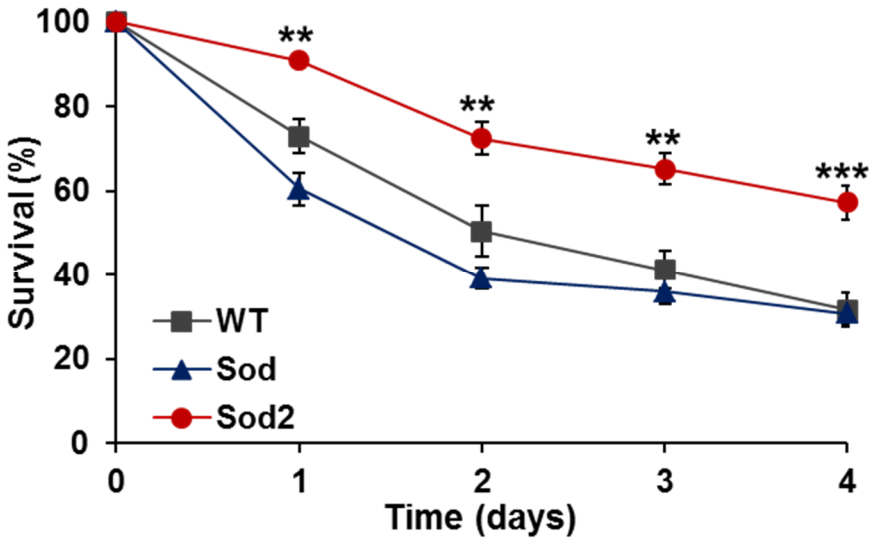

Fig.3.14. Sod2 protects *Drosophila melanogaster* against lethal treatment with PQ. The GAL4/UAS system was used to drive the expression of either Sod or Sod2 in a tissue specific manner. The proteins were expressed ubiquitously through the da-GAL4 driver. The survival of da-GAL4/+ (WT), da-GAL4>Sod and da-GAL4>Sod2 flies was monitored upon exposure to 5 mM PQ. Data are expressed as mean ± SEM. Statistical significance was determined by one-way ANOVA with Bonferroni correction (**p<0.01, ***p<0.001). At least 150 flies were assessed for each genotype.

Considering that in humans the chronic exposure to PQ was significantly correlated with the onset of PD, we decided to investigate *in vivo* the toxic effects associated to sub-lethal concentrations PQ. When flies were exposed to 1 mM PQ for 7 days the survival was not affected but defects in locomotor performance, as resulting from negative geotaxis climbing assays, were observed. After PQ treatment,

control flies showed a strong impairment in locomotion. Interestingly, the ubiquitous over-expression of Sod *via* the da-GAL4 driver was able to almost completely rescue this motor dysfunction. In contrast, even though Sod2 over-expression improved the behavioral phenotype in a statistically significant manner, the rescue was only partial and less evident than with Sod (Fig.3.15A). To better understand whether these results might be linked to DAergic system, the Sods over-expression was achieved only into DAergic neurons using the TH-GAL4 driver (Fig.3.15B). Surprisingly, in these experiments over-expressing Sod2 did not improve the motor dysfunction induced by the herbicide. In contrast, Cu,Zn-Sod was able to significantly counteract the oxidative damage in dopaminergic neurons.

These findings suggest that in presence of a chronic PQ concentration, the damage appears to be mostly related to the cytosolic production of superoxide radical, which interferes with the correct functioning of this subpopulation of neurons. As described in the Introduction, DAergic neurons seem to be particularly vulnerable to oxidative damage conditions and dopamine metabolism is widely considered the main candidate for this vulnerability. Actually, the redox chemistry of dopamine, which occurs in the cytosol, represents in itself another pathway for superoxide radicals production. As mentioned in the Section 1.2.6, after its synthesis, DA is transferred into synaptic vesicles while, approximately 10% of the total cellular DA content is present in the cytoplasm where its self-oxidation can produce both superoxide anion radicals and hydrogen peroxide (Eisenhofer et al, 2004). In this context, the presence of a ROS generator, such as PQ, could promote dopamine self-oxidation leading to a sort of vicious cycle. Accordingly, in a previous work, the concomitant administration of the herbicide with a nontoxic concentration of DA significantly increased either ROS production and cell death, supporting the hypothesis that DA itself may contribute to the vulnerability of DA neurons to PQ toxicity (Rappold et al, 2011).

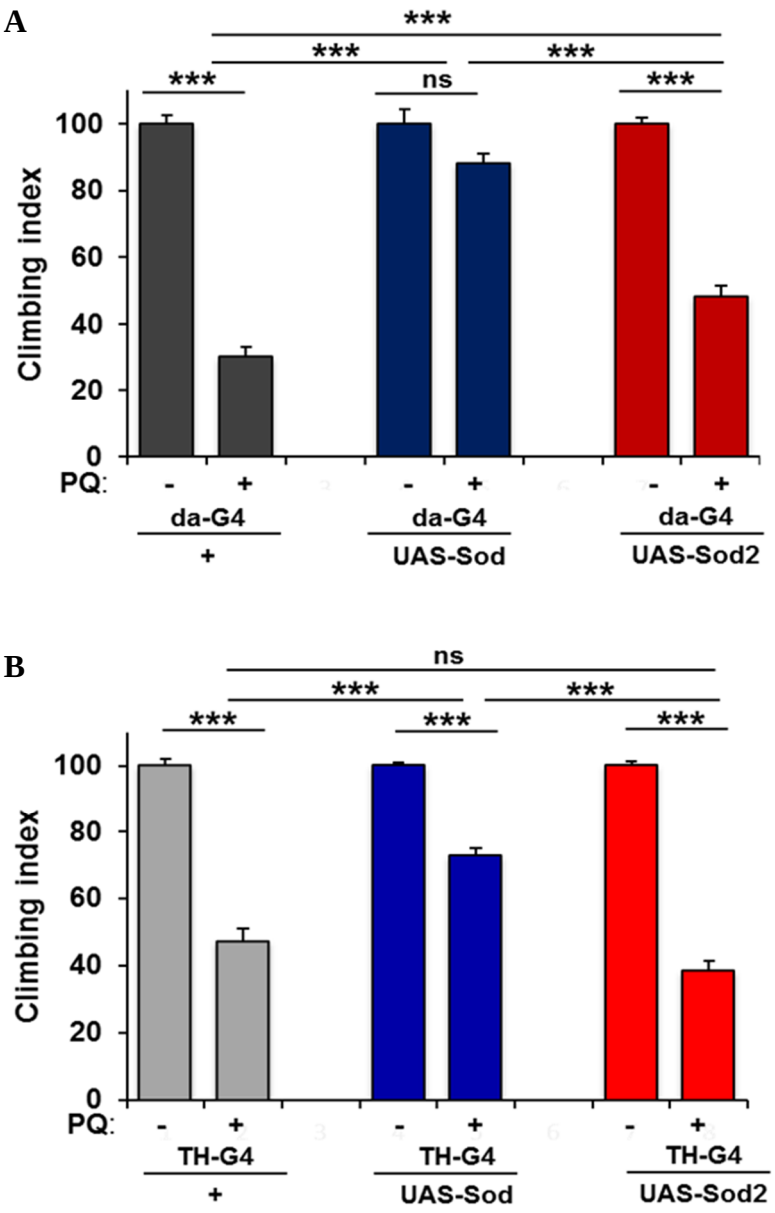

Fig.3.15. Sod and Sod2 differentially protect *Drosophila melanogaster* against PQ toxicity. The proteins were overexpressed ubiquitously through the da-GAL4 driver **(A)** or in dopaminergic neurons by means of the TH-GAL4 driver. **(B).** The locomotion behavior of flies was measured after a 7 days exposure to a sub-lethal concentration (1 mM) of PQ. Data are expressed as mean ± SEM. Statistical significance was determined by one-way ANOVA with Bonferroni correction (**p<0.01, ***p<0.001). In each experiment at least 150 flies were assessed for each genotype.

3.8 Sod mimetic compounds

The use of the SODs native proteins presents some disadvantages, such as immunogenicity and the inability to cross the BBB. To overcome these limitations, several SOD mimetics have been developed. Like the native enzymes, these molecules are able to catalytically dismutate superoxide, which represents a great advantage in comparison to other antioxidant compounds. Currently, four classes of molecules possessing SOD-like activity have been described, which include metalloporphyrin, nitroxides, Mn(III)-salen complexes and Mn(II)-pentaazamacrocyclic-based complexes (Paragraph 1.4.3). Considering that our previously reported data support the beneficial activity of SOD enzymes in both *in vitro* and *in vivo* models, in this thesis, we also investigated the potential protective effect of SOD mimetics. In particular, for each of the aforementioned classes the activity of one specific compound, namely Mn(III)TMPyP, Tempol, EUK-134 and M40403, has been studied. Before testing their protective effects, the specific activity of each molecule has been measured through a widely used assay based on cytochrome c (McCord, 2001). In this assay, superoxide anion reduces cytochrome c resulting in the increase of its absorbance at 550 nm. This assay allows an indirect quantification of SOD activity based on the competition for superoxide between cytochrome c and the competitors, SOD or SOD mimetics, producing a measurable decrease of cytochrome reduction rate (Fig.3.16A). The slope of this lines obtained by plotting the temporal evolution of absorbance represents the % of inhibition of cytochrome c reduction induced by each compound. Therefore, by plotting the % of inhibition versus SOD concentrations an hyperbolic curve was obtained that allowed to calculate the specific activity of each drug (Fig.3.16B). Commercial human SOD1 was used as control to compare the measured activities. The results obtained by these experiments are summarized in Tab.3.2. All the molecules tested showed scavenger/catalytic activity against superoxide anions, although their specific activity was lower than human SOD1 enzyme. Among them, the porphyrin Mn(III)TMPyP was the most active compound while Tempol was the least active; actually its activity is approximately 26000 times lower than the SOD1.

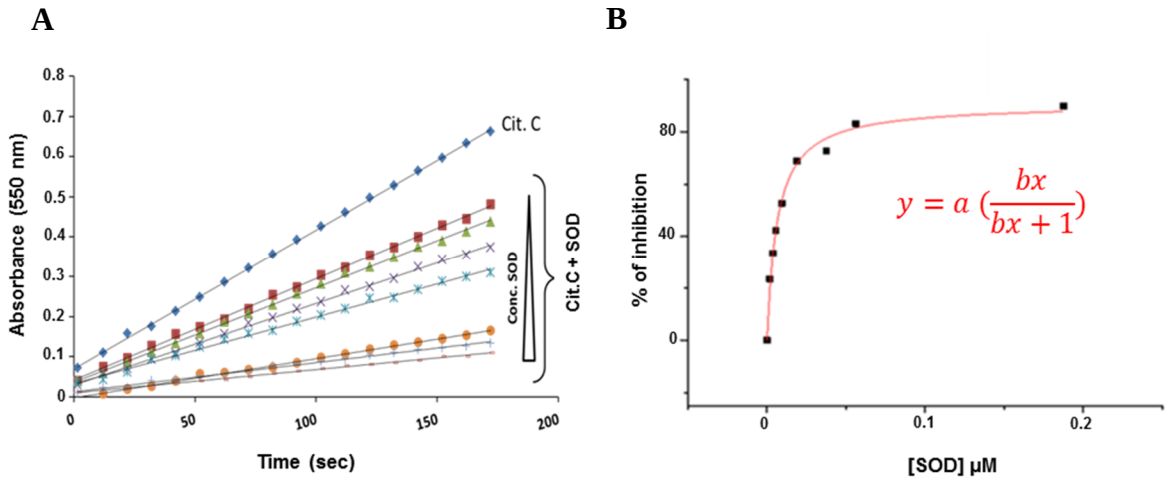

Fig.3.16. Rapresentative graphs of cytochrome c reduction assay (A) Rapresentative lines of cytochrome reduction obtained by plotting the temporal evolution of absorbance (550 nm). The presence of a competitor for superoxide, such as SOD1,induce a slope decrease was observed. **(B)** Rapresentative rectangular hyperbolic curve prepared by plotting the % of inhinition versus concentration of SOD or SOD mimetics.

	units/µmol
SOD1	158 ± 6
Mn-TmPyP	31 ± 7
M40403	0.44 ± 0.06
EUK-134	0.15 ± 0.01
Tempol	0.006 ± 0.001

Tab.3.2. Specific activity (units/µmol) of the SOD-mimetic molecules. These data were calculated by the previous curve and are expressed as mean ± SEM of at least three indipendent experiments.

3.9 Beneficial effect of M40403 against PQ toxicity in SH-SY5Y cells

Once the specific activity of each compound was established, their potential protective effect against PQ toxicity was investigated in SH-SY5Y cells. Considering that the four compounds interfered with the CCK-8 colorimetric assay, their antioxidant activity was tested through cytofluorimetric measurements. Specifically, cell cultures were treated with 500 μM PQ for 48 hours in presence or in absence of these SOD mimetics. The concentration to be used for each drug has been established based on their specific activity: we added in the medium the same catalytic units for each molecule. Therefore, the final concentrations utilized in these experiments were: 150 nM Mn-TMPyP, 10 μM M40403, 25 μM EUK-134 and 800 μM Tempol. In Fig.3.17, the results of these analysis showed that, among the different drugs used, only M40403 was able to significantly rescue PQ toxicity.

Consistent with our observations, a recent work demonstrated that, in SH-SY5Y cells, the metalloporphyrin Mn-TMPyP failed to reduce either ROS accumulation and cell death induced by PQ (Rodriguez-Rocha et al, 2013). Meanwhile, Mollace *et al.*, demonstrated that in rat microinfusion of PQ into the SN was followed by an increased lipid peroxidation, which was rescued by pre-treatment with the novel SOD mimetic M40401, analog of M40403 used in the present study (Mollace et al, 2003). In contrast with our results, in literature it has been demonstrated that also Tempol and EUK-134 can have a protective effects rescuing PQ toxicity. Indeed, it has been previously reported that in a renal cellular model the nephrotoxic action extended by PQ was significantly reduced by treatment with EUK-134 and tempol (Samai et al, 2007). Additionally, it has been shown that pretreatment of DAergic cultures *in vitro* as well as an *in vivo* systemic treatment of with SOD/Catalase mimetic, EUK-134 , conferred neuroprotection against selective PQ-mediated DAergic cell loss (Peng et al, 2005).

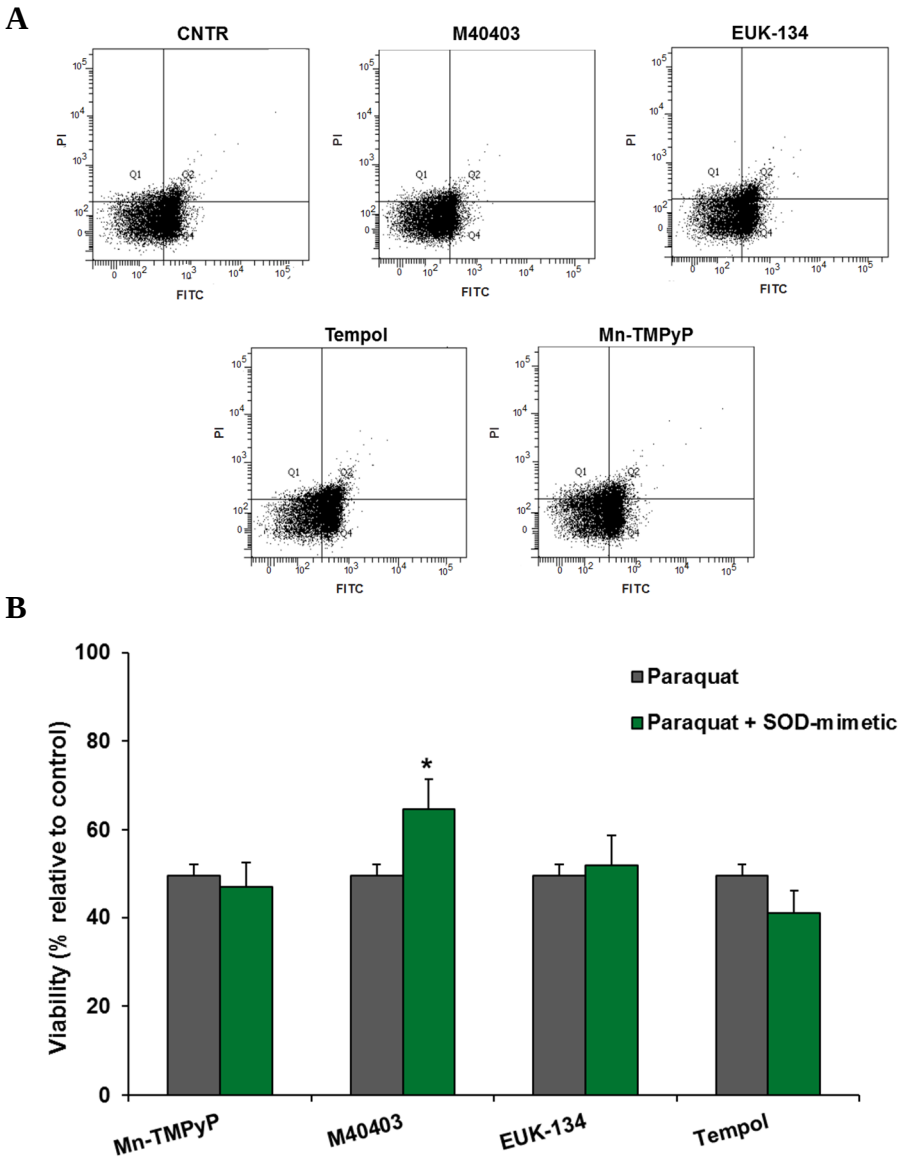

Fig.3.17. The SOD-mimetic M40403 rescues PQ toxicity in SH-SY5Y cells. Cytofluorimetric analysis carried out on WT cells, treated for 48 hours with 500 μM PQ in the absence or presence of the different SOD-mimetic compounds. Before analysis cells were labeled with PI and annexin V-FITC and 10^4 cells were analyzed for each condition. **(A)** Dot plots PI vs FITC. .. The staining pattern resulting from the simultaneous use of these dyes allows to distinguish viable, apoptotic and necrotic cells. Plots are divided in four regions corresponding to viable (PI/FITC -/-; Q3), apoptotic (PI/FITC -/+; Q4), late apoptotic (PI/FITC +/+; Q2) and necrotic (PI/FITC +/-; Q1) cell populations .**(B)** Quantification of cell viability (PI/FITC -/-, Q3 events) relative to WT cells. Data are expressed as mean of at least three different experiments ± SEM. Statistical significance was determined by t-test comparing cells exposed to PQ in absence and in presence of Sod mimetics. (*$p<0.05$).

As shown in Fig.3.11B, PQ induced profound alterations in mitochondrial morphology resulting in a severe fragmentation. Therefore, it was of interest to check the effects of M40403 on mitochondrial network upon 24 hours exposure to PQ. As reported in Fig.3.18, the presence of M40403 significantly reduced mitochondrial fragmentation induced by PQ and, concurrently, increase the number of cells presenting a tubular shape.

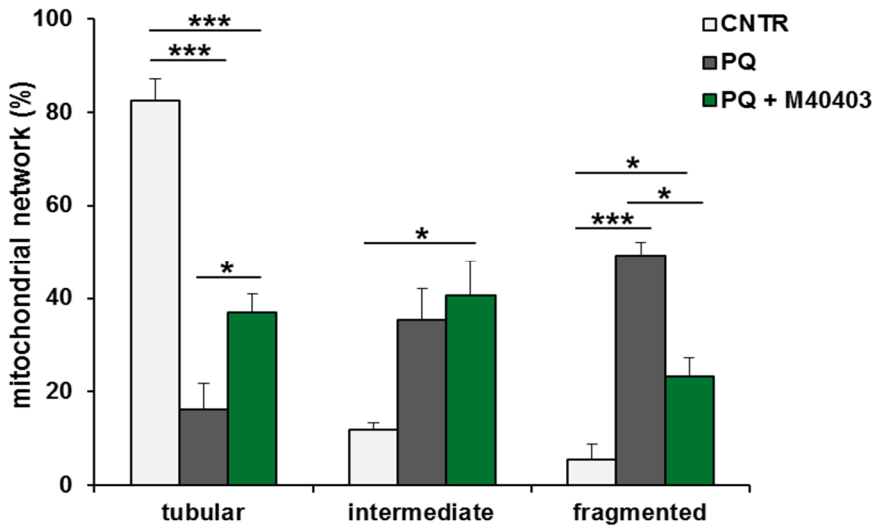

Fig.3.18. M40403 rescues mitochondrial fragmentation induced by PQ. SH-SY5Y cells were transfected for 24 hours with mito- RFP, which allowed visualizing the mitochondrial network. Afterwards samples were treated with 500 μM PQ in the absence or presence of M40403 and compared with untreated sample (CNTR). Images were acquired using epifluorescence microscope with a magnification of 100x. Mitochondrial network was scored as follows: fragmented, small and round; intermediate, mixture of round and shorter tubular; and tubular, long and higher interconnectivity. The percentage of cells with a specific mitochondrial network was determined as a percentage of the total number of transfected cells counted (≥50 cells per experiment). The data analysis was performed in a blind manner. Data are expressed as mean ± SEM of 3 independent experiments. Statistical significance was assessed by One way ANOVA with Bonferroni correction (*$p<0.05$, **$p<0.01$, p***<0.001).

To summarize, these findings support the hypothesis that the use of this class of novel and selective SOD mimetics may be helpul in the prevention of oxidative injury associated to neurodegenerative disorders such as PD.

3.10 Protective role of M40403 against PQ in *Drosophila*

The antioxidant activity exerted by M40403 against PQ toxicity was also investigated *in vivo* in *Drosophila* flies. Once again the two different conditions of treatment previously discussed, lethal and chronic, have been analyzed. First, fly survival was evaluated by exposing flies to 5 mM PQ in the absence or presence of M40403 (200 μM and 1 mM). Consistent with the results presented above, fly survival was strongly affected by the presence of 5 mM PQ with less than 50% of flies surviving after 4 days. The presence of M40403 increased fly survival in a dose-dependent manner and at the highest concentration used the rescue was almost complete (Fig3.19A). Afterwards, the locomotion behavior of flies after a sub-lethal exposure to PQ (1 mM for 7 days) was assessed in the absence or presence of SOD mimetic. As expected, PQ administration strongly affected motor performance (Fig.3.19B), however the presence of M40403, at both concentration tested, resulted in a significant improvement of the climbing ability. These data confirmed the rescuing activity of this compound against oxidative stress generated through acute or chronic PQ exposure.

It is worth mentioning that, in previous experiments, Magwere and colleagues tested the effects of feeding with the superoxide dismutase (SOD) mimetic drugs, EUK-8, EUK-134 and the mitochondria-targeted mitoquinone, on lifespan and oxidative stress resistance in *Drosophila* flies. Instead of a beneficial effect, all these drugs showed a dose-dependent increase in toxicity that was exacerbated in the presence of PQ (Magwere et al, 2006). In light of these observations, the protective activity of M40403 that we observed, *in vivo*, against PQ toxicity should be considered particularly relevant.

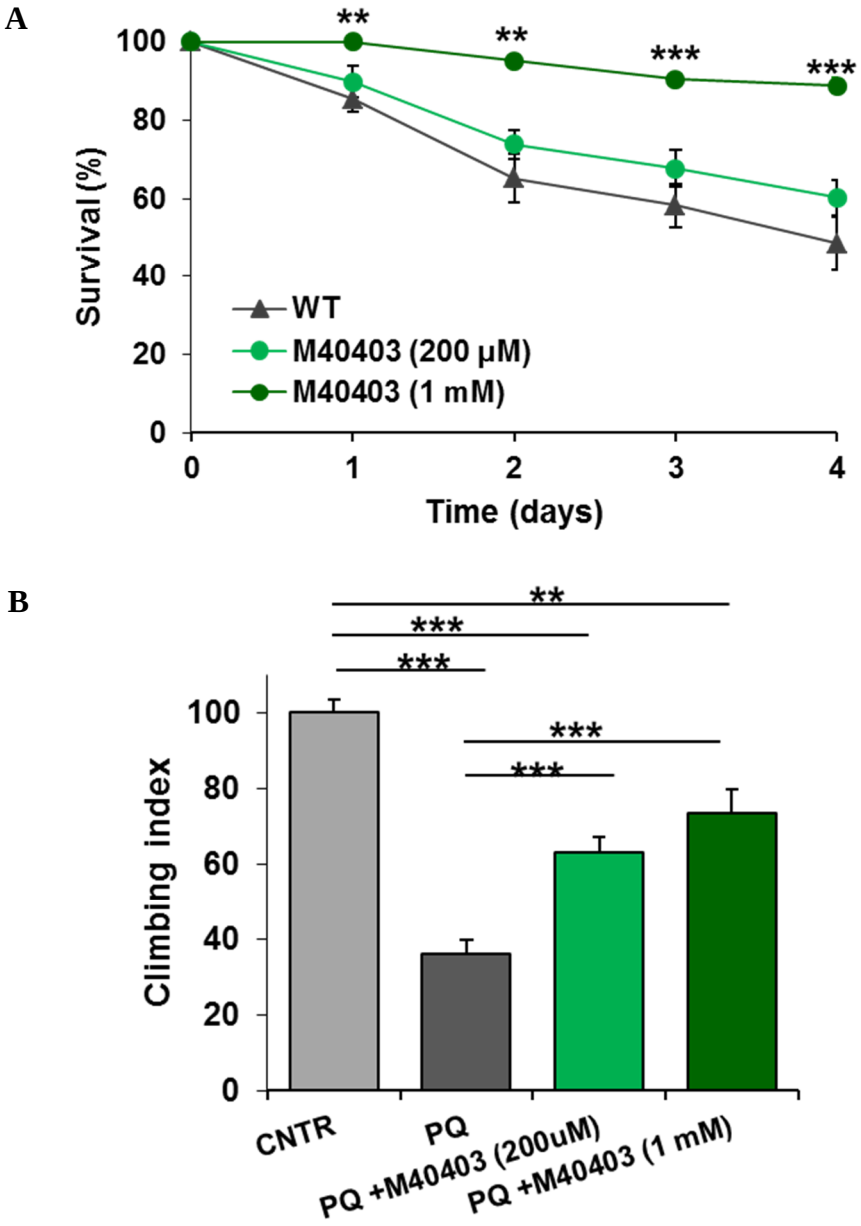

Fig.3.19 M40403 rescues PQ toxicity in flies. (A) Survival of wild type *Drosophila* (w, Dah) was monitored upon exposure to 5 mM PQ, in the absence or presence of different amounts of M40403. **(B)** Locomotion behaviour of wild type flies was analyzed after treatment with a sub-lethal concentration (1 mM) of PQ for 7 days, in the absence or presence of different amounts of M40403. Data are expressed as mean ± SEM. Statistical significance was determined by one-way ANOVA with Bonferroni correction (**p<0.01, ***p<0.001). At least 60 flies were tested for each condition.

3.11 Mitochondrial fragmentation in *PINK1 knock out* cells

In the experiments discussed until now, PQ toxicity has been chosen and used as an experimental paradigm to mimic sporadic PD in cells and flies. In the next sections, the role of SODs and SOD mimetics against oxidative injury related to genetic forms of PD will be analyzed. Specifically, PINK1 deficiency has been studied as model of genetic parkinsonism *in vitro* and *in vivo* studies. As described in the Paragraph 1.3.1.3, PINK1 is serine/threonine kinase with a putative mitochondrial targeting sequence. Increasing evidence indicates that this protein regulates mitochondrial morphology and mitophagy as well as oxidative stress (Dagda et al, 2009). Actually, an impairment of the respiratory activity, an increase of lipid peroxidation and an hypersensitivity to oxidative stress have been observed in primary fibroblasts isolated from PD patients carrying PINK1 mutations (Hoepken et al, 2007). Furthermore, it has been reported that PINK1 deficiency in human DAergic neurons, obtained through the differentiation of neuronal stem cells, induced a chronic mitochondrial dysfunction and an increase in oxidative stress (Wood-Kaczmar et al, 2008). In a recent study, a novel mutation in *PINK1* gene (P209A) has been identified in a cohort of 68 patients with early onset PD. The transfection of SH-SY5Y cells with the *PINK1* P209A mutant enhanced the oxidative stress-induced cell death, supporting the involvement of this kinase in regulation of cellular oxidative status (Chien et al, 2013). Moreover, it has been demonstrated that RNA silencing of *PINK1* impacted on mitochondrial network causing fragmentation in HeLa cells. The same mitochondrial phenotype has been identified in fibroblasts of PD patients carrying mutations in *PINK1* gene (Exner et al, 2007) as well in *PINK1 knock down* SH-SY5Y cells (Dagda et al, 2009).

In this work, *PINK1 knock out* cells were generated using the *CRISPR/CAS* technology. This system is a novel powerful tool for genome editing. It is based on two distinct components: a guide RNA (gRNA) and the nuclease, Cas9. The gRNA is a combination of the CRISP target RNA (crRNA) and trans-activating crRNA (tracrRNA). It can combine the targeting specificity of the crRNA, in this case a specific sequence for PINK1, with the scaffolding/binding ability for Cas9 nuclease of the tracrRNA into a single transcript. When the gRNA and the Cas9 are expressed

in the cell, the genomic target sequence can be modified or permanently disrupted. In particular, the gRNA/Cas9 complex is recruited to the target sequence, which is present in the genomic DNA, through the complementarity with the gRNA sequence. Once this complex binds the target sequence, Cas9 can cut both strands of DNA generating a Double Strand Break (DSB). Even if DSBs can be repaired through repairing pathways, the result is very often the disruption of the open reading frame (ORF) of the targeted gene.

To obtain *PINK1 knock out* cells, two different sequences, namely KO1 and KO2, were designed. Each sequence, able to recognized a specific region of the PINK1 genomic DNA, was cloned in an expression vector, containing as gene reporter the CD4 sequence, used to label transfected cells. First, to test the ability of these sequences to induce gene disruption, HeLa cells were transfected with KO1 or KO2 plasmids. In contrast to SH-SY5Y cells, this cell line presented a higher transfection efficiency (about 80%) that permitted to evaluate the reduction of PINK1 expression level through WB analysis. After 24 hours of transfection, cells were exposed to carbonyl cyanide m-chlorophenyl hydrazone (CCCP) for 4 hours. This uncoupler was utilized to induce mitochondrial membrane depolarization, necessary for PINK1 stabilization and accumulation on the outer mitochondrial membrane. As reported in Fig.3.20, Both KO1 and KO2 sequences were able to decrease PINK1 protein levels, confirming their ability to induce gene disruption.

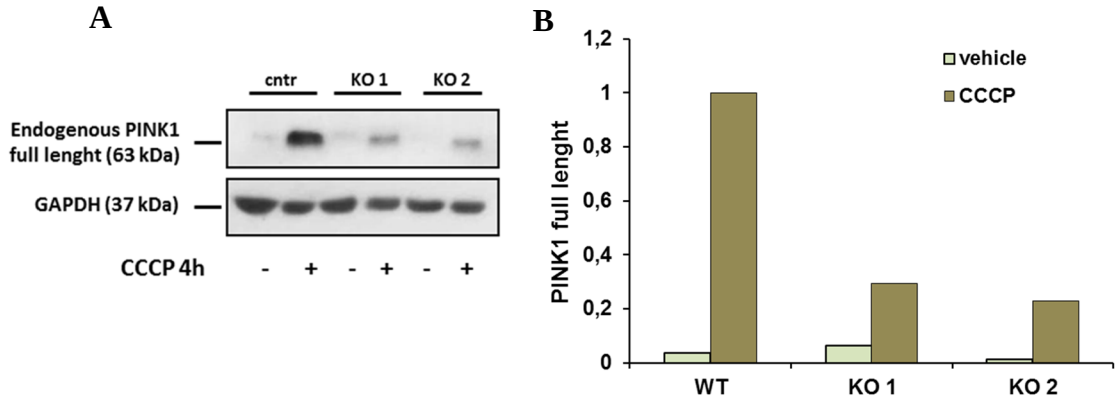

Fig.3.20 PINK1 knockout in Hela cells. Hela cells were transfected with vector containig PINK1 crispr/cas sequences (KO1 or KO2) for 24 hours and then were treated with 10 μM CCCP for 4 hours in order to have PINK1 stabilization on OMM. **(A)** Alterations in endogenous full-length protein levels were assessed by western blot in a single expreiment. **(B)** Densitometric quantification of full-length endogenous PINK1 levels using Image J. Glyceraldehyde 3-phosphate dehydrogenase (GAPDH) was used as a loading control.

Afterwards, considering that the most pronounced phenotype of PINK1 deficiency in mammalian cellular model is mitochondrial fragmentation, the effect of *PINK1 knock out* was evalauted in terms of alterations of the mitochondrial network in human SH-SY5Y cells. Therefore, cells were co-transfected with KO1 or KO2 and mito-RFP for 24 hours and then samples were fixed and stained with CD4 antibody conjugated with Alexafluor 488-antibody. Through fluorescence microscopy, the mitochondrial network in CD4+ (transfected) cells has been evaluated and compared with CD4- (untransfected) cells used as control. The quantification was obtained using the same classification previously described (Paragraph 3.6). In agreement with the aforamentioned works (Dagda et al, 2009; Exner et al, 2007), PINK1 deficiency, obtained through either KO1 and KO2 sequences, significantly affected mitochondrial network inducing fragmentation (Fig.3.21).

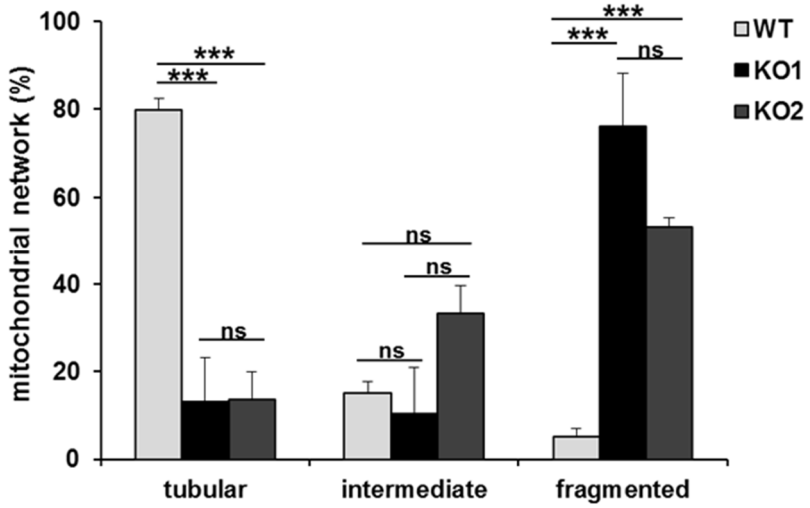

Fig.3.21. PINK1 deficiency affects mitochondrial network leading to fragmentation. SH-SY5Y cells were co-transfected for 24 hours with KO1 or KO2 and mito-RFP, which allowed visualizing the mitochondrial network. Images were acquired using epifluorescence microscope with a magnification 100x. Mitochondrial network was scored as follows: tubular, long and higher interconnectivity; intermediate, mixture of round and shorter tubular and fragmented multiple punctiform organelle. Quantification of the percentage of cells with the indicated mitochondrial network. The values represent the percentage of the total number of transfected cells counted (≥30 cells per experiment). The analysis was performed in a blind manner. Data are expressed as mean ± SEM of 3 independent experiments. Statistical significance was assessed by One way ANOVA with Bonferroni correction.

3.12 SODs reverse mitochondrial fragmentation in *PINK1 knock out* cells

The PINK1 deficiency was used as experimental paradigm to explore the effect of SODs overexpression at the level of mitochondrial morphology. Using the same protocol described above, SOD1 and SOD2 stably overexpressing cells were co-transfected with KO1 or KO2 and mito-RFP and analyzed after 24 hours. Preliminary results of these experiments are reported in Fig.3.22. Once again, the expression of the cytosolic and mitochondrial isoforms produced different effects. Indeed, while SOD1 overexpression seemed to partially reduce the mitochondrial fragmentation induced by *PINK1* gene disruption (KO1 WT and KO2 WT), increasing the number of cells with an intermediated morphology (Fig.3.22A); the

mitochondrial SOD2 appeared able to reverse mitochondrial fragmentation allowing the maintenance of a healthy mitochondrial network (Fig.3.22B).

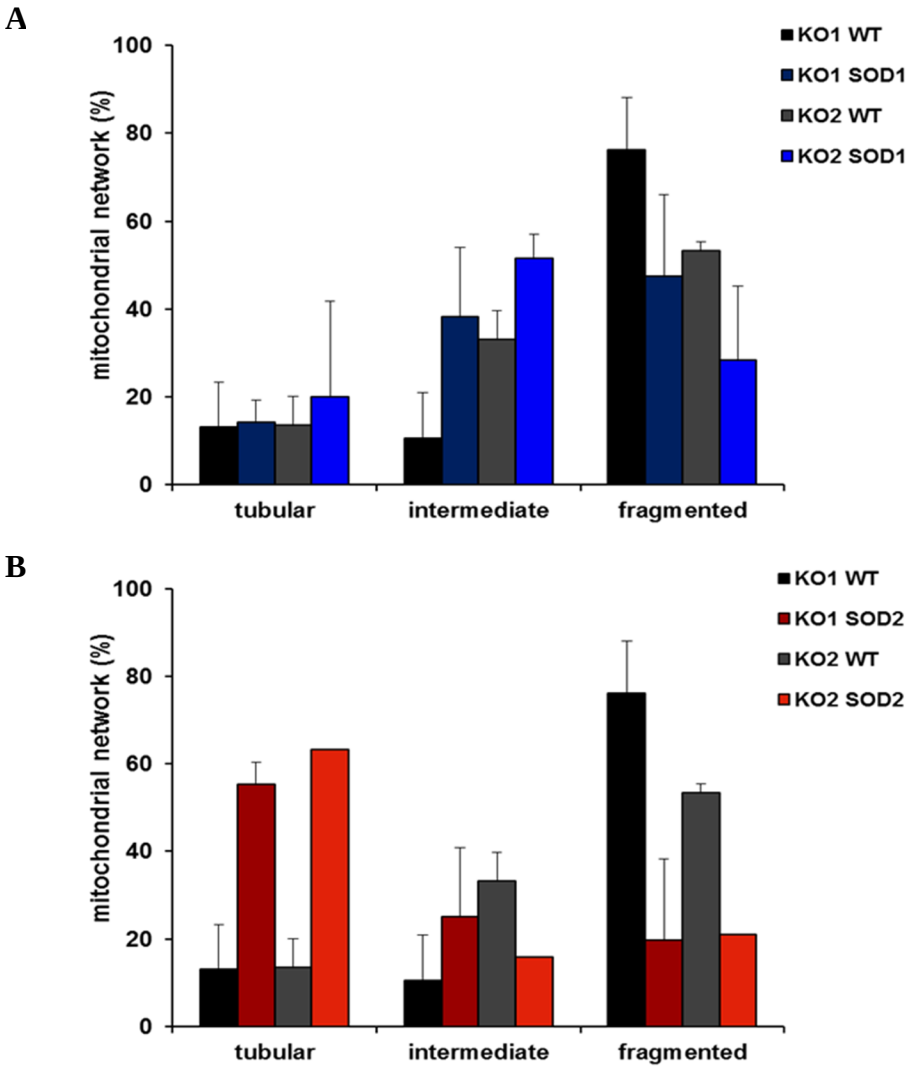

Fig.3.22. SODs overexpression appears e protective against mitochondrial fragmentation induced by *PINK1 knock out.* SH-SY5Y WT, **(A)** SOD1, and **(B)** SOD2 stably overexpressing cells were co-transfected for 24 hours with KO1 or KO2 and mito-RFP, which allowed to visualize the mitochondrial network. Images were acquired using epifluorescence microscope with a magnification of 100x. Mitochondrial network was scored as follows: tubular, long and higher interconnectivity; intermediate, mixture of round and shorter tubular and fragmented multiple punctiform organelle.. The values represent the percentage of the total number of transfected cells counted (≥30 cells per experiment). Data are expressed as mean ± maximum error of two independent experiments.

If these results will be further confirmed, they support the involvement of oxidative stress and, specially of superoxide anion, in the mitochondrial fragmentation in *PINK1 knock out* cells. Coherently with the observed SOD2 protection, it has been previoulsy reported that, in SH-SY5Y cells, *PINK1 knock down* increased the level of mitochondrial superoxide which, in turn, promoted mitochondrial fragmentation. Indeed, superoxide has been proposed an essential mediator in triggering fragmentation of the mitochondrial network (Dagda et al, 2009). Moreover, it has been demonstrated that the absence of PINK1, in SH-SY5Y cells and in human neurons derived from fetal mesencephalic stem cells, was associated with a significant increase of ROS production in two separate sites, the mitochodria and the cytosol (Gandhi et al, 2009). These observations revealed the involvement of both these compartment in oxidative stress linked to PINK1 dysfunction and might explain the partial protective effect of SOD1 overexpression.

3.13 Sod recues motor deficits in *Drosophila* PINK1 mutants

To investigate the role of PINK1, several animal models have been generated. Among them, *Drosophila PINK1* mutants exhibited a strong phenotype that included shorter lifespan, male sterility, motor impairment, muscle and DAergic neuron degeneration. Additionally, at mitochondrial level these flies revealed prominent defects, such as enlarged and swollen mitochondria, fragmented cristae, decreased ATP production (Clark et al, 2006). Therefore, *Drosophila* is considered a valid animal model which recapitulates mitochondrial dysfunction and age-related neuronal death observed in PD patients. To evaluate the involvement of oxidative stress in *PINK1* mutant flies ($PINK1^{B9}$), the previously described UAS/GAL4 system was used to overexpress Sod and Sod2 in an ubiquitous manner via the da-GAL4 driver. RT-PCR was first used to verify the overexpression of each Sod isoform (Fig.3.23A). Afterwards, the protective function of each enzyme was examined by taking into consideration the ability to improve the motor performance of the mutants ($PINK1^{B9}$/Y; da/+). Our results indicated that Sod and Sod2 overexpression produced a very different and selective effect. Surprisingly, climbing assays showed that, while the mitochondrial isoform did not ameliorate the motor impairment, the

overexpression of the cytosolic Cu,Zn-Sod increased locomotor activity of PINK1^{B9}mutant flies (Fig.3.23B).

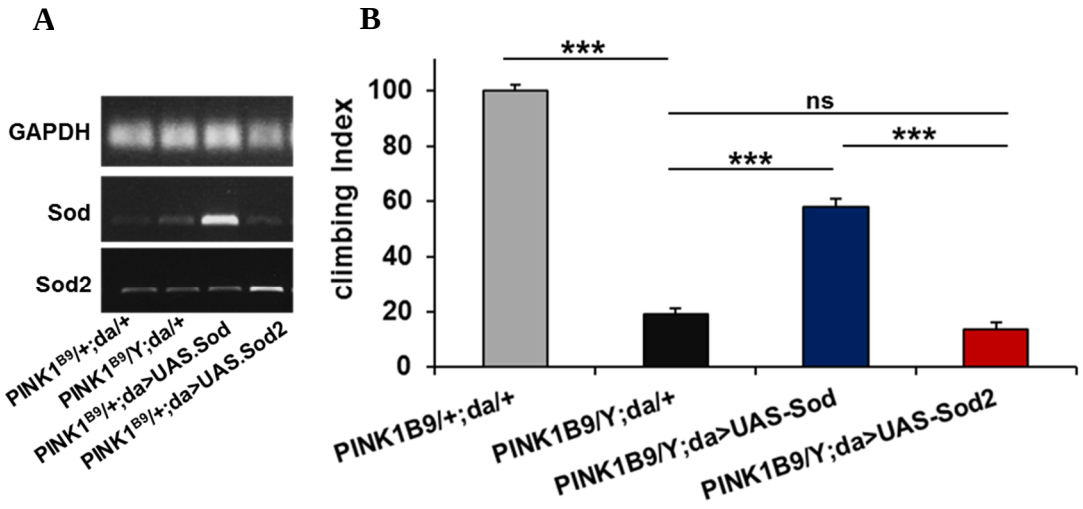

Fig.3.23 Sod overexperssion partially rescues PINK1^{B9} motor impairment. (A) Ubiquitous Sod and Sod2 overexpression in mutant flies was verified by semi-quantitative RT-PCR analysis. The da-GAL4/UAS system was used to ubiquitously drive the expression of either Sod or Sod2 in flies. GAPDH mRNA level was used as loading control. **(B)** Locomotion behavior of PINK1^{B9}/Y; da/+ flies (male mutants) was analyzed and compared with PINK1^{B9}/+;da/+ (females used as control) trought climbing assay. PINK1^{B9}/Y;da>UAS.Sod flies presented an improvement of motor dysfunction; while PINK1^{B9}/Y;da>UAS.Sod2 flies behaved as PINK1^{B9} mutants. Climbing assays were performed with 1-2 day old flies. Data are expressed as mean ± SEM. Statistical significance was determined by one-way ANOVA with Bonferroni correction (*p<0.05, **p<0.01, ***p<0.001). For each genotype at least 150 flies were tested.

Our data are in agreement with a previous work in which the overexpression of human SOD1 was able to rescue the degeneration of DAergic neurons in *PINK1 RNAi* fly lines, although the mechanism underlying the selective protection extended by cytosolic Sod, *in vivo*, remains unclear (Wang et al, 2006). To date, several studies demonstrated the involvement of PINK1 in maintaining mitochondrial homeostasis (Chu, 2010); however, our *in vitro* and *in vivo* results suggest another possible action of this kinase in the regulation of oxidative stress through other processes not directly connected to mitochondria functioning and maintenance.

Indeed, although PINK1 is predominantly localized in mitochondria, this protein can also be found in the cytoplasm (Weihofen et al, 2008), where it might be involved in different molecular pathways. For instance, recently a novel function of the cytosolic PINK1 has been proposed (Zhou et al, 2014), in which the kinase, controlling negatively the TH and DA levels in DAergic neurons, regulates the sensitivity to oxidative stress. According to this hypothesis, PINK1 dysfunction promotes an up-regulation of DA synthesis and content, which might strongly increase the cytosolic ROS production.

3.14 M40403 reverses mitochondrial alterations in *PINK1 knock out* cells

To investigate whether M40403 was able to rescue the mitochondrial fragmentation observed in PINK1 deficient cells, SH-SY5Y cells were co-transfected with KO1 or KO2 and mito-RFP in presence or absence of 10 μM M40403. The effect of this compound on mitochondrial network was then analyzed through fluorescence microscopy, as previously described. When cells were transfected with the KO1 sequence, M40403 decreased the fragmentation increasing the intermediate shape. On the contrary, when the *knock out* was induced by the KO2 sequence, of the presence of M40403 increased the percentage of cells with the tubular shape with a concomitant reduction of those with an intermediate morphology. Even though the results obtained with the two sequences used are different, they both indicate a protective effect of M40403. Although further analyses are required to validate the effect, our preliminary data suggested that this treatment with M40403 was slightly protective rescuing the mitochondrial phenotype due to the absence of PINK1.

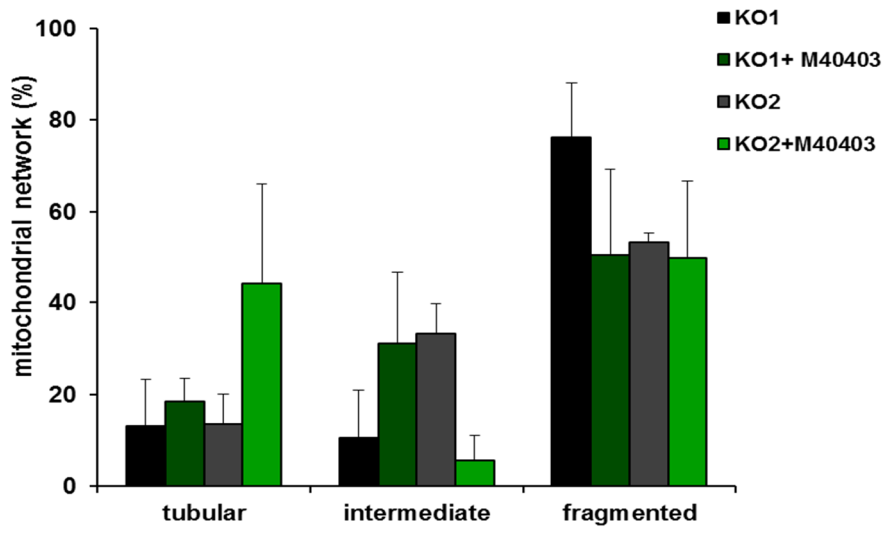

Fig.3.24 M40403 seems to partially ameliorate the mitochondrial fragmentation due to the loss of PINK1. SH-SY5Y cells were co-transfected for 24 hours with KO1 or KO2 and mito-RFP, which allowed to visualize the mitochondrial network. Images were acquired using an epifluorescence microscope with a magnification of 100x. Mitochondrial network was scored as follows: tubular, long and higher interconnectivity; intermediate, mixture of round and shorter tubular; fragmented, multiple punctiform organelles. Quantification of the percentage of cells with the indicated mitochondrial network. The values represent the percentage of the total number of transfected cells counted (≥30 cells per experiment). Data are expressed as mean ± maximum error of two independent experiments.

3.15 M40403 administration improves motor performance in *PINK1* fly mutants

Considering the promising results obtained by overexpressing Sod proteins in *PINK1* fly mutants and in light of the partial beneficial activity of M40403 in rescuing PINK1 deficiency *in vitro*, the activity of this SOD mimetic has been further explored in *Drosophila PINK1* mutants. Immediately after eclosion, these flies exhibited an abnormal wing posture associated with muscle degeneration. For this reason, while, PQ and M40403 were previously administered to adult flies using a sucrose/drug-soaked filter paper, in these experiments M40403 was administered during the larval phase (from mating to eclosion). adding the drug directly to the solid standard food. The thermal stability of the SOD mimetic has been first assessed at 70°C, temperature necessary to melt fly food (data not shown). As it is well known that during larval stage, flies eat more than in the adulthood, treatments carried out

during this phase are usually used with lower doses of drug than in adult administration, for instance see (Tain et al, 2009). Thus,, the drug was tested in *PINK1* mutants using increasing concentrations (0.01-0.3 mM). Our results indicated that this treatment resulted in a significant suppression of the climbing deficits in *PINK1* mutant flies (Fig.3.25), although other pathological phenotypes, such as thorax indentations and abnormal wing posture, were still evident.

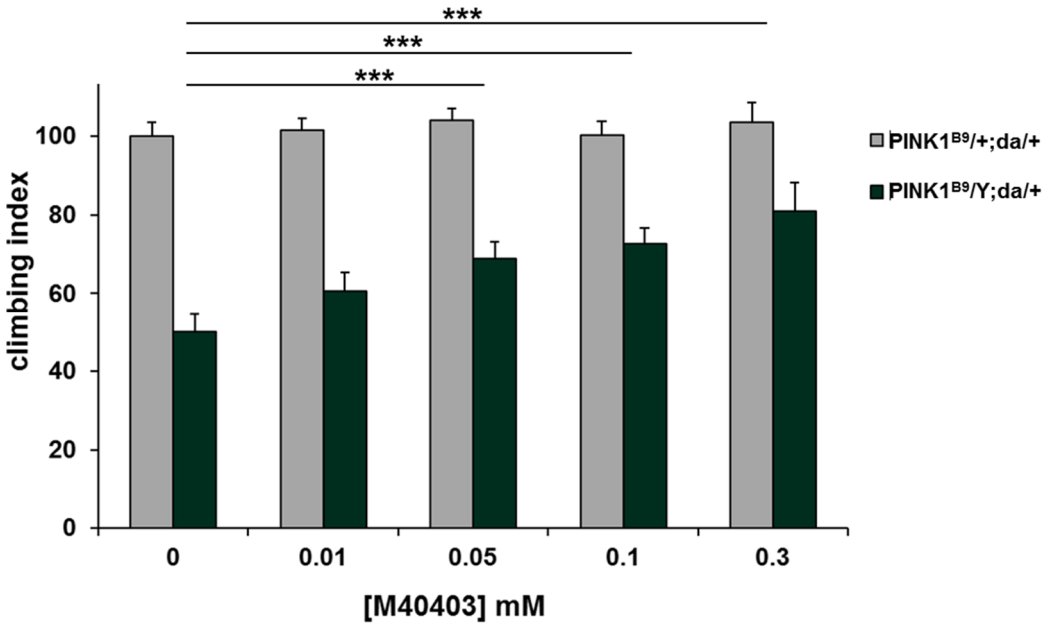

Fig.3.25 The M40403 SOD-mimetic rescues PINK1^{B9} motor impairment. PINK1^{B9}/Y; da/+ flies (male mutants) PINK1^{B9}/+; da/+(females used as control) were fed from mating to enclosion with a medium containg increasing concentrations (0.01-0.3 mM) of drug. 0-4 day old flies were collected and used to assess climbing index. The exposure to M40403 significantly restored motor dysfucntion in PINK1^{B9}/Y; da/+ flies in a dose dependent manner; while, its presence did not have any effect on control flies. Data are expressed as mean ± SEM. Statistical significance was determined by one-way ANOVA with Bonferroni correction multiple comparison- selected pairs (***p<0.001). For each genotype at least 40 flies were tested.

Our observations might be considered particularly relevant because for the first time the exposure to a SOD mimetic proved to rescue significantly one of the most pronounced phenotypes, which characterized *Drosophila PINK1* mutants.

3.16 Lethality rescue by M40403 in Sod- and Sod2- *knock down* flies

Overall, from the results presented it appears evident that M40403 was able to act similarly to SOD2 in scavenging superoxide radicals produced at mitochondrial level through acute exposure to PQ and PINK1 deficiency. Additionally, the protection exerted by this SOD mimetic against PQ sub-lethal treatment as well as PINK1 loss of function in flies supported the hypothesis that the drug could act also at cytosolic level. To address this important issue and to better characterize the properties of this molecule, its protective activity has been tested in Sod and Sod2 deficient flies, generated through the transgenic RNAi technology coupled with the da-GAL4 driver. The ubiquitous down-regulation of the enzymes has been described to lead to early adult mortality and elevated endogenous oxidative damage production (Kirby et al, 2002; Wicks et al, 2009). The survival of each fly line was assed and was comparable, with a median survival of 13 days. The treatment of these flies with M40403 increased the survival for both genotypes, but with differential effects. In the case of Sod-deficient flies, the presence of M40403 appeared to be strongly protective in the first period of treatment (12 days), after which the survival rapidly decreased reaching the values similar to the untreated flies (Fig.3.26A). In contrast, the drug was not able to reduce the mortality of Sod2-deficient flies in the first period of treatment but showed protection starting from the 6th day until the end of the experiment (Fig.3.26B). The survival distribution of the untreated and M40403-treated flies was compared through the logrank test, which indicated that in both cases the two curves are significantly different ($p=0.004$ and $p<0.001$ for Sod-and Sod2-knockdown flies, respectively).

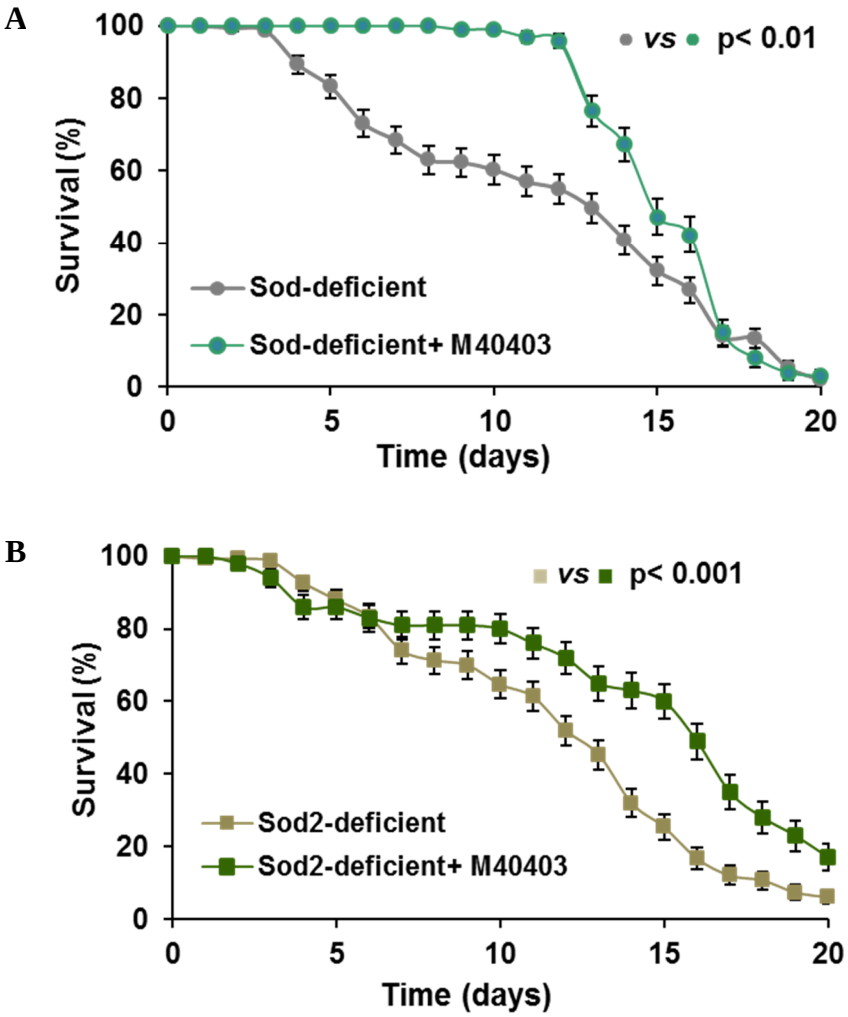

Fig.3.26. The M40403 SOD-mimetic rescues the lethality in Sod- and Sod2-deficient flies. Sod- and Sod2-knockdown flies were generated through the expression of a UAS inverted repeat transgene, to induce RNA interference, coupled with the da-GAL4 driver. The survival of **(A)** Sod- or **(B**) Sod2-deficient flies was measured over a period of 20 days in the absence or presence of 1 mM M40403. The survival distribution of the untreated and M40403-treated flies was compared using the logrank test.

In conclusion, the data presented here indicated that the SOD-mimetic molecule M40403 is able to partially rescue, *in vivo*, the loss of either Sod or Sod2 suggesting that it can act both at cytosolic and mitochondrial level. Nevertheless, as that mitochondria are widely considered the primary source or ROS, recently a mitochondria-targeted SOD mimetic, MitoSOD, was synthesized by conjugating M40403 with a mitochondria-targeting triphenylphosphonium group (Kelso et al, 2012). Using energized mitochondria it has been demonstrated a greater uptake of

MitoSOD than M40403. Even if M40403 uptake seemed negligible, the results obtained in this thesis support at least a partial mitochondrial uptake.

Overall, the potential ability of M40403 to act both at mitochondrial and cytosolic level could have a particular importance when cytosolic processes contribute to and exacerbate the production of superoxide radicals, as supposed in our experimental paradigms. Thus, from a therapeutic point of view the use of a SOD mimetic less selective and not specific for mitochondrial import, like M40403, could be more advantageous.

Chapter 4

Results and Discussion

Neuroblastoma cell lines as in vitro models for catecholaminergic neurons

A s mentioned in the Introduction (Paragraph 1.5), cellular models are largely used to study *in vitro* the molecular mechanisms underlying the preferential DAergic cell death, that affects PD patients. This selective loss might be correlated to the dopamine metabolism itself; thus, a suitable and reliable cellular model should exhibits a DAergic phenotype. Beside the use of primary rodent cells or of stem cell-derived dopaminergic neurons, an alternative cell system is represented by human neuroblastoma cells. These cell lines have a number of advantages that make them useful as models: they are easy to obtain and to grow using standard tissue culture plastic and media, and they can be stored indefinitely in liquid nitrogen. In addition, they continuously divide and can provide the required quantity of cells for different experiments, without exhibiting a large variability. The downside of these cell lines is the lack of many features that define neurons, including neuronal morphology, inhibited cell division, and expression of neuron-specific markers (Andres et al, 2013). Hopefully, neuronal cell lines can be induced to differentiate by adding different drugs or growth factors to the media. Differentiation results in non-dividing cells with many of the characteristics of a neuron, including the extension of neurites.

The human neuroblastoma SH-SY5Y cell line has been largely used in neuroscience research and, in particular, as a PD cell system (Lopes et al, 2010; Xie et al, 2010). These cells, which were subcloned from the SK-N-SH cell line, are neuronal in origin, express tyrosine hydroxylase (TH) and exhibit moderate levels of dopamine-β-hydroxylase (DßH) activity, specific for noradrenergic (NAergic) neurons (Ross et al, 1983). A variety of agents, including retinoic acid (RA) (Pahlman et al, 1984), phorbol ester 12-O-tetradecanoylphorbol-13-acetate (TPA) (Pahlman et al, 1981; Pahlman et al, 1983), brain-derived neurotrophic factor (Spinelli et al, 1982), dibutyryl cyclic AMP (Kume et al, 2008) and staurosporine (Jalava et al, 1992) have been used to induce differentiation. Much less is known about the BE(2)-M17 cell line. These cells have been cloned from the SK-N-BE(2) neuroblatoma cell line isolated from a 2 years old male. Even though the first biochemical characterizations of these cells date back to the 80s (Ciccarone et al, 1989; Rettig et al, 1987), their use has been limited, most probably because of the larger diffusion of the SH-SY5Y cell line. However, little research has been

performed on the analysis of the DAergic pathway of BE(2)-M17, in both undifferentiated and differentiated state.

In this chapter, results concerning the neuronal differentiation of SH-SY5Y and BE(2)-M17 will be presented. Even though SH-SY5Y cells are largely adopted in PD studies, the phenotype acquired after differentiation is still debated, because of their ability to synthetize different neurotransmitter, including the catecholamines DA and noradrenaline (NA). For this reason, we decided to re-evaluate morphological and neurochemical changes induced by neuronal differentiation in this cell line. In addition, we analyzed and characterized the phenotype of BE(2)-M17 cells before and after differentiation. To this aim, here we investigated the capability of three differentiating agents, TPA, RA and staurosporine, to drive the differentiation toward a DAergic phenotype in terms of growth inhibition, morphological properties, expression profiles of genes involved in catecholamine synthesis and storage and the cellular content of the neurotransmitters DA and NA. TPA, RA, and staurosporine have been selected on the basis of their inexpensiveness and ease of manipulation. Each of these compounds induces differentiation through a different mechanism. RA regulates neurite outgrowth and growth inhibition through the regulation of the transcription of neurotrophin receptors, modulation of the Wnt signaling pathways and participation of type II protein kinase A (Xie et al, 2010). The differentiating properties of TPA and staurosporine are primarily mediated by protein kinase C (PKC) isoforms. Nevertheless, TPA is a PKC activator, while staurosporine is a potent PKC inhibitor (Leli et al, 1992).

3.1 Effect of differentiation on growth inhibition

Upon differentiation, SH-SY5Y and BE(2)-M17 cells can cease to proliferate, becoming a stable population with morphological similarity to neuronal cells, such as an extensive neurite outgrowth. To find the optimal experimental conditions for differentiation, growth inhibition was first evaluated in both cell lines, using various concentrations of each differentiating agent. On the basis of previous reports on SH-SY5Y cells (Jalava et al, 1992; Pahlman et al, 1984; Pahlman et al, 1983) the following ranges of concentration were tested: 1.5-150 nM for TPA, 1-50 μM for RA

and 3-15 nM for staurosporine. Consistent with the literature results, in the case of SH-SY5Y cells, we observed that the most pronounced effects on growth inhibition were obtained with 15 nM TPA, 10 μM RA and 10 nM staurosporine. With BE(2)-M17 cells the most effective concentrations found were 30 nM TPA, 5 μM RA and 8 nM staurosporine, not much dissimilar from those obtained for SH-SY5Y cells.

Cells were then treated with the optimized concentration of each differentiating agent for 4 and 7 days and growth inhibition was assessed by cell counting using a hemocytometer. As shown in Fig.3.1, all of the drugs altered cell proliferation, but with variable efficiency depending on the treatment and on the cell line. In the case of SH-SY5Y, after 4 days the inhibition levels in the presence of RA and TPA were very similar (~40%), whereas RA promoted a more marked effect compared to TPA after 7 days (~70% and ~45%, respectively). Interestingly, staurosporine induced the most pronounced inhibition. In fact, after 4 days treatment, cell proliferation was almost completely blocked with a growth inhibition of ~80%, and the effect became more evident after an incubation time of 7 days (~95%) (Fig.3.1A). The results obtained with BE(2)-M17 cells were quite different. After 4 days of treatment, the effects of staurosporine were almost absent while the growth inhibition in the presence of TPA reached ~20%. The strongest inhibition (~40%) was obtained in the presence of RA. After 7 days, RA still induced the strongest inhibition (~70%), whereas staurosporine promoted a more marked effect compared to TPA (~45% and ~20%, respectively), although very small in comparison with the effects observed on SH-SY5Y cells (Fig3.1B). In agreement with other studies (Constantinescu et al, 2007; Mattsson et al, 1984), in SH-SY5Y cells, TPA only partially inhibits cell growth and was less effective than staurosporine, which arrested proliferation almost completely. Indeed, in literature it has been reported that staurosporine, used in a range between 10 and 25 nM, induced a total inhibition of DNA synthesis in SH-SY5Y cell line, coherently with the complete block of cell proliferation observed here (Constantinescu et al, 2007). A different response was obtained in BE(2)-M17 cultures, where RA resulted the most effective agent in arresting cell cycle.

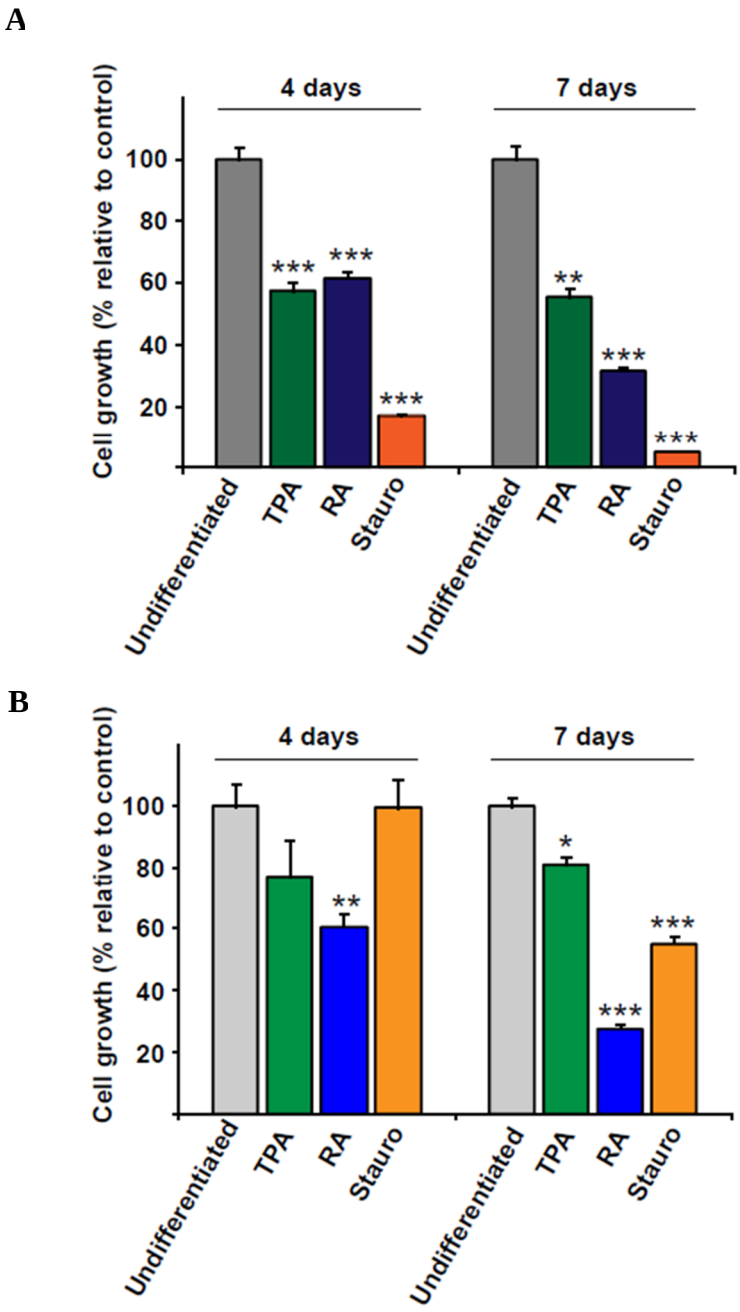

Fig.3.1. Cell growth of undifferentiated and differentiated SH-SY5Y and BE(2)-M17 cells. Cell growth has been evaluated after 4 and 7 days of differentiation in **(A)** SH-SY5Y **(B)** BE(2)-M17 All the examined drugs inhibited cell proliferation. In SH-SY5Y, the effect of staurosporine was the most pronounced, while in BE(2)-M17 the strongest inhibition was achieved with RA treatment. Data are expressed as mean ± S.E.M. of three experiments. Differences between differentiated and undifferentiated were tested for significance using Student's t-test. *(*P<0.05, **P<0.01, ***P<0.001).*

3.2 Morphological differentiation and neurite outgrowth

Neuronal differentiation is also associated with the acquisition of a specific morphology characterized by a small cell body, called soma, which contains the nucleus, and specialized elongated neuritic processes arising from the soma. In this work, the effects of the treatment with TPA, RA and staurosporine have been further analyzed in their ability to induce morphological changes.

Undifferentiated SH-SY5Y neuroblastoma cells display a characteristic morphology with rounded cell bodies and few short processes (Fig.3.2A). A similar morphology is also present in undifferentiated BE(2)-M17 cells although they are smaller and the processes are less evident (Fig.3.2B). To explore whether and how the differentiation alters cell morphology, cells were treated with TPA, RA or staurosporine for 7 days. After treatment, cells were analyzed using a phase contrast light microscope. Depending on the chemical used, cells displayed different levels of neurite length and branching. Differentiation induced by TPA resulted in the formation of short processes only in both cell lines. In contrast, both RA- and staurosporine-differentiated cultures showed a morphology more similar to neurons with a complex network of neuritic extensions.

To better characterize the morphological changes and to quantify the effect of each differentiating agent in terms of neurite outgrowth, cells were transfected with a cytosolic fluorescent probe that allowed tracking of the neurites at single-cell level. Three parameters were used to analyze the outgrowth of neurites: i) the longest neurite length, ii) the average of neurite length and iii) the number of neurites per cell. Results are summarized in Fig.3.3.

In SH-SY5Y cells, TPA slightly increased neuritic length as compared with undifferentiated cells; in presence of RA this increment was more evident, although not statistically significant. Consistent with our results, RA has been reported to be an inducer of neurite outgrowth and axonal elongation in several cell models (Clagett-Dame et al, 2006). Staurosporine-induced differentiation resulted again the best condition tested: neurite length significantly increased compared with

undifferentiated and RA- or TPA- differentiated cells (Fig.3.3B). However, none of these drugs impacted on the number of neurites per cell.

In BE(2)-M17 cell line, TPA only partially stimulated neuritic outgrowth; in contrast the effects with the other two agents were more marked. Staurosporine induced a significant elongation of processes; although the best morphological differentiation was accomplished by the addition of RA, that not only increased neurite length but also promoted branching, as clearly showed with the increase of the number of processes per cell (Fig.3.3F).

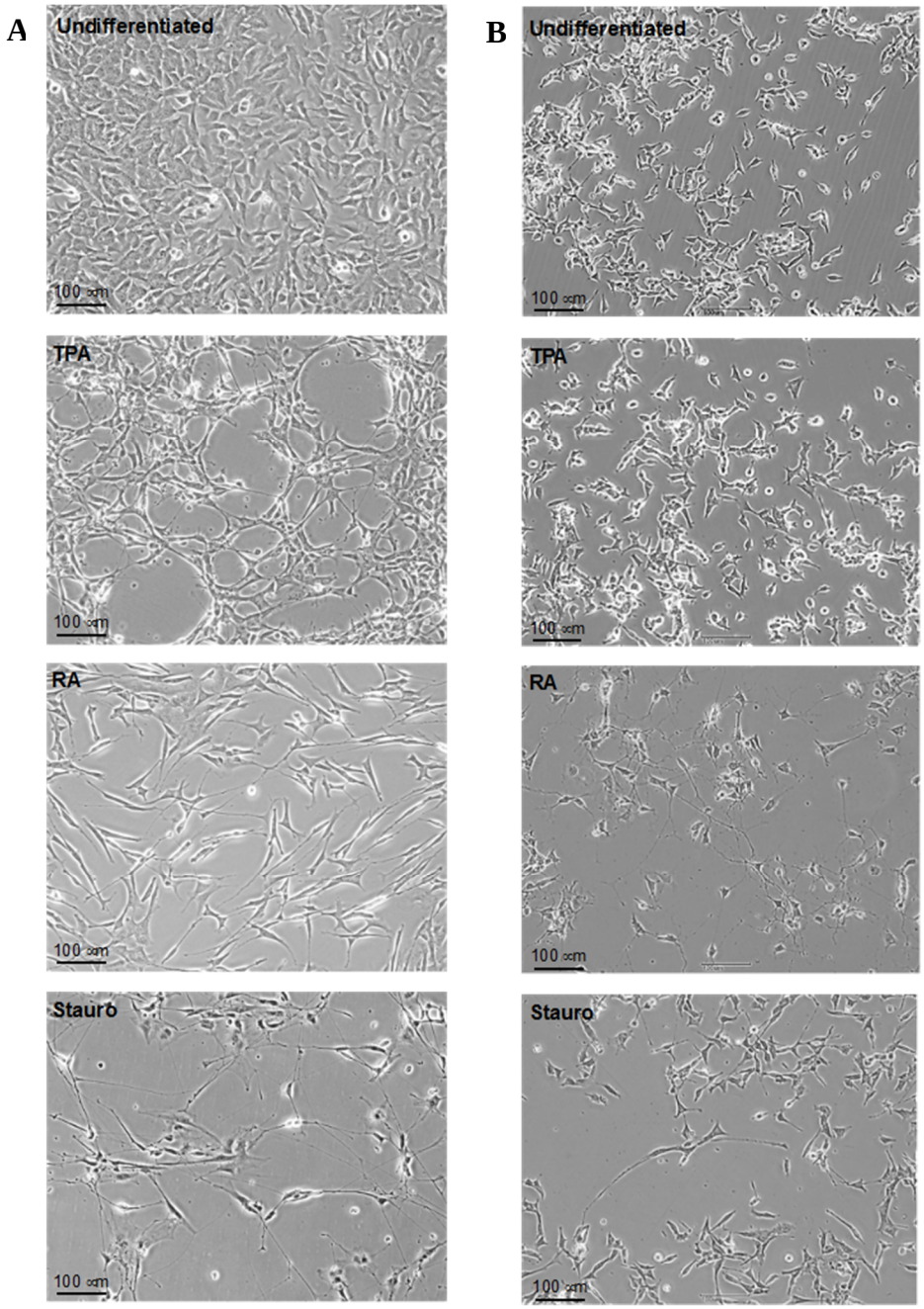

Fig.3.2. Cellular morphology after differentiation. Representative phase contrast images of undifferentiated and differentiated **(A)** SH-SY5Y and **(B)** BE(2)-M17 cells after 7 days of treatment with different differentiating agents. TPA: phorbol ester 12-O-tetradecanoylphorbol-13-acetate, RA: Retinoic acid, Stauro: Staurosporine.. After 7 days of treatment, staurosporine and RA promoted the most remarkable neurite extension, respectively, in SH-SY5Y cells and BE(2)-M17. Scale bar = 100 µM.

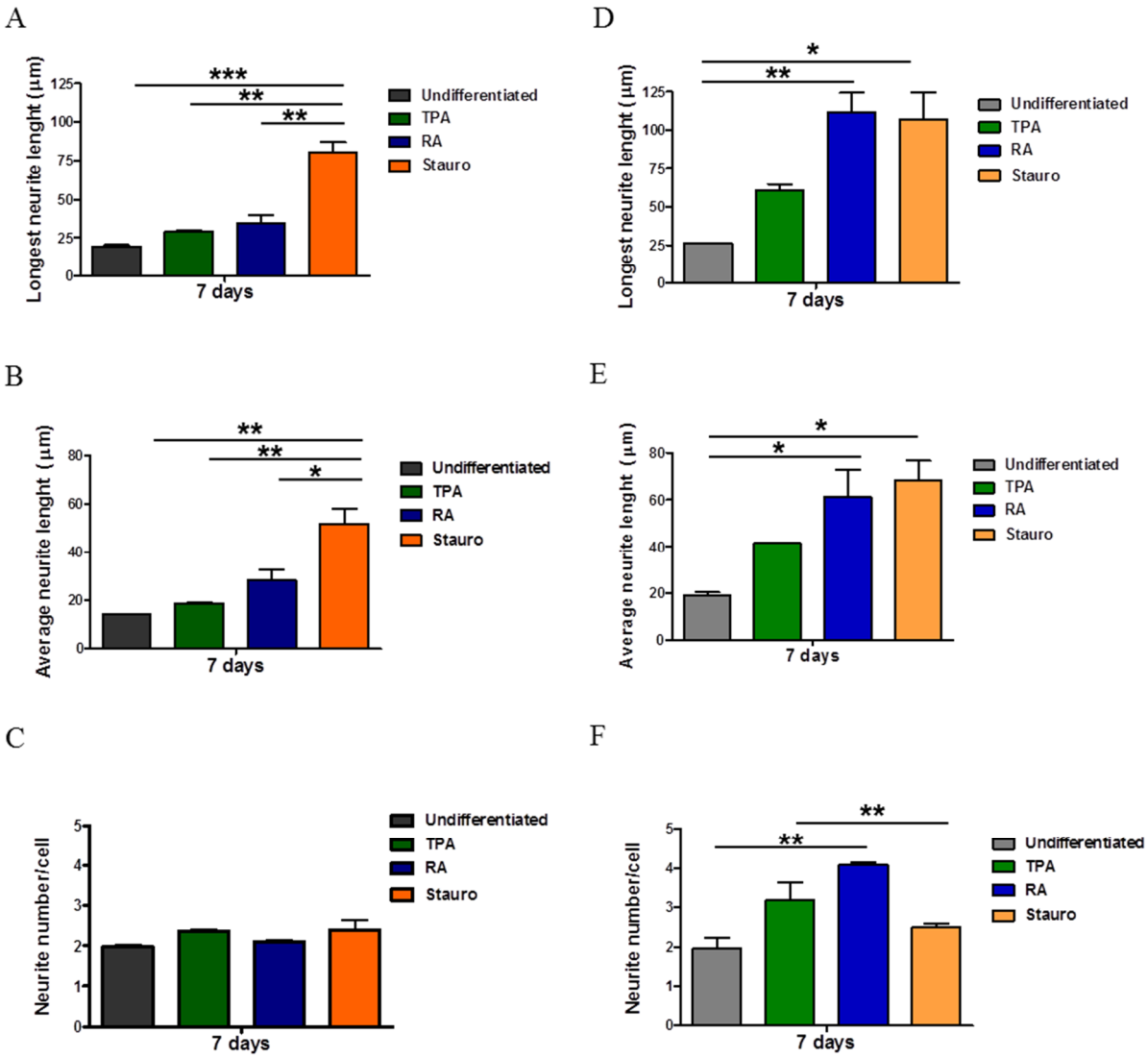

Fig.3.3. Neurite outgrowth after differentiation. Three different parameters have been quantified: the length of the longest neurite, the average of neurite length and the neurite number per cells. Each parameter was measured in undifferentiated and differentiated **(A, B, C)** SH-SY5Y or **(D, E, F)** BE(2)-M17 cells after 7 days treatment with differentiating agents phorbol ester 12-O-tetradecanoylphorbol-13-acetate (TPA), Retinoic acid (RA), Staurosporine (Stauro). Staurosporine and RA promoted the most remarkable neurite lenght, respectively, in SH-SY5Y cells and BE(2)-M17. Additionally, RA treatment increased neurite branching in BE(2)-M17. Data are expressed as mean ± SEM of three experiment. For each condition at least 90 cells were analyzed. Statistical significance was determined by one-way ANOVA with Bonferroni (*p<0.05; **p<0.01; ***p<0.001).

3.3 Immunofluorescence analysis of neuronal markers.

To study whether differentiated cells expressed late neuronal markers, we stained undifferentiated and differentiated SH-SY5Y and BE(2)-M17 cultures using specific antibodies against neuron-specific proteins such as β-tubulin III and neurofilament. β-tubulin III is a neuron-specific class of tubulin. During development, the relative abundance of this protein increases with the rate of neuronal differentiation (Lee et al, 1990). Neurofilaments are intermediate filaments, components of the mature cytoskeleton of neurons and present mainly in axons. After 7 days of incubation in the presence of each differentiating agent, cells were fixed and immunocytochemistry was performed. Consistent with our previous , TPA induced marked variations in cell morphology leading to neuron-like appearance (Fig.3.4). Accordingly, while TPA-treated cells showed only moderate neurite outgrowth and did not exhibit detectable neuronal-marker-positive processes; on the contrary, the differentiation with RA and staurosporine promoted in both cell lines a significant increase in processes positive to both β-tubulin III and neurofilament.

In agreement with these observations, it has been previously shown that the differentiation induced by RA in SH-SY5Y and BE(2)-M17 increased the expression of late neuronal markers, not only β-tubulin III but also microtubule-associated protein 2, (Andres et al, 2013; Constantinescu et al, 2007) which is an abundant neuronal cytoskeletal phosphoprotein essential for the development and maintenance of neuronal morphology, cytoskeleton dynamics and organelle trafficking (Binder et al, 1985). The expression of these markers was concomitant with the down-regulation of nestin, that a member of the intermediate filament family not expressed in mature neuronal cells (Lopes et al, 2010). Furthermore, the induction of mature neuronal markers, observed upon differentiation with staurosporine, confirmed previous studies ,which showed that this molecule stimulated SH-SY5Y cells to express mature neuronal markers, such as microtubule-associated protein 2 (Borland et al, 2008) and growth associated protein 43 (Jalava et al, 1992). The latter is involved in axonal growth and the modulation of synaptic connection (Benowitz et al, 1987).

Taken together, our data demonstrate that in both cell lines the treatment with RA and staurosporine generate cell populations with variably extended neuritic processes, which are positive to the neuronal markers used, suggesting the acquisition of a mature neuronal-like phenotype.

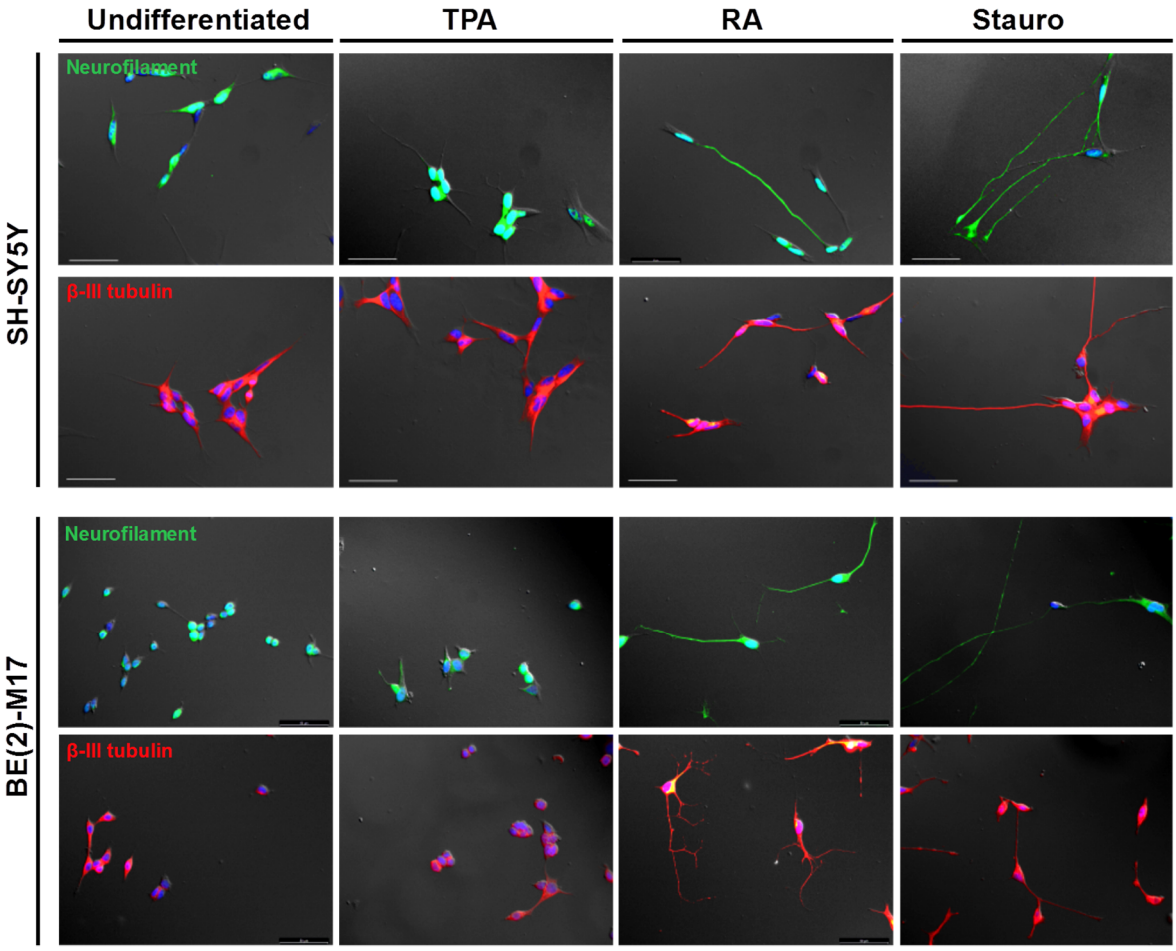

Fig.3.4. Immunofluorescence staining for two components of the cytoskeleton of mature neurons:, neurofilament and β-III tubulin. The comparison was made between undifferentiated and differentiated SH-SY5Y and BE(2)-M17 cells after 7 days of treatment with . phorbol ester 12-O-tetradecanoylphorbol-13-acetate (TPA), retinoic acid (RA) and staurosporine (Stauro). RA and staurosporine differentiation induced the formation of long processes positive for neurofilament and β-III tubulin in both cell lines. Blue: Hoechst; Green: neurofilaments; Red: β-III tubulin; Gray: phase contrast. Scale bar = 50 µM.

3.4 Expression profile of DA-and NA-related genes

To analyze the effects of differentiation on the CAergic pathway in both SH-SY5Y and BE(2)-M17 cells, variations in gene expression profile before and after differentiation has been assessed through qRT-PCR experiments. Specifically, we decided to focus on the key genes involved in DA and NA synthesis and storage: TH and aromatic L-amino acid decarboxylase (AADC), which are both involved in the synthesis of DA; vesicular monoamine transporter 2 (VMAT2), which rapidly sequester DA from the cytosol into synaptic vesicles; DβH, which synthesizes NA from DA inside synaptic vesicles.

The results obtained with SH-SY5Y cells after addition of the differentiating agents are summarized in Tab.3.1 and plotted in Fig.3.4. After 4 days, the expression profiles of TPA-differentiated cells were slightly down-regulated relative to the undifferentiated controls. This trend was more evident after 7 days of TPA treatment. A similar trend of general down-regulation was also observed when the cells were treated with RA, where the effects were visible as early as 4 days after treatment. Analysis at 7 days revealed that the *TH* and *AADC* genes were the most affected, suggesting that DA synthesis was specifically inhibited. In contrast, cells treated with staurosporine exhibited an up-regulation of all these markers both at 4 and 7 days after differentiation. Interestingly, while the expression of the *TH* gene was only slightly increased, *VMAT2* expression was increased more than 80 and 100 times at 4 and 7 days, respectively. Also expression of the *DβH* gene was considerably enhanced (~7 and ~8 times at 4 and 7 days, respectively). Overall, these results indicate that while DA synthesis appears to be only slightly increases by staurosporine-induced differentiation, the potential for DA storage inside vesicles and subsequent conversion into NA are clearly increased.

In literature, SH-SY5Y cells have been largely characterized in terms of expression profile of genes and proteins involved in neurotransmitter synthesis, metabolism and storage. So far, an unequivocal characterization of the neurotransmitter phenotype of differentiated SH-SY5Y cells is still lacking. For instance, treatment with RA, which was the most extensively analyzed, produced controversial results (Korecka et al, 2013). Actually, it has been shown that

differentiating agent induced the expression of TH, suggesting a shift towards a DAergic phenotype (Lopes et al, 2010). However, other authors did not observe changes in the expression of key DAergic-cell markers in RA treated cells (Cheung et al, 2009). Moreover, RA treatment has been reported to induce a cholinergic phenotype (Zimmermann et al, 2004), evaluated as the increase of acetylcholinesterase and acetyltransferase activity compared with non-treated cells (Adem et al, 1987). In our analyses, it was observed that RA promoted the down-regulation of all DA- and NA- related genes suggesting the loss catecholaminergic phenotype and supporting the possibility that these cells could acquire a cholinergic phenotype. In literature, it has been proposed that TPA-induced differentiation leads to a NAergic phenotype, as consequence of the TH stimulation and of a significant increment (200 fold) of NA content compared to undifferentiated cells (Jalava et al, 1992; Pahlman et al, 1984). However, in this work we observed a general down-regulation of catecholaminergic markers, which does not support the previously described phenotype. Finally, consistent with the NAergic phenotype ascribed to staurosporine-differentiated cells (Jalava et al, 1993), we found that this agent was responsible for a general increase of all DA/NA-related gene expression and, in particular of VMAT2 and DβH, key enzymes for NA synthesis.

SH-SY5Y				
TPA	**TH**	**AADC**	**VMAT2**	**DβH**
4 days	0.75±0.02	0.68 ± 0.08	0.74 ± 0.04	0.73 ± 0.05
7 days	0.18±0.06	0.33 ± 0.04	0.38 ± 0.03	0.25 ± 0.03
RA	**TH**	**AADC**	**VMAT2**	**DβH**
4 days	0.14 ± 0.03	0.40 ± 0.03	0.30 ± 0.01	0.79 ± 0.05
7 days	0.05 ± 0.02	0.10 ± 0.01	0.34 ± 0.02	0.40 ± 0.04
Stauro	**TH**	**AADC**	**VMAT2**	**DβH**
4 days	1.42 ± 0.03	3.3 ± 0.2	83 ± 3	7.3 ± 0.4
7 days	1.12 ± 0.03	2.7 ± 0.3	105 ± 2	7.9 ± 1.0

Tab.3.1. Gene expression profile of the primary catecholaminergic markers after differentiation in SH-SY5Y cells after 4 and 7 day of differentiation. Tyrosine hydroxylase (*TH*), aromatic L-amino acid decarboxylase (*AADC*), vesicular monoamine transporter 2 (*VMAT2*) and dopamine beta hydroxylase (*DβH*) mRNAs were analyzed using qRT-PCR and compared with undifferentiated cells, using Glyceraldehyde 3-phosphate dehydrogenase (*GAPDH*) and RNA polymerase II (*RPII*) as housekeeping genes. Values higher and lower than 1 represent, respectively, up- and down-regulation of the genes after cell differentiation. The data are expressed as the mean ± SEM of three experiments.

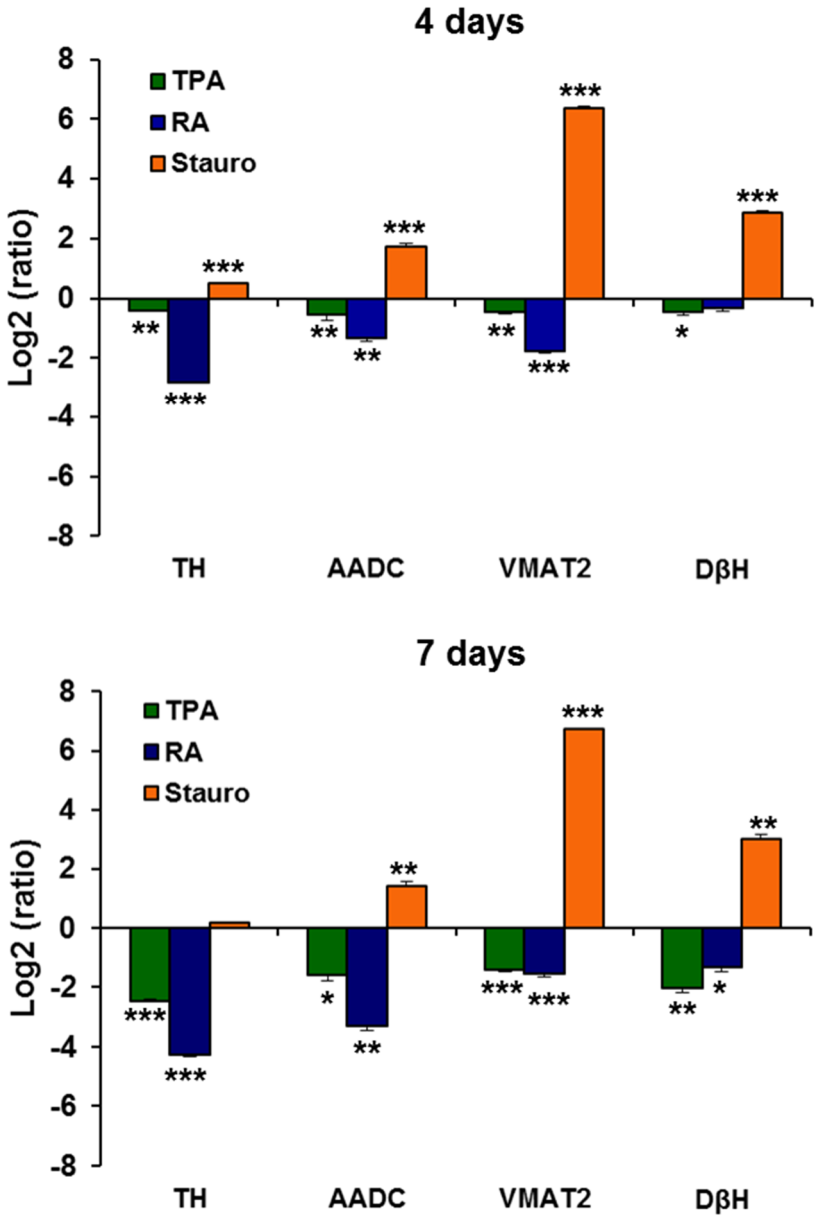

Fig.3.5. Gene expression profile of CAergic markers in differentiated SH-SY5Y. After 4 and 7 days of differentiation with TPA, RA and staurosporine, Tyrosine hydroxylase (*TH*), aromatic L-amino acid decarboxylase (*AADC*), vesicular monoamine transporter 2 (*VMAT2*) and dopamine beta hydroxylase (*DβH*) mRNA levels were compared with levels in undifferentiated cells using qRT-PCR. Expression is displayed on a Log_2 scale. Positive and negative values indicated, respectively, up- and down-regulation of the genes relative to control cells (undifferentiated cells). For each gene, differences between differentiated and undifferentiated were tested for significance using Student's t-test. (*P<0.05, **P<0.01, ***P<0.001).

The effects observed in the BE(2)-M17 cell line after differentiation were less straightforward (Tab.3.2 and Fig.3.6). In general, for each differentiating agent used, the expression profiles observed at 4 and 7 days of treatment were very similar. The effects observed in the presence of TPA were rather mild (with the exception of the *TH* gene that was up-regulated ~3 times) and the phenotype did not seem to change in comparison to undifferentiated cells. Even in the presence of RA, the expression profiles of *TH*, *AADC* and *DβH* genes were only slightly different from undifferentiated control, while *VMAT2* resulted from 6 to10 times down-regulated. As in the case of the SH-SY5Y cell line, among the differentiating agents tested staurosporine was the only one that increased the catecholaminergic phenotype of the cells. Nevertheless, in addition to *VMAT2* and *DβH* genes, also the TH gene was strongly up-regulated (~8 times), in contrast with SH-SY5Y. BE(2)-M17 cells have been previously described to express choline acetyltransferase, acetylcholinesterase and dopamine-β-hydroxylase suggesting both cholinergic and NAergic properties (Andres et al, 2013). However, this is the only work available in literature, no further investigations have been described. Thus, our results become particularly relevant considering the current scanty characterization of this cell line.

BE(2)-M17				
TPA	**TH**	**AADC**	**VMAT2**	**DβH**
4 days	3 ±0.2	1.3 ± 0.10	0.67 ± 0.08	1.93 ± 0.19
7 days	2.6 ±0.2	1.19 ± 0.10	0.75 ± 0.06	1.31 ± 0.15
RA	**TH**	**AADC**	**VMAT2**	**DβH**
4 days	0.93 ± 0.06	1.34 ± 0.08	0.14 ± 0.01	0.58 ± 0.05
7 days	0.85 ± 0.05	1.48 ± 0.12	0.11 ± 0.01	0.87 ± 0.07
Stauro	**TH**	**AADC**	**VMAT2**	**DβH**
4 days	7.9 ± 1.5	1.49 ± 0.09	19.1 ± 1.5	21 ± 2
7 days	8.2 ± 0.6	1.54 ± 0.11	36 ± 2	16.8 ± 1.1

Tab.3.2. Gene expression profile of the primary catecholaminergic markers after differentiation in BE(2)-M17 cells after 4 and 7 day of differentiation. Tyrosine hydroxylase (*TH*), aromatic L-amino acid decarboxylase (*AADC*), vesicular monoamine transporter 2 (*VMAT2*) and dopamine beta hydroxylase (*DβH*) mRNAs were analyzed using qRT-PCR and compared with undifferentiated cells, using Glyceraldehyde 3-phosphate dehydrogenase (*GAPDH*) and RNA polymerase II (*RPII*) as housekeeping genes. Values higher and lower than 1 represent, respectively, up- and down-regulation of the genes after cell differentiation. The data are expressed as the mean ± SEM.

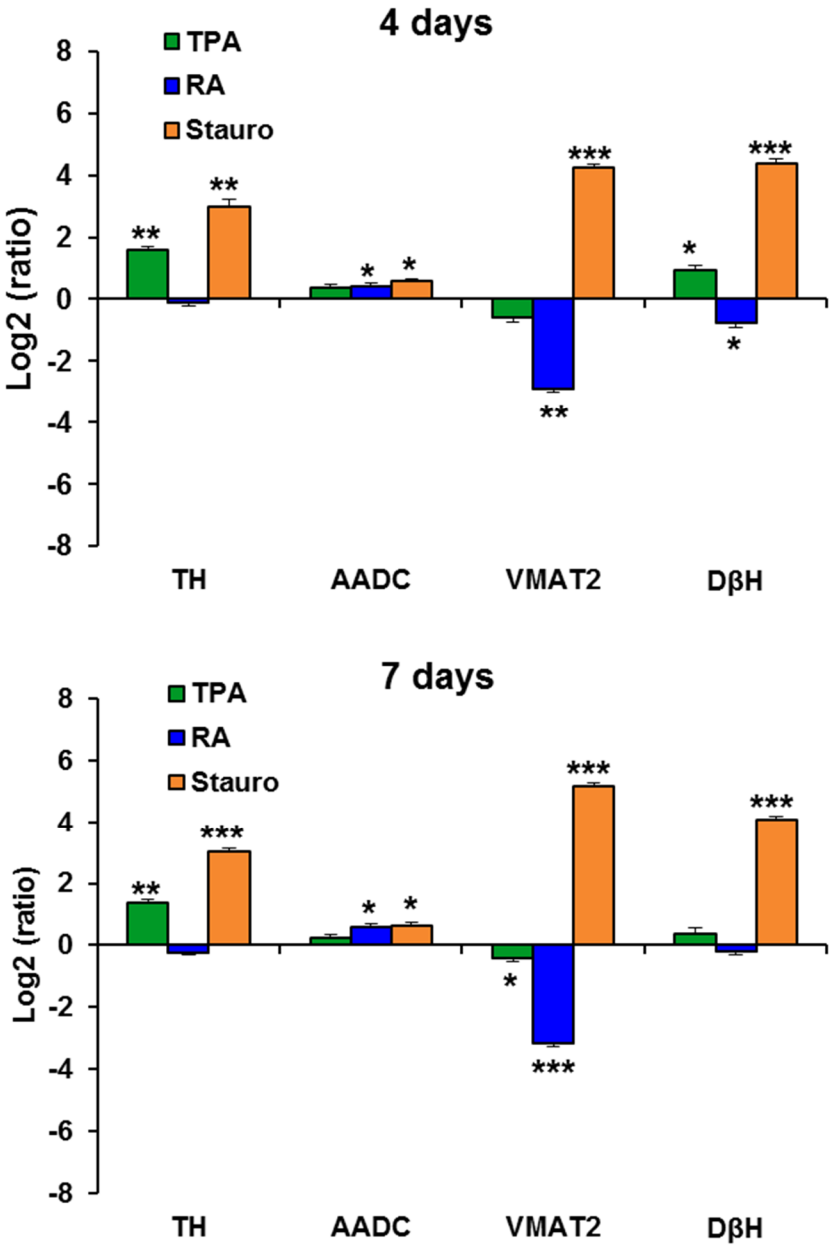

Fig.3.6. Gene expression profile of CAergic markers in differentiated BE(2)-M17 cells. After 4 and 7 days of differentiation with TPA, RA and staurosporine, Tyrosine hydroxylase (*TH*), aromatic L-amino acid decarboxylase (*AADC*), vesicular monoamine transporter 2 (*VMAT2*) and dopamine beta hydroxylase (*DβH*) mRNA levels were compared with levels in undifferentiated cells using qRT-PCR. Expression is displayed on a Log_2 scale. Positive and negative values indicated, respectively, up- and down-regulation of the genes with respect to control cells (undifferentiated cells). For each gene, differences between differentiated and undifferentiated were tested for significance using Student's t-test. (*P<0.05, **P<0.01, ***P<0.001).

3.5 Quantification of catecholamine levels

To investigate whether the alterations of gene expression profile were associated to changes in the cellular content of the neurotransmitters DA and NA, their intracellular level (expressed as nanomoles per gram total proteins) has been quantified by HPLC coupled with an electrochemical detector. These analyses were performed in SH-SY5Y and BE(2)-M17 cells, before and after 7 days differentiation with the three differentiating agents (Tab.3.3).

The DA and NA intracellular contents detected in undifferentiated SH-SY5Y cells were, respectively, 0.7 ± 0.1 and 1.7 ± 0.6 nmol g^{-1}. Consistent with the down-regulation of the four analyzed genes, treatment with TPA and RA decreased the content of neurotransmitter. Actually, the level of DA was below detection level, while NA content was reduced to 0.4 ± 0.2 with TPA and 0.2 ± 0.1 nmol g^{-1} with RA, supporting a potential shift from catecholaminergic to cholinergic phenotype. As expected, the effect observed after staurosporine-differentiation was particularly different. Indeed, DA and NA amounts were augmented to 2.4 ± 0.6 and 11 ± 3 nmol g^{-1}, respectively, indicating that differentiation promotes a more pronounced NAergic phenotype.

In SH-SY5Y cells, NA content was already measured in another study, upon TPA-, RA- and staurosporine differentiation. In agreement with our observations, it has been found that staurosporine treatment induced a consistent increase in intracellular NA levels (Prince & Oreland, 1997). In the same work, a moderate effects after TPA exposure was also identified, however this increase was not appreciated by other investigators (Jalava et al, 1993). As mentioned before, the phenotype of RA-treated SH-SY5Y cells is the subject of some controversy in the literature. Recently, RA has been described to suppress serotonergic, noradrenergic and cholinergic characteristics and actively promoted DA (Korecka et al, 2013), although others reported that this treatment developed a cholinergic phenotype (Zimmermann et al, 2004). In agreement with the latter study, here we found that RA differentiation inhibited DA and NA synthesis.

In undifferentiated BE(2)-M17 cells, these analyses revealed that the DA and NA content (9.2 ± 1.2 and 5.4 ± 1.7 nmol g^{-1}, respectively) was higher than the values measured in SH-SY5Y cells. TPA treatment slightly increased the level of both neurotransmitters (11.3 ± 1.9 and 17.7 ± 3.0), which might be explained with the modest up-regulation of *TH* and *DβH* genes observed through qRT-PCR. Coherently with our gene expression analysis, treatment with RA did not affected DA and NA content, while the presence of staurosporine induced a strong increase of both DA and NA content. Even though few data are available regarding this cell line, it is worth mentioning that, consistent with our results, also in the case of SK-N-BE(2) cells, from which BE(2)-M17 were subcloned, high levels of DA were detected although DβH activity was measured (Biedler et al, 1978).

	DA	**NA**
SH-SY5Y undifferentiated	0.7 ± 0.1	1.7 ± 0.6
SH-SY5Y TPA	nd	0.4 ± 0.2
SH-SY5Y RA	nd	0.2 ± 0.1
SH-SY5Y Stauro	2.4 ±0.6	11 ± 3
BE(2)-M17 undifferentiated	9.2 ± 1.2	5.4 ± 1.7
BE(2)-M17 TPA	11.3 ± 1.9	17.7 ± 3.0
BE(2)-M17 RA	9.7 ± 1.5	7.5 ± 1.5
BE(2)-M17 Stauro	40 ± 12	45 ± 14

Tab.3.3. DA and NA contents detected in SH-SY5Y and BE(2)-M17 cell lines before and after 7 days of differentiation. The values represent nanomoles of catecholamine per gram of proteins. The data were expressed as the mean ± SEM of at least 3 experiments. Nd: not detectable.

To summarize, the proliferating and differentiating effects of three agents, RA, TPA and staurosporine, in SH-SY5Y and BE(2)-M17 human neuroblastoma cell lines were analyzed. Our results indicate that the BE(2)-M17 cell line, which has been poorly characterized in the past, emerges as a new experimental paradigm with

catecholaminergic phenotype more pronounced than that one observed in SH-SY5Y cells. Additionally, the differentiation induced with staurosporine not only promotes a mature neuronal-like phenotype but also enhances the this phenotype.

Chapter 5

Conclusions

Aim of this thesis was to investigate the potential protective role of SODs and SOD mimetics against oxidative injury related to PD.

Although the ethiopathogenic mechanisms of Parkinson's disease (PD) are still unclear, several literature evidence suggest that oxidative stress plays a central role in both sporadic and familial forms of PD (Hwang, 2013). In the disorder, the dysregulation of ROS homeostasis and the consequent oxidative stress are the results of a complex scenario of molecular pathways. Indeed, different sources and molecular pathways have been associated to ROS generation, including protein aggregation, UPS impairment, mitochondrial dysfunction, neuroinflammation and dopamine (DA) metabolism (Dias et al, 2013). The key hypothesis of this work was that the inhibition of ROS overproduction, through antioxidant enzymes or molecules could block, delay or prevent the degeneration of dopaminergic (DArgic) neurons. In particular, we focused on SOD enzymes, because of their ability to dismutate superoxide anions, which are responsible for the downstream generation of more toxic species. Thus, the role of these enzymes as well as of small compounds, that mimic the native protein activity, has been investigated *in vitro* and *in vivo* as protective mechanism against oxidative injuries, related to PD. To this aim, two different experimental paradigms have been used: the first one was paraquat (PQ), whose chronic exposure has been identified as a risk factor for sporadic form of PD; the second one was PINK1 deficiency, which has been chosen as a model of genetic parkinsonism.

PQ is a widely used herbicide, the main mechanism of its toxicity resides in its redox cycling within cells, that generates a massive oxidative stress leading to a consistent cell damage (Franco et al, 2010). In this thesis, PQ toxicity has been first estimated in human neuroblastoma SH-SY5Y cells. Our cytofluorimetric analyses showed that, after 48 hours of exposure, PQ induced cell death, through the apoptotic pathway. Afterwards, to explore whether SODs might counteract the PQ-induced oxidative damage, the cytosolic and the mitochondrialproteins were stably overexpressed in neuroblastoma cells. It resulted that only the mitochondrial SOD2 significantly rescued the cytotoxicity induced by PQ. The selective effect of this enzyme suggests that this treatment directly impacts on mitochondrial functions. To

better elucidate and characterize the potential involvement of mitochondria in PQ toxicity, we measured ROS production in SH-SY5Y cells using the genetically encoded redox sensor roGFP2. Specifically, two isoforms of this indicator have been expressed, one localized in the cytosol (roGFP2) and the second one in the mitochondria (mt-roGFP2). Considering that ROS generation might precede cell death, our analyses were performed after 6 and 12 hours of PQ exposure. In agreement with this hypothesis, we found that the treatment significantly increased oxidative stress at mitochondrial level, while the cytosolic compartment was not affected. Being that mitochondrial ROS have been proposed to modulate the morphology of these organelles (Dagda et al, 2009), we also analyzed the effects of PQ on mitochondrial network using the fluorescent probe, mito-RFP. Indeed, we observed that PQ-induced oxidative stress triggered mitochondrial fragmentation. Overall, in our *in vitro* model, PQ toxicity affected extensively mitochondria, increasing ROS production in these organelles, which in turn promoted mitochondrial fragmentation. These observations are consistent with the protection exerted by mitochondrial SOD2 against the herbicide and support the hypothesis that this enzyme might have a relevant function in hampering oxidative damage in PD.

To further validate our results, the role of SODs has been studied *in vivo*, using *Drosophila melanogaster*. Thus, fly lines, ubiquitously overexpressing either the cytosolic or mitochondrial homolog proteins, were exposed to a lethal concentration of PQ (5 mM). The treatment strongly impacted on fly survival, which was significantly recovered only by Sod2 overexpression. Coherently with our *in vitro* results, this selective protection of the mitochondrial isoform confirmed that acute PQ exposure induced toxicity through a mechanism that mainly involved mitochondria. The picture that emerges using a sub-lethal concentration of PQ is different and quite complex. Actually, when flies were exposed to 1 mM PQ, the treatment did not affected survival but motor performance. Under these conditions, the mitochondrial Sod2 only partially ameliorated the motor phenotype, which was, on the contrary, almost completely restored by the overexpression of the cytosolic isoform. Considering that the chronic exposure to PQ was correlated to PD onset, we overexpressed each enzyme exclusively into the dopaminergic neurons. In this case,

Sod2 did not improve at all the motor dysfunction induced by 1 mM of PQ, while the cytosolic Sod reversed the locomotor defects. Our results support the view that the chronic exposure to PQ is mostly related to a cytosolic damage, which seems to be particularly relevant for the correct functioning of DAergic neurons. Our hypothesis is that some cytosolic processes, such as DA metabolism, occur inside these neurons, which might amplify the toxicity derived from the PQ- induced production of free radical species resulting in a particular vulnerability of DAergic neurons to oxidative stress.

Having demonstrated the protective role of both SODs against PQ toxicity, we thoroughly investigated the effects of a SOD mimetic. Although the direct administration of SOD enzymes, from bovine origin, proved to have beneficial effects in many diseases, both pre-clinically and clinically [see (Salvemini et al, 2002)], SOD-mimetic compounds were developed to circumvent several drawbacks associated with the use of native enzymes, such as immunogenicity and the inability to cross the BBB. Like the native enzymes, these compounds are molecules able to catalytically dismutate superoxide, which represents a great advantage in comparison to other antioxidant compounds. In this study, we tested the activity of the Mn(II)-pentaazamacrocyclic-based complex M40403, that acts selectively as scavenger for superoxide anion (Salvemini et al, 2002). The effect of this compound was first compared with other SOD mimetics against PQ toxicity in SH-SY5Y cells. Interestingly, among the different molecules tested, only M40403 showed significant beneficial properties decreasing PQ-induced cell death. In addition, this molecule reversed the mitochondrial fragmentation promoted by PQ. Moreover, when tested *in vivo*, M40403 succeeded in rescuing the lethality generated by elevated concentration of PQ as well as the locomotion behaviour of flies exposed to a chronic concentration. Taken together, these analyses reveal that M40403 is able to rescue oxidative damage induced by PQ both *in vitro* and *in vivo*, supporting a potential use as therapeutic agent.

In this research line we focused also on PINK1 deficiency. *PINK1* gene mutations have been identified as causes of recessive early onset parkinsonism (Valente et al, 2004). This gene encodes for a serine/threonine kinase that has been

reported as important regulator of mitochondrial quality control (Chu, 2010). Furthermore, several evidence suggested that the protein is also involved in the regulation of the cellular oxidative status (Chien et al, 2013). Thus, it has been selected to explore the effects of SODs overexpression and M40403 treatment.

First, we induced *PINK1* gene disruption in SH-SY5Y cells, using CRISPR/CAS technology for genome editing. In literature, it has been largely demonstrated that one of the most prominent phenotype in PINK1-deficient mammalian cells is mitochondrial fragmentation (Dagda et al, 2009; Exner et al, 2007). Coherently with previous works, we found that loss of PINK1 strongly perturbed the mitochondrial network resulting in its fragmentation. To evaluate whether SODs overexpression might ameliorate the observed phenotype, *PINK1 knock out* has been induced in SOD1 and SOD2 stably overexpressing cells and mitochondrial morphology was investigated. Even though further experiments are required, our preliminary analyses suggest promising results. Indeed, the cytosolic SOD1 seemed able to slightly reduce the mitochondrial morphological alterations; while the effect of the mitochondrial SOD2 appeared more evident, reducing mitochondrial fragmentation and allowing the maintenance of a healthy mitochondrial network.

The potential protective activity of Sods has been also investigated in PINK1 mutant flies, which exhibited a strong phenotype, that includes a severe motor impairment (Clark et al, 2006). In these mutants, the ubiquitous overexpression of Sods was achieved using the UAS/GAL4 system and the effects were analyzed in terms of motor performance. Surprisingly, we observed that only the overexpression of cytosolic Sod was able to significantly improve the locomotor activity of these flies. Although the mechanism underlying this selective protection remains unclear, the data suggest that PINK1 might be also involved in other pathways that are not strictly correlated with mitochondrial maintenance and functioning.

PINK1 deficient condition has also been used to test the effect of M40403 *in vitro* and *in vivo*. In SH-SY5Y cells, the compound seemed able to partially reverse mitochondrial fragmentation, although other experiments are necessary to confirm

this improvement. Coherently with our preliminary data in cells, the M40403 administration during larval development was able to rescue the motor impairment observed in PINK1 mutant flies. In agreement with our findings concerning PQ toxicity, these results highlight the protective effect of this compound against oxidative stress in PD models.

Finally, to better characterize the properties of the SOD mimetic M40403 and to understand whether this molecule can act as superoxide scavenger both in the cytosol and mitochondria, its protective effect has been tested in Sod and Sod2 deficient flies. These fly lines were characterized by a reduced life span (Wicks et al, 2009). Therefore, the effect of this drug was tested for 20 days in terms of survival. The results of these experiments demonstrated that M40403 was able to partially replace the loss of either Sod or Sod2 suggesting that it can act both at cytosolic and mitochondrial level.

Starting from the data presented in this thesis, it might be worth reconsidering the use of antioxidants in PD therapy, by testing the protective role of M40403 molecule (or its analogues) in clinical trials. Specifically, SOD mimetic compounds belonging to the M40403 family could be evaluated for their use as a complementary therapy to the currently adopted treatments for PD. Unlike other SOD mimetics, these molecules could offer several advantages. First, they are be able to cross the BBB (Salvemini et al, 1999), which is crucial requirement of a potential drug aimed to neurodegenerative disorders. Actually, the *in vivo* distribution of M40403 has been described in rats and after injection the drug was found widely distributed, also in the brain (Salvemini et al, 1999). Furthermore, M40403 presents a great stability and selectivity as scavenger for superoxide anion (Muscoli et al, 2003). Finally, this compound was already tested in phase I and phase II clinical trials for inflammatory diseases resulting safe and well-tolerated.

In parallel to the study described above, we carried out a second project line aimed to the characterization of two human neuroblastoma cell lines, SH-SY5Y and BE(2)-M17, in order to identify between them the most reliable model for PD studies.

Neuroblastoma cell lines are widely used in *in vitro* studies to analyze cellular pathways involved in the pathogenesis of PD. Although their use presents several advantages, these cells are undergo mitosis, are unsynchronized and do not exhibit the typical markers of mature neurons (Xie et al, 2010). In some circumstances, undifferentiated SH-SY5Y and BE(2)-M17 can be appropriately used, while in other studies their differentiation toward a neuronal-like phenotype could be preferred. Because DA metabolism is considered a key factor for the preferential degeneration of nigrostriatal neurons in PD, to provide a reliable cellular model we investigated the ability of three different agents, phorbol ester 12-O-tetradecanoylphorbol-13-acetate (TPA), Retinoic acid (RA), staurosporine , to drive a neuronal differentiation of these cell lines toward a DAergic phenotype. Although SH-SY5Y cells are largely used in PD research, an unequivocal characterization of their phenotype is still lacking, due to their ability to synthetize different neurotransmitter, including the catecholamines DA and noradrenaline (NA). For this reason, we decided to re-evaluate morphological and neurochemical changes induced by neuronal differentiation in this cell line. Additionally, we decided to analyze BE(2)-M17 cell line before and after differentiation, owing to the current scarce of knowledge of their phenotype.

The effects induced by TPA , RA and staurosporine, were first explored for their effects on promoting neuronal differentiation of both cell lines. To this aim, growth inhibition, cell morphology and expression of late neuronal markers were analyzed. Our results indicate that all the analyzed chemicals affect cell proliferation and morphological features with efficacies that depend on the treatment and on the cell line. Indeed, staurosporine and RA treatments were the most efficient to inhibit cell growth, respectively, in SH-SY5Y and BE(2)-M17. Moreover, while TPA resulted in the formation of few and short processes in each cell line, RA and staurosporine promoted the formation of a complex network of neuritic extensions.

In addition, immunofluorescence analysis revealed that these two compounds induced the expression of mature neuronal markers, β-III-tubulin and neurofilament, in SH-SY5Y and as well as in BE(2)-M17 cells.

Once the capability of each cell line to differentiate and acquire a neuron-like phenotype was evaluated, we investigated whether the differentiation impacts on catecholaminergic pathways in these cells. To address this issue, we first assessed the consequence of the three differentiating treatments on the expression profile of the major genes involved in DA and NA metabolism, *tyrosine hydroxylase (TH), aromatic L-amino acid decarboxylase (AADC), vesicular monoamine transporter 2 (VMAT2) and dopamine beta hydroxylase (DβH).* In the case of SH-SY5Y cells, both RA and TPA promoted the down-regulation of all the considered genes, suggesting a loss of the DA/NAergic phenotype. In contrast, staurosporine treatment resulted in up-regulation of all DA- and NA-related genes and, in particular, of *VMAT2* and *DβH*. Although the effects of TPA and RA on BE(2)-M17 cells were less pronounced, even in this case staurosporine induced the up-regulation of the genes involved in metabolism of DA and NA neurotransmitters. These data demonstrate that the cathecholaminergic phenotype in both SH-SY5Y and BE(2)-M17 cells can be modulated through differentiation. Moreover, HPLC Analyses showed that undifferentiated SH-SY5Y cells accumulate both DA and NA, but the NA amount was higher than DA level. Coherently with the observed gene down-regulation, TPA and RA-induced differentiation decreased the content of both neurotransmitters. Upon staurosporine treatment, consistent with the increased expression of *DβH* gene, we observed a large increase of the NA content relative to control cells. In conclusion, SH-SY5Y cells exhibit a more marked NAergic phenotype, which is further enhanced following staurosporine-induced differentiation. The amounts of DA and NA detected in undifferentiated BE(2)-M17 cells were considerably more elevated in comparison with SH-SY5Y , indicating a more pronounced DA/NAergic phenotype. In spite of the presence of DβH, which is expected to convert DA into NA, DA level was even higher than NA content. Consistent with the gene expression profile analysis, RA and TPA did not substantially alter the amount of each neurotransmitter. On the contrary, following the treatment with staurosporine,

we observed a large increase of both DA and NA. Overall, BE(2)-M17 cells exhibit a clear catecholaminergic phenotype and the differentiation induced with staurosporine not only promotes a mature neuronal-like morphology but also enhances this phenotype.

In conclusion, our results indicate that the BE(2)-M17 cell line emerges as a new and alternative experimental paradigm with with a catecholaminergic phenotype that differ substantially from that of the SH-SY5Y cells, suggesting different fields of application for the two cell lines. As the presence of DA appears to be an important requirement for a cell model, the use of the BE(2)-M17 cell line appears more suitable. On the contrary, the use of the SH-SY5Y cell line should be preferred to carry out studies in which the interference due to the presence of DA needs to be minimized.

In light of these results, we might better understand some data obtained in the first part of this thesis. Actually, studying the protective role of SODs *in vitro* and *in vivo* we observed some differences. Indeed, in SH-SY5Y cells SOD2 rescued PQ toxicity and PINK1 deficiency, while in *Drosophila* the cytosolic isoform was particularly protective in DAergic neurons. The different effects identified in these two approaches might be explained with the prominent NAergic phenotype of undifferentiated SH-SY5Y cells. Therefore, this model could not allow to thoroughly evaluate the contribution of DA metabolism in oxidative stress damage induced by PQ toxicity or PINK1 deficiency. In contrary, BE(2)-M17 cells might be a more suitable model to further investigate this issue.

Bibliography

Abeliovich A (2014) Neurological disorders: Quality-control pathway unlocked. *Nature* 510: 44-45

Abreu IA, Cabelli DE (2010) Superoxide dismutases-a review of the metal-associated mechanistic variations. *Biochim Biophys Acta* 1804: 263-274

Adem A, Mattsson ME, Nordberg A, Pahlman S (1987) Muscarinic receptors in human SH-SY5Y neuroblastoma cell line: regulation by phorbol ester and retinoic acid-induced differentiation. *Brain Res* 430: 235-242

Afanas'ev I (2010) Signaling and Damaging Functions of Free Radicals in Aging-Free Radical Theory, Hormesis, and TOR. *Aging Dis* 1: 75-88

Alam ZI, Daniel SE, Lees AJ, Marsden DC, Jenner P, Halliwell B (1997) A generalised increase in protein carbonyls in the brain in Parkinson's but not incidental Lewy body disease. *J Neurochem* 69: 1326-1329

Andersen JK (2004) Oxidative stress in neurodegeneration: cause or consequence? *Nat Med* 10 Suppl: S18-25

Andreassen OA, Ferrante RJ, Dedeoglu A, Albers DW, Klivenyi P, Carlson EJ, Epstein CJ, Beal MF (2001) Mice with a partial deficiency of manganese superoxide dismutase show increased vulnerability to the mitochondrial toxins malonate, 3-nitropropionic acid, and MPTP. *Exp Neurol* 167: 189-195

Andres D, Keyser BM, Petrali J, Benton B, Hubbard KS, McNutt PM, Ray R (2013) Morphological and functional differentiation in BE(2)-M17 human neuroblastoma cells by treatment with Trans-retinoic acid. *BMC Neurosci* 14: 49

Antonyuk SV, Strange RW, Marklund SL, Hasnain SS (2009) The structure of human extracellular copper-zinc superoxide dismutase at 1.7 A resolution: insights into heparin and collagen binding. *J Mol Biol* 388: 310-326

Auburger G, Klinkenberg M, Drost J, Marcus K, Morales-Gordo B, Kunz WS, Brandt U, Broccoli V, Reichmann H, Gispert S, Jendrach M (2012) Primary skin fibroblasts as a model of Parkinson's disease. *Mol Neurobiol* 46: 20-27

Bartus RT, Weinberg MS, Samulski RJ (2014) Parkinson's disease gene therapy: success by design meets failure by efficacy. *Mol Ther* 22: 487-497

Batinic-Haberle I, Benov L, Spasojevic I, Fridovich I (1998) The ortho effect makes manganese(III) meso-tetrakis(N-methylpyridinium-2-yl)porphyrin a powerful and potentially useful superoxide dismutase mimic. *J Biol Chem* 273: 24521-24528

Batinic-Haberle I, Reboucas JS, Spasojevic I (2010) Superoxide dismutase mimics: chemistry, pharmacology, and therapeutic potential. *Antioxid Redox Signal* 13: 877-918

Beilina A, Van Der Brug M, Ahmad R, Kesavapany S, Miller DW, Petsko GA, Cookson MR (2005) Mutations in PTEN-induced putative kinase 1 associated with recessive parkinsonism have differential effects on protein stability. *Proc Natl Acad Sci U S A* 102: 5703-5708

Beitz JM (2014) Parkinson's disease: a review. *Front Biosci (Schol Ed)* 6: 65-74

Benabid AL (2003) Deep brain stimulation for Parkinson's disease. *Curr Opin Neurobiol* 13: 696-706

Benarroch EE (2009) Brain iron homeostasis and neurodegenerative disease. *Neurology* 72: 1436-1440

Bender A, Krishnan KJ, Morris CM, Taylor GA, Reeve AK, Perry RH, Jaros E, Hersheson JS, Betts J, Klopstock T, Taylor RW, Turnbull DM (2006) High levels of mitochondrial DNA deletions in substantia nigra neurons in aging and Parkinson disease. *Nat Genet* 38: 515-517

Benowitz LI, Perrone-Bizzozero NI, Finklestein SP (1987) Molecular properties of the growth-associated protein GAP-43 (B-50). *J Neurochem* 48: 1640-1647

Beraud D, Hathaway HA, Trecki J, Chasovskikh S, Johnson DA, Johnson JA, Federoff HJ, Shimoji M, Mhyre TR, Maguire-Zeiss KA (2013) Microglial activation and antioxidant responses induced by the Parkinson's disease protein alpha-synuclein. *J Neuroimmune Pharmacol* 8: 94-117

Beraud D, Twomey M, Bloom B, Mittereder A, Ton V, Neitzke K, Chasovskikh S, Mhyre TR, Maguire-Zeiss KA (2011) alpha-Synuclein Alters Toll-Like Receptor Expression. *Front Neurosci* 5: 80

Berman SB, Hastings TG (1999) Dopamine oxidation alters mitochondrial respiration and induces permeability transition in brain mitochondria: implications for Parkinson's disease. *J Neurochem* 73: 1127-1137

Bharath S, Hsu M, Kaur D, Rajagopalan S, Andersen JK (2002) Glutathione, iron and Parkinson's disease. *Biochem Pharmacol* 64: 1037-1048

Bhaskar A, Chawla M, Mehta M, Parikh P, Chandra P, Bhave D, Kumar D, Carroll KS, Singh A (2014) Reengineering redox sensitive GFP to measure mycothiol redox potential of Mycobacterium tuberculosis during infection. *PLoS Pathog* 10: e1003902

Biedler JL, Roffler-Tarlov S, Schachner M, Freedman LS (1978) Multiple neurotransmitter synthesis by human neuroblastoma cell lines and clones. *Cancer Res* 38: 3751-3757

Binder LI, Frankfurter A, Rebhun LI (1985) The distribution of tau in the mammalian central nervous system. *J Cell Biol* 101: 1371-1378

Bisaglia M, Filograna R, Beltramini M, Bubacco L (2014) Are dopamine derivatives implicated in the pathogenesis of Parkinson's disease? *Ageing Res Rev* 13: 107-114

Bisaglia M, Greggio E, Beltramini M, Bubacco L (2013) Dysfunction of dopamine homeostasis: clues in the hunt for novel Parkinson's disease therapies. *FASEB J* 27: 2101-2110

Bjelakovic G, Nikolova D, Gluud LL, Simonetti RG, Gluud C (2012) Antioxidant supplements for prevention of mortality in healthy participants and patients with various diseases. *Cochrane Database Syst Rev* 3: CD007176

Block ML, Zecca L, Hong JS (2007) Microglia-mediated neurotoxicity: uncovering the molecular mechanisms. *Nat Rev Neurosci* 8: 57-69

Blum-Degen D, Muller T, Kuhn W, Gerlach M, Przuntek H, Riederer P (1995) Interleukin-1 beta and interleukin-6 are elevated in the cerebrospinal fluid of Alzheimer's and de novo Parkinson's disease patients. *Neurosci Lett* 202: 17-20

Bonifati V (2012) Autosomal recessive parkinsonism. *Parkinsonism Relat Disord* 18 Suppl 1: S4-6

Bonifati V (2014) Genetics of Parkinson's disease--state of the art, 2013. *Parkinsonism Relat Disord* 20 Suppl 1: S23-28

Bonifati V, Rizzu P, van Baren MJ, Schaap O, Breedveld GJ, Krieger E, Dekker MC, Squitieri F, Ibanez P, Joosse M, van Dongen JW, Vanacore N, van Swieten JC, Brice A, Meco G, van Duijn CM, Oostra BA, Heutink P (2003) Mutations in the DJ-1 gene associated with autosomal recessive early-onset parkinsonism. *Science* 299: 256-259

Borgstahl GE, Parge HE, Hickey MJ, Beyer WF, Jr., Hallewell RA, Tainer JA (1992) The structure of human mitochondrial manganese superoxide dismutase reveals a novel tetrameric interface of two 4-helix bundles. *Cell* 71: 107-118

Borland MK, Trimmer PA, Rubinstein JD, Keeney PM, Mohanakumar K, Liu L, Bennett JP, Jr. (2008) Chronic, low-dose rotenone reproduces Lewy neurites found in early stages of Parkinson's disease, reduces mitochondrial movement and slowly kills differentiated SH-SY5Y neural cells. *Mol Neurodegener* 3: 21

Brooks AI, Chadwick CA, Gelbard HA, Cory-Slechta DA, Federoff HJ (1999) Paraquat elicited neurobehavioral syndrome caused by dopaminergic neuron loss. *Brain Res* 823: 1-10

Castello PR, Drechsel DA, Patel M (2007) Mitochondria are a major source of paraquat-induced reactive oxygen species production in the brain. *J Biol Chem* 282: 14186-14193

Celotto AM, Liu Z, Vandemark AP, Palladino MJ (2012) A novel Drosophila SOD2 mutant demonstrates a role for mitochondrial ROS in neurodevelopment and disease. *Brain Behav* 2: 424-434

Chang X, Lu W, Dou T, Wang X, Lou D, Sun X, Zhou Z (2013) Paraquat inhibits cell viability via enhanced oxidative stress and apoptosis in human neural progenitor cells. *Chem Biol Interact* 206: 248-255

Cheung YT, Lau WK, Yu MS, Lai CS, Yeung SC, So KF, Chang RC (2009) Effects of all-trans-retinoic acid on human SH-SY5Y neuroblastoma as in vitro model in neurotoxicity research. *Neurotoxicology* 30: 127-135

Chien WL, Lee TR, Hung SY, Kang KH, Wu RM, Lee MJ, Fu WM (2013) Increase of oxidative stress by a novel PINK1 mutation, P209A. *Free Radic Biol Med* 58: 160-169

Choi HS, An JJ, Kim SY, Lee SH, Kim DW, Yoo KY, Won MH, Kang TC, Kwon HJ, Kang JH, Cho SW, Kwon OS, Park J, Eum WS, Choi SY (2006) PEP-1-SOD fusion protein efficiently protects against paraquat-induced dopaminergic neuron damage in a Parkinson disease mouse model. *Free Radic Biol Med* 41: 1058-1068

Chu CT (2010) A pivotal role for PINK1 and autophagy in mitochondrial quality control: implications for Parkinson disease. *Hum Mol Genet* 19: R28-37

Church SL, Grant JW, Meese EU, Trent JM (1992) Sublocalization of the gene encoding manganese superoxide dismutase (MnSOD/SOD2) to 6q25 by fluorescence in situ hybridization and somatic cell hybrid mapping. *Genomics* 14: 823-825

Ciccarone V, Spengler BA, Meyers MB, Biedler JL, Ross RA (1989) Phenotypic diversification in human neuroblastoma cells: expression of distinct neural crest lineages. *Cancer Res* 49: 219-225

Clagett-Dame M, McNeill EM, Muley PD (2006) Role of all-trans retinoic acid in neurite outgrowth and axonal elongation. *J Neurobiol* 66: 739-756

Clark IE, Dodson MW, Jiang C, Cao JH, Huh JR, Seol JH, Yoo SJ, Hay BA, Guo M (2006) Drosophila pink1 is required for mitochondrial function and interacts genetically with parkin. *Nature* 441: 1162-1166

Cocheme HM, Murphy MP (2008) Complex I is the major site of mitochondrial superoxide production by paraquat. *J Biol Chem* 283: 1786-1798

Collier TJ, Kanaan NM, Kordower JH (2011) Ageing as a primary risk factor for Parkinson's disease: evidence from studies of non-human primates. *Nat Rev Neurosci* 12: 359-366

Collins LM, Toulouse A, Connor TJ, Nolan YM (2012) Contributions of central and systemic inflammation to the pathophysiology of Parkinson's disease. *Neuropharmacology* 62: 2154-2168

Constantinescu R, Constantinescu AT, Reichmann H, Janetzky B (2007) Neuronal differentiation and long-term culture of the human neuroblastoma line SH-SY5Y. *J Neural Transm Suppl*: 17-28

Costa AC, Loh SH, Martins LM (2013) Drosophila Trap1 protects against mitochondrial dysfunction in a PINK1/parkin model of Parkinson's disease. *Cell Death Dis* 4: e467

Coune PG, Schneider BL, Aebischer P (2012) Parkinson's disease: gene therapies. *Cold Spring Harb Perspect Med* 2: a009431

Dagda RK, Cherra SJ, 3rd, Kulich SM, Tandon A, Park D, Chu CT (2009) Loss of PINK1 function promotes mitophagy through effects on oxidative stress and mitochondrial fission. *J Biol Chem* 284: 13843-13855

Dawson TM, Ko HS, Dawson VL (2010) Genetic animal models of Parkinson's disease. *Neuron* 66: 646-661

Day BJ, Batinic-Haberle I, Crapo JD (1999) Metalloporphyrins are potent inhibitors of lipid peroxidation. *Free Radic Biol Med* 26: 730-736

Day BJ, Fridovich I, Crapo JD (1997) Manganic porphyrins possess catalase activity and protect endothelial cells against hydrogen peroxide-mediated injury. *Arch Biochem Biophys* 347: 256-262

de Rijk MC, Tzourio C, Breteler MM, Dartigues JF, Amaducci L, Lopez-Pousa S, Manubens-Bertran JM, Alperovitch A, Rocca WA (1997) Prevalence of parkinsonism and Parkinson's disease in Europe: the EUROPARKINSON Collaborative Study. European Community Concerted Action on the Epidemiology of Parkinson's disease. *J Neurol Neurosurg Psychiatry* 62: 10-15

Debattisti V, Scorrano L (2013) D. melanogaster, mitochondria and neurodegeneration: small model organism, big discoveries. *Mol Cell Neurosci* 55: 77-86

Dennis KE, Aschner JL, Milatovic D, Schmidt JW, Aschner M, Kaplowitz MR, Zhang Y, Fike CD (2009) NADPH oxidases and reactive oxygen species at different stages of chronic hypoxia-induced pulmonary hypertension in newborn piglets. *Am J Physiol Lung Cell Mol Physiol* 297: L596-607

Dexter DT, Carter CJ, Wells FR, Javoy-Agid F, Agid Y, Lees A, Jenner P, Marsden CD (1989) Basal lipid peroxidation in substantia nigra is increased in Parkinson's disease. *J Neurochem* 52: 381-389

Di Napoli M, Papa F (2005) M-40403 Metaphore Pharmaceuticals. *IDrugs* 8: 67-76

Dias V, Junn E, Mouradian MM (2013) The role of oxidative stress in Parkinson's disease. *J Parkinsons Dis* 3: 461-491

Dobbs RJ, Charlett A, Purkiss AG, Dobbs SM, Weller C, Peterson DW (1999) Association of circulating TNF-alpha and IL-6 with ageing and parkinsonism. *Acta Neurol Scand* 100: 34-41

Doctrow SR, Huffman K, Marcus CB, Musleh W, Bruce A, Baudry M, Malfroy B (1997) Salen-manganese complexes: combined superoxide dismutase/catalase mimics with broad pharmacological efficacy. *Adv Pharmacol* 38: 247-269

Domingues AF, Arduino DM, Esteves AR, Swerdlow RH, Oliveira CR, Cardoso SM (2008) Mitochondria and ubiquitin-proteasomal system interplay: relevance to Parkinson's disease. *Free Radic Biol Med* 45: 820-825

Dooley CT, Dore TM, Hanson GT, Jackson WC, Remington SJ, Tsien RY (2004) Imaging dynamic redox changes in mammalian cells with green fluorescent protein indicators. *J Biol Chem* 279: 22284-22293

Dorsey ER, Constantinescu R, Thompson JP, Biglan KM, Holloway RG, Kieburtz K, Marshall FJ, Ravina BM, Schifitto G, Siderowf A, Tanner CM (2007) Projected number of people with Parkinson disease in the most populous nations, 2005 through 2030. *Neurology* 68: 384-386

Drechsel DA, Patel M (2008) Role of reactive oxygen species in the neurotoxicity of environmental agents implicated in Parkinson's disease. *Free Radic Biol Med* 44: 1873-1886

Duttaroy A, Paul A, Kundu M, Belton A (2003) A Sod2 null mutation confers severely reduced adult life span in Drosophila. *Genetics* 165: 2295-2299

Eisenhofer G, Kopin IJ, Goldstein DS (2004) Catecholamine metabolism: a contemporary view with implications for physiology and medicine. *Pharmacol Rev* 56: 331-349

Esteves AR, Swerdlow RH, Cardoso SM (2014) LRRK2, a puzzling protein: insights into Parkinson's disease pathogenesis. *Exp Neurol* 261: 206-216

Evans JR, Mason SL, Barker RA (2012) Current status of clinical trials of neural transplantation in Parkinson's disease. *Prog Brain Res* 200: 169-198

Exner N, Treske B, Paquet D, Holmstrom K, Schiesling C, Gispert S, Carballo-Carbajal I, Berg D, Hoepken HH, Gasser T, Kruger R, Winklhofer KF, Vogel F, Reichert AS, Auburger G, Kahle PJ, Schmid B, Haass C (2007) Loss-of-function of human PINK1 results in mitochondrial pathology and can be rescued by parkin. *J Neurosci* 27: 12413-12418

Farrer M, Chan P, Chen R, Tan L, Lincoln S, Hernandez D, Forno L, Gwinn-Hardy K, Petrucelli L, Hussey J, Singleton A, Tanner C, Hardy J, Langston JW (2001) Lewy bodies and parkinsonism in families with parkin mutations. *Ann Neurol* 50: 293-300

Fattman CL, Schaefer LM, Oury TD (2003) Extracellular superoxide dismutase in biology and medicine. *Free Radic Biol Med* 35: 236-256

Finkel T (2011) Signal transduction by reactive oxygen species. *J Cell Biol* 194: 7-15

Finkel T, Holbrook NJ (2000) Oxidants, oxidative stress and the biology of ageing. *Nature* 408: 239-247

Floor E, Wetzel MG (1998) Increased protein oxidation in human substantia nigra pars compacta in comparison with basal ganglia and prefrontal cortex measured with an improved dinitrophenylhydrazine assay. *J Neurochem* 70: 268-275

Franco R, Li S, Rodriguez-Rocha H, Burns M, Panayiotidis MI (2010) Molecular mechanisms of pesticide-induced neurotoxicity: Relevance to Parkinson's disease. *Chem Biol Interact* 188: 289-300

Frank S, Gaume B, Bergmann-Leitner ES, Leitner WW, Robert EG, Catez F, Smith CL, Youle RJ (2001) The role of dynamin-related protein 1, a mediator of mitochondrial fission, in apoptosis. *Dev Cell* 1: 515-525

Friedman A, Galazka-Friedman J, Koziorowski D (2009) Iron as a cause of Parkinson disease - a myth or a well established hypothesis? *Parkinsonism Relat Disord* 15 Suppl 3: S212-214

Fujioka S, Wszolek ZK (2012) Update on genetics of parkinsonism. *Neurodegener Dis* 10: 257-260

Furukawa Y, Torres AS, O'Halloran TV (2004) Oxygen-induced maturation of SOD1: a key role for disulfide formation by the copper chaperone CCS. *EMBO J* 23: 2872-2881

Gandhi S, Abramov AY (2012) Mechanism of oxidative stress in neurodegeneration. *Oxid Med Cell Longev* 2012: 428010

Gandhi S, Wood-Kaczmar A, Yao Z, Plun-Favreau H, Deas E, Klupsch K, Downward J, Latchman DS, Tabrizi SJ, Wood NW, Duchen MR, Abramov AY (2009) PINK1-associated Parkinson's disease is caused by neuronal vulnerability to calcium-induced cell death. *Mol Cell* 33: 627-638

Gaweda-Walerych K, Zekanowski C (2013) Integrated pathways of parkin control over mitochondrial maintenance - relevance to Parkinson's disease pathogenesis. *Acta Neurobiol Exp (Wars)* 73: 199-224

Gemma C, Vila J, Bachstetter A, Bickford PC (2007) Oxidative Stress and the Aging Brain: From Theory to Prevention.

George JM (2002) The synucleins. *Genome Biol* 3: REVIEWS3002

Gertz B, Wong M, Martin LJ (2012) Nuclear localization of human SOD1 and mutant SOD1-specific disruption of survival motor neuron protein complex in transgenic amyotrophic lateral sclerosis mice. *J Neuropathol Exp Neurol* 71: 162-177

Giasson BI, Murray IV, Trojanowski JQ, Lee VM (2001) A hydrophobic stretch of 12 amino acid residues in the middle of alpha-synuclein is essential for filament assembly. *J Biol Chem* 276: 2380-2386

Girotto S, Cendron L, Bisaglia M, Tessari I, Mammi S, Zanotti G, Bubacco L (2014) DJ-1 is a copper chaperone acting on SOD1 activation. *J Biol Chem* 289: 10887-10899

Girotto S, Sturlese M, Bellanda M, Tessari I, Cappellini R, Bisaglia M, Bubacco L, Mammi S (2012) Dopamine-derived quinones affect the structure of the redox sensor DJ-1 through modifications at Cys-106 and Cys-53. *J Biol Chem* 287: 18738-18749

Gispert S, Ricciardi F, Kurz A, Azizov M, Hoepken HH, Becker D, Voos W, Leuner K, Muller WE, Kudin AP, Kunz WS, Zimmermann A, Roeper J, Wenzel D, Jendrach M, Garcia-Arencibia M, Fernandez-Ruiz J, Huber L, Rohrer H, Barrera M, Reichert

AS, Rub U, Chen A, Nussbaum RL, Auburger G (2009) Parkinson phenotype in aged PINK1-deficient mice is accompanied by progressive mitochondrial dysfunction in absence of neurodegeneration. *PLoS One* 4: e5777

Goldberg MS, Fleming SM, Palacino JJ, Cepeda C, Lam HA, Bhatnagar A, Meloni EG, Wu N, Ackerson LC, Klapstein GJ, Gajendiran M, Roth BL, Chesselet MF, Maidment NT, Levine MS, Shen J (2003) Parkin-deficient mice exhibit nigrostriatal deficits but not loss of dopaminergic neurons. *J Biol Chem* 278: 43628-43635

Gomes LC, Scorrano L (2013) Mitochondrial morphology in mitophagy and macroautophagy. *Biochim Biophys Acta* 1833: 205-212

Good PF, Hsu A, Werner P, Perl DP, Olanow CW (1998) Protein nitration in Parkinson's disease. *J Neuropathol Exp Neurol* 57: 338-342

Graham DG (1978) Oxidative pathways for catecholamines in the genesis of neuromelanin and cytotoxic quinones. *Mol Pharmacol* 14: 633-643

Greene JC, Whitworth AJ, Kuo I, Andrews LA, Feany MB, Pallanck LJ (2003) Mitochondrial pathology and apoptotic muscle degeneration in Drosophila parkin mutants. *Proc Natl Acad Sci U S A* 100: 4078-4083

Guzman JN, Sanchez-Padilla J, Chan CS, Surmeier DJ (2009) Robust pacemaking in substantia nigra dopaminergic neurons. *J Neurosci* 29: 11011-11019

Guzman JN, Sanchez-Padilla J, Wokosin D, Kondapalli J, Ilijic E, Schumacker PT, Surmeier DJ (2010) Oxidant stress evoked by pacemaking in dopaminergic neurons is attenuated by DJ-1. *Nature* 468: 696-700

Halliwell B, Gutteridge JM, Cross CE (1992) Free radicals, antioxidants, and human disease: where are we now? *J Lab Clin Med* 119: 598-620

Harman D (1956) Aging: a theory based on free radical and radiation chemistry. *J Gerontol* 11: 298-300

Harman D (1972) The biologic clock: the mitochondria? *J Am Geriatr Soc* 20: 145-147

Hastings TG, Zigmond MJ (1997) Loss of dopaminergic neurons in parkinsonism: possible role of reactive dopamine metabolites. *J Neural Transm Suppl* 49: 103-110

Herman GE (2002) Mouse models of human disease: lessons learned and promises to come. *ILAR J* 43: 55-56

Heumann R, Moratalla R, Herrero MT, Chakrabarty K, Drucker-Colin R, Garcia-Montes JR, Simola N, Morelli M (2014) Dyskinesia in Parkinson's disease: mechanisms and current non-pharmacological interventions. *J Neurochem* 130: 472-489

Hirth F (2010) Drosophila melanogaster in the study of human neurodegeneration. *CNS Neurol Disord Drug Targets* 9: 504-523

Hoepken HH, Gispert S, Morales B, Wingerter O, Del Turco D, Mulsch A, Nussbaum RL, Muller K, Drose S, Brandt U, Deller T, Wirth B, Kudin AP, Kunz WS, Auburger G (2007) Mitochondrial dysfunction, peroxidation damage and changes in glutathione metabolism in PARK6. *Neurobiol Dis* 25: 401-411

Hosamani R (2013) Acute exposure of Drosophila melanogaster to paraquat causes oxidative stress and mitochondrial dysfunction. *Arch Insect Biochem Physiol* 83: 25-40

Hwang O (2013) Role of oxidative stress in Parkinson's disease. *Exp Neurobiol* 22: 11-17

Ii K, Ito H, Tanaka K, Hirano A (1997) Immunocytochemical co-localization of the proteasome in ubiquitinated structures in neurodegenerative diseases and the elderly. *J Neuropathol Exp Neurol* 56: 125-131

Im JY, Lee KW, Junn E, Mouradian MM (2010) DJ-1 protects against oxidative damage by regulating the thioredoxin/ASK1 complex. *Neurosci Res* 67: 203-208

Irrcher I, Aleyasin H, Seifert EL, Hewitt SJ, Chhabra S, Phillips M, Lutz AK, Rousseaux MW, Bevilacqua L, Jahani-Asl A, Callaghan S, MacLaurin JG, Winklhofer KF, Rizzu P, Rippstein P, Kim RH, Chen CX, Fon EA, Slack RS, Harper ME, McBride HM, Mak TW, Park DS (2010) Loss of the Parkinson's disease-linked gene DJ-1 perturbs mitochondrial dynamics. *Hum Mol Genet* 19: 3734-3746

Islinger M, Li KW, Seitz J, Volkl A, Luers GH (2009) Hitchhiking of Cu/Zn superoxide dismutase to peroxisomes--evidence for a natural piggyback import mechanism in mammals. *Traffic* 10: 1711-1721

Jagasia R, Grote P, Westermann B, Conradt B (2005) DRP-1-mediated mitochondrial fragmentation during EGL-1-induced cell death in C. elegans. *Nature* 433: 754-760

Jalava A, Akerman K, Heikkila J (1993) Protein kinase inhibitor, staurosporine, induces a mature neuronal phenotype in SH-SY5Y human neuroblastoma cells through an alpha-, beta-, and zeta-protein kinase C-independent pathway. *J Cell Physiol* 155: 301-312

Jalava A, Heikkila J, Lintunen M, Akerman K, Pahlman S (1992) Staurosporine induces a neuronal phenotype in SH-SY5Y human neuroblastoma cells that resembles that induced by the phorbol ester 12-O-tetradecanoyl phorbol-13 acetate (TPA). *FEBS Lett* 300: 114-118

Javitch JA, D'Amato RJ, Strittmatter SM, Snyder SH (1985) Parkinsonism-inducing neurotoxin, N-methyl-4-phenyl-1,2,3,6 -tetrahydropyridine: uptake of the metabolite N-methyl-4-phenylpyridine by dopamine neurons explains selective toxicity. *Proc Natl Acad Sci U S A* 82: 2173-2177

Jenner P (2003) Oxidative stress in Parkinson's disease. *Ann Neurol* 53 Suppl 3: S26-36; discussion S36-28

Jin K (2010) Modern Biological Theories of Aging. *Aging Dis* 1: 72-74

Jinek M, East A, Cheng A, Lin S, Ma E, Doudna J (2013) RNA-programmed genome editing in human cells. *Elife* 2: e00471

Kamel F (2013) Epidemiology. Paths from pesticides to Parkinson's. *Science* 341: 722-723

Kane LA, Lazarou M, Fogel AI, Li Y, Yamano K, Sarraf SA, Banerjee S, Youle RJ (2014) PINK1 phosphorylates ubiquitin to activate Parkin E3 ubiquitin ligase activity. *J Cell Biol* 205: 143-153

Kang MJ, Gil SJ, Koh HC (2009) Paraquat induces alternation of the dopamine catabolic pathways and glutathione levels in the substantia nigra of mice. *Toxicol Lett* 188: 148-152

Kawamata H, Manfredi G (2010) Import, maturation, and function of SOD1 and its copper chaperone CCS in the mitochondrial intermembrane space. *Antioxid Redox Signal* 13: 1375-1384

Kayatekin C, Cohen NR, Matthews CR (2012) Enthalpic barriers dominate the folding and unfolding of the human Cu, Zn superoxide dismutase monomer. *J Mol Biol* 424: 192-202

Kazlauskaite A, Kondapalli C, Gourlay R, Campbell DG, Ritorto MS, Hofmann K, Alessi DR, Knebel A, Trost M, Muqit MM (2014) Parkin is activated by PINK1-dependent phosphorylation of ubiquitin at Ser65. *Biochem J* 460: 127-139

Kelso GF, Maroz A, Cocheme HM, Logan A, Prime TA, Peskin AV, Winterbourn CC, James AM, Ross MF, Brooker S, Porteous CM, Anderson RF, Murphy MP, Smith RA (2012) A mitochondria-targeted macrocyclic Mn(II) superoxide dismutase mimetic. *Chem Biol* 19: 1237-1246

Kim RH, Smith PD, Aleyasin H, Hayley S, Mount MP, Pownall S, Wakeham A, You-Ten AJ, Kalia SK, Horne P, Westaway D, Lozano AM, Anisman H, Park DS, Mak TW (2005) Hypersensitivity of DJ-1-deficient mice to 1-methyl-4-phenyl-1,2,3,6-tetrahydropyrindine (MPTP) and oxidative stress. *Proc Natl Acad Sci U S A* 102: 5215-5220

Kim SU, de Vellis J (2009) Stem cell-based cell therapy in neurological diseases: a review. *J Neurosci Res* 87: 2183-2200

Kinumi T, Kimata J, Taira T, Ariga H, Niki E (2004) Cysteine-106 of DJ-1 is the most sensitive cysteine residue to hydrogen peroxide-mediated oxidation in vivo in human umbilical vein endothelial cells. *Biochem Biophys Res Commun* 317: 722-728

Kirby K, Hu J, Hilliker AJ, Phillips JP (2002) RNA interference-mediated silencing of Sod2 in Drosophila leads to early adult-onset mortality and elevated endogenous oxidative stress. *Proc Natl Acad Sci U S A* 99: 16162-16167

Kitada T, Asakawa S, Hattori N, Matsumine H, Yamamura Y, Minoshima S, Yokochi M, Mizuno Y, Shimizu N (1998) Mutations in the parkin gene cause autosomal recessive juvenile parkinsonism. *Nature* 392: 605-608

Kitada T, Pisani A, Porter DR, Yamaguchi H, Tscherter A, Martella G, Bonsi P, Zhang C, Pothos EN, Shen J (2007) Impaired dopamine release and synaptic plasticity in the striatum of PINK1-deficient mice. *Proc Natl Acad Sci U S A* 104: 11441-11446

Knott C, Stern G, Wilkin GP (2000) Inflammatory regulators in Parkinson's disease: iNOS, lipocortin-1, and cyclooxygenases-1 and -2. *Mol Cell Neurosci* 16: 724-739

Kondapalli C, Kazlauskaite A, Zhang N, Woodroof HI, Campbell DG, Gourlay R, Burchell L, Walden H, Macartney TJ, Deak M, Knebel A, Alessi DR, Muqit MM (2012) PINK1 is activated by mitochondrial membrane potential depolarization and stimulates Parkin E3 ligase activity by phosphorylating Serine 65. *Open Biol* 2: 120080

Korecka JA, van Kesteren RE, Blaas E, Spitzer SO, Kamstra JH, Smit AB, Swaab DF, Verhaagen J, Bossers K (2013) Phenotypic characterization of retinoic acid differentiated SH-SY5Y cells by transcriptional profiling. *PLoS One* 8: e63862

Koyano F, Okatsu K, Kosako H, Tamura Y, Go E, Kimura M, Kimura Y, Tsuchiya H, Yoshihara H, Hirokawa T, Endo T, Fon EA, Trempe JF, Saeki Y, Tanaka K, Matsuda N (2014) Ubiquitin is phosphorylated by PINK1 to activate parkin. *Nature* 510: 162-166

Kozak M (1986) Point mutations define a sequence flanking the AUG initiator codon that modulates translation by eukaryotic ribosomes. *Cell* 44: 283-292

Krebiehl G, Ruckerbauer S, Burbulla LF, Kieper N, Maurer B, Waak J, Wolburg H, Gizatullina Z, Gellerich FN, Woitalla D, Riess O, Kahle PJ, Proikas-Cezanne T, Kruger R (2010) Reduced basal autophagy and impaired mitochondrial dynamics due to loss of Parkinson's disease-associated protein DJ-1. *PLoS One* 5: e9367

Kregel KC, Zhang HJ (2007) An integrated view of oxidative stress in aging: basic mechanisms, functional effects, and pathological considerations. *Am J Physiol Regul Integr Comp Physiol* 292: R18-36

Kumar H, Lim HW, More SV, Kim BW, Koppula S, Kim IS, Choi DK (2012) The role of free radicals in the aging brain and Parkinson's disease: convergence and parallelism. *Int J Mol Sci* 13: 10478-10504

Kume T, Kawato Y, Osakada F, Izumi Y, Katsuki H, Nakagawa T, Kaneko S, Niidome T, Takada-Takatori Y, Akaike A (2008) Dibutyryl cyclic AMP induces differentiation of human neuroblastoma SH-SY5Y cells into a noradrenergic phenotype. *Neurosci Lett* 443: 199-203

Kuroda Y, Mitsui T, Kunishige M, Shono M, Akaike M, Azuma H, Matsumoto T (2006) Parkin enhances mitochondrial biogenesis in proliferating cells. *Hum Mol Genet* 15: 883-895

Langston JW, Ballard P, Tetrud JW, Irwin I (1983) Chronic Parkinsonism in humans due to a product of meperidine-analog synthesis. *Science* 219: 979-980

Lashuel HA, Overk CR, Oueslati A, Masliah E (2013) The many faces of alpha-synuclein: from structure and toxicity to therapeutic target. *Nat Rev Neurosci* 14: 38-48

LaVoie MJ, Ostaszewski BL, Weihofen A, Schlossmacher MG, Selkoe DJ (2005) Dopamine covalently modifies and functionally inactivates parkin. *Nat Med* 11: 1214-1221

Le W, Sayana P, Jankovic J (2014) Animal models of Parkinson's disease: a gateway to therapeutics? *Neurotherapeutics* 11: 92-110

Lee MH, Hyun DH, Jenner P, Halliwell B (2001) Effect of proteasome inhibition on cellular oxidative damage, antioxidant defences and nitric oxide production. *J Neurochem* 78: 32-41

Lee MK, Tuttle JB, Rebhun LI, Cleveland DW, Frankfurter A (1990) The expression and posttranslational modification of a neuron-specific beta-tubulin isotype during chick embryogenesis. *Cell Motil Cytoskeleton* 17: 118-132

Lehmann S, Martins LM (2013) Insights into mitochondrial quality control pathways and Parkinson's disease. *J Mol Med (Berl)* 91: 665-671

Leli U, Cataldo A, Shea TB, Nixon RA, Hauser G (1992) Distinct mechanisms of differentiation of SH-SY5Y neuroblastoma cells by protein kinase C activators and inhibitors. *J Neurochem* 58: 1191-1198

Lesage S, Brice A (2012) Role of mendelian genes in "sporadic" Parkinson's disease. *Parkinsonism Relat Disord* 18 Suppl 1: S66-70

Lev N, Ickowicz D, Melamed E, Offen D (2008) Oxidative insults induce DJ-1 upregulation and redistribution: implications for neuroprotection. *Neurotoxicology* 29: 397-405

Levanon D, Lieman-Hurwitz J, Dafni N, Wigderson M, Sherman L, Bernstein Y, Laver-Rudich Z, Danciger E, Stein O, Groner Y (1985) Architecture and anatomy of the chromosomal locus in human chromosome 21 encoding the Cu/Zn superoxide dismutase. *EMBO J* 4: 77-84

Li XP, Xie WJ, Zhang Z, Kansara S, Jankovic J, Le WD (2012) A mechanistic study of proteasome inhibition-induced iron misregulation in dopamine neuron degeneration. *Neurosignals* 20: 223-236

Li Y, Huang TT, Carlson EJ, Melov S, Ursell PC, Olson JL, Noble LJ, Yoshimura MP, Berger C, Chan PH, Wallace DC, Epstein CJ (1995) Dilated cardiomyopathy and neonatal lethality in mutant mice lacking manganese superoxide dismutase. *Nat Genet* 11: 376-381

Lin W, Kang UJ (2008) Characterization of PINK1 processing, stability, and subcellular localization. *J Neurochem* 106: 464-474

Liu Z, Celotto AM, Romero G, Wipf P, Palladino MJ (2012) Genetically encoded redox sensor identifies the role of ROS in degenerative and mitochondrial disease pathogenesis. *Neurobiol Dis* 45: 362-368

Loewenbruck K, Storch A (2011) Stem cell-based therapies in Parkinson's disease: future hope or current treatment option? *J Neurol* 258: S346-353

LoPachin RM, Jr., Saubermann AJ (1990) Disruption of cellular elements and water in neurotoxicity: studies using electron probe X-ray microanalysis. *Toxicol Appl Pharmacol* 106: 355-374

Lopes FM, Schroder R, da Frota ML, Jr., Zanotto-Filho A, Muller CB, Pires AS, Meurer RT, Colpo GD, Gelain DP, Kapczinski F, Moreira JC, Fernandes Mda C, Klamt F (2010) Comparison between proliferative and neuron-like SH-SY5Y cells as an in vitro model for Parkinson disease studies. *Brain Res* 1337: 85-94

Lutz AK, Exner N, Fett ME, Schlehe JS, Kloos K, Lammermann K, Brunner B, Kurz-Drexler A, Vogel F, Reichert AS, Bouman L, Vogt-Weisenhorn D, Wurst W, Tatzelt J, Haass C, Winklhofer KF (2009) Loss of parkin or PINK1 function increases Drp1-dependent mitochondrial fragmentation. *J Biol Chem* 284: 22938-22951

Macarthur H, Westfall TC, Riley DP, Misko TP, Salvemini D (2000) Inactivation of catecholamines by superoxide gives new insights on the pathogenesis of septic shock. *Proc Natl Acad Sci U S A* 97: 9753-9758

Machida Y, Chiba T, Takayanagi A, Tanaka Y, Asanuma M, Ogawa N, Koyama A, Iwatsubo T, Ito S, Jansen PH, Shimizu N, Tanaka K, Mizuno Y, Hattori N (2005) Common anti-apoptotic roles of parkin and alpha-synuclein in human dopaminergic cells. *Biochem Biophys Res Commun* 332: 233-240

Magwere T, West M, Riyahi K, Murphy MP, Smith RA, Partridge L (2006) The effects of exogenous antioxidants on lifespan and oxidative stress resistance in Drosophila melanogaster. *Mech Ageing Dev* 127: 356-370

Mardones L, Zuniga FA, Villagran M, Sotomayor K, Mendoza P, Escobar D, Gonzalez M, Ormazabal V, Maldonado M, Onate G, Angulo C, Concha, II, Reyes AM, Carcamo JG, Barra V, Vera JC, Rivas CI (2012) Essential role of intracellular glutathione in controlling ascorbic acid transporter expression and function in rat hepatocytes and hepatoma cells. *Free Radic Biol Med* 52: 1874-1887

Marklund SL (1990) Expression of extracellular superoxide dismutase by human cell lines. *Biochem J* 266: 213-219

Masini E, Cuzzocrea S, Mazzon E, Marzocca C, Mannaioni PF, Salvemini D (2002) Protective effects of M40403, a selective superoxide dismutase mimetic, in myocardial ischaemia and reperfusion injury in vivo. *Br J Pharmacol* 136: 905-917

Matsuda N, Sato S, Shiba K, Okatsu K, Saisho K, Gautier CA, Sou YS, Saiki S, Kawajiri S, Sato F, Kimura M, Komatsu M, Hattori N, Tanaka K (2010) PINK1 stabilized by mitochondrial depolarization recruits Parkin to damaged mitochondria and activates latent Parkin for mitophagy. *J Cell Biol* 189: 211-221

Mattsson ME, Ruusala AI, Pahlman S (1984) Changes in inducibility of ornithine decarboxylase activity in differentiating human neuroblastoma cells. *Exp Cell Res* 155: 105-112

McCord JM (2001) Analysis of superoxide dismutase activity. *Curr Protoc Toxicol* Chapter 7: Unit7 3

McCormack AL, Thiruchelvam M, Manning-Bog AB, Thiffault C, Langston JW, Cory-Slechta DA, Di Monte DA (2002) Environmental risk factors and Parkinson's disease: selective degeneration of nigral dopaminergic neurons caused by the herbicide paraquat. *Neurobiol Dis* 10: 119-127

McGeer PL, Itagaki S, Boyes BE, McGeer EG (1988) Reactive microglia are positive for HLA-DR in the substantia nigra of Parkinson's and Alzheimer's disease brains. *Neurology* 38: 1285-1291

McNaught KS, Belizaire R, Isacson O, Jenner P, Olanow CW (2003) Altered proteasomal function in sporadic Parkinson's disease. *Exp Neurol* 179: 38-46

McNaught KS, Jenner P (2001) Proteasomal function is impaired in substantia nigra in Parkinson's disease. *Neurosci Lett* 297: 191-194

McNaught KS, Mytilineou C, Jnobaptiste R, Yabut J, Shashidharan P, Jennert P, Olanow CW (2002) Impairment of the ubiquitin-proteasome system causes dopaminergic cell death and inclusion body formation in ventral mesencephalic cultures. *J Neurochem* 81: 301-306

McNaught KS, Olanow CW, Halliwell B, Isacson O, Jenner P (2001) Failure of the ubiquitin-proteasome system in Parkinson's disease. *Nat Rev Neurosci* 2: 589-594

McNaught KS, Perl DP, Brownell AL, Olanow CW (2004) Systemic exposure to proteasome inhibitors causes a progressive model of Parkinson's disease. *Ann Neurol* 56: 149-162

Melov S, Doctrow SR, Schneider JA, Haberson J, Patel M, Coskun PE, Huffman K, Wallace DC, Malfroy B (2001) Lifespan extension and rescue of spongiform encephalopathy in superoxide dismutase 2 nullizygous mice treated with superoxide dismutase-catalase mimetics. *J Neurosci* 21: 8348-8353

Meulener M, Whitworth AJ, Armstrong-Gold CE, Rizzu P, Heutink P, Wes PD, Pallanck LJ, Bonini NM (2005) Drosophila DJ-1 mutants are selectively sensitive to environmental toxins associated with Parkinson's disease. *Curr Biol* 15: 1572-1577

Meyer AJ, Dick TP (2010) Fluorescent protein-based redox probes. *Antioxid Redox Signal* 13: 621-650

Miao L, St Clair DK (2009) Regulation of superoxide dismutase genes: implications in disease. *Free Radic Biol Med* 47: 344-356

Miriyala S, Spasojevic I, Tovmasyan A, Salvemini D, Vujaskovic Z, St Clair D, Batinic-Haberle I (2012) Manganese superoxide dismutase, MnSOD and its mimics. *Biochim Biophys Acta* 1822: 794-814

Mogi M, Harada M, Kondo T, Riederer P, Inagaki H, Minami M, Nagatsu T (1994) Interleukin-1 beta, interleukin-6, epidermal growth factor and transforming growth factor-alpha are elevated in the brain from parkinsonian patients. *Neurosci Lett* 180: 147-150

Mogi M, Kondo T, Mizuno Y, Nagatsu T (2007) p53 protein, interferon-gamma, and NF-kappaB levels are elevated in the parkinsonian brain. *Neurosci Lett* 414: 94-97

Mollace V, Iannone M, Muscoli C, Palma E, Granato T, Rispoli V, Nistico R, Rotiroti D, Salvemini D (2003) The role of oxidative stress in paraquat-induced neurotoxicity in rats: protection by non peptidyl superoxide dismutase mimetic. *Neurosci Lett* 335: 163-166

Moran JM, Ortiz-Ortiz MA, Ruiz-Mesa LM, Fuentes JM (2010) Nitric oxide in paraquat-mediated toxicity: A review. *J Biochem Mol Toxicol* 24: 402-409

Morgan B, Sobotta MC, Dick TP (2011) Measuring E(GSH) and H2O2 with roGFP2-based redox probes. *Free Radic Biol Med* 51: 1943-1951

Murphy CK, Fey EG, Watkins BA, Wong V, Rothstein D, Sonis ST (2008) Efficacy of superoxide dismutase mimetic M40403 in attenuating radiation-induced oral mucositis in hamsters. *Clin Cancer Res* 14: 4292-4297

Murphy MP (2014) Antioxidants as therapies: can we improve on nature? *Free Radic Biol Med* 66: 20-23

Muscoli C, Cuzzocrea S, Riley DP, Zweier JL, Thiemermann C, Wang ZQ, Salvemini D (2003) On the selectivity of superoxide dismutase mimetics and its importance in pharmacological studies. *Br J Pharmacol* 140: 445-460

Narendra D, Tanaka A, Suen DF, Youle RJ (2008) Parkin is recruited selectively to impaired mitochondria and promotes their autophagy. *J Cell Biol* 183: 795-803

Narendra DP, Jin SM, Tanaka A, Suen DF, Gautier CA, Shen J, Cookson MR, Youle RJ (2010) PINK1 is selectively stabilized on impaired mitochondria to activate Parkin. *PLoS Biol* 8: e1000298

Navarro-Yepes J, Zavala-Flores L, Anandhan A, Wang F, Skotak M, Chandra N, Li M, Pappa A, Martinez-Fong D, Del Razo LM, Quintanilla-Vega B, Franco R (2014) Antioxidant gene therapy against neuronal cell death. *Pharmacol Ther* 142: 206-230

Navarro A, Boveris A (2009) Brain mitochondrial dysfunction and oxidative damage in Parkinson's disease. *J Bioenerg Biomembr* 41: 517-521

Ndengele MM, Muscoli C, Wang ZQ, Doyle TM, Matuschak GM, Salvemini D (2005) Superoxide potentiates NF-kappaB activation and modulates endotoxin-induced cytokine production in alveolar macrophages. *Shock* 23: 186-193

Olanow CW, Goetz CG, Kordower JH, Stoessl AJ, Sossi V, Brin MF, Shannon KM, Nauert GM, Perl DP, Godbold J, Freeman TB (2003) A double-blind controlled trial of bilateral fetal nigral transplantation in Parkinson's disease. *Ann Neurol* 54: 403-414

Olanow CW, Schapira AH (2013) Therapeutic prospects for Parkinson disease. *Ann Neurol* 74: 337-347

Orr WC, Sohal RS (1993) Effects of Cu-Zn superoxide dismutase overexpression of life span and resistance to oxidative stress in transgenic Drosophila melanogaster. *Arch Biochem Biophys* 301: 34-40

Orrenius S, Zhivotovsky B, Nicotera P (2003) Regulation of cell death: the calcium-apoptosis link. *Nat Rev Mol Cell Biol* 4: 552-565

Pahlman S, Odelstad L, Larsson E, Grotte G, Nilsson K (1981) Phenotypic changes of human neuroblastoma cells in culture induced by 12-O-tetradecanoyl-phorbol-13-acetate. *Int J Cancer* 28: 583-589

Pahlman S, Ruusala AI, Abrahamsson L, Mattsson ME, Esscher T (1984) Retinoic acid-induced differentiation of cultured human neuroblastoma cells: a comparison with phorbolester-induced differentiation. *Cell Differ* 14: 135-144

Pahlman S, Ruusala AI, Abrahamsson L, Odelstad L, Nilsson K (1983) Kinetics and concentration effects of TPA-induced differentiation of cultured human neuroblastoma cells. *Cell Differ* 12: 165-170

Palacino JJ, Sagi D, Goldberg MS, Krauss S, Motz C, Wacker M, Klose J, Shen J (2004) Mitochondrial dysfunction and oxidative damage in parkin-deficient mice. *J Biol Chem* 279: 18614-18622

Pan-Montojo F, Reichmann H (2014) Considerations on the role of environmental toxins in idiopathic Parkinson's disease pathophysiology. *Transl Neurodegener* 3: 10

Parashar V, Frankel S, Lurie AG, Rogina B (2008) The effects of age on radiation resistance and oxidative stress in adult Drosophila melanogaster. *Radiat Res* 169: 707-711

Park J, Kim SY, Cha GH, Lee SB, Kim S, Chung J (2005) Drosophila DJ-1 mutants show oxidative stress-sensitive locomotive dysfunction. *Gene* 361: 133-139

Park J, Kim Y, Chung J (2009) Mitochondrial dysfunction and Parkinson's disease genes: insights from Drosophila. *Dis Model Mech* 2: 336-340

Park J, Lee SB, Lee S, Kim Y, Song S, Kim S, Bae E, Kim J, Shong M, Kim JM, Chung J (2006) Mitochondrial dysfunction in Drosophila PINK1 mutants is complemented by parkin. *Nature* 441: 1157-1161

Parker WD, Jr., Boyson SJ, Parks JK (1989) Abnormalities of the electron transport chain in idiopathic Parkinson's disease. *Ann Neurol* 26: 719-723

Peng J, Mao XO, Stevenson FF, Hsu M, Andersen JK (2004) The herbicide paraquat induces dopaminergic nigral apoptosis through sustained activation of the JNK pathway. *J Biol Chem* 279: 32626-32632

Peng J, Stevenson FF, Doctrow SR, Andersen JK (2005) Superoxide dismutase/catalase mimetics are neuroprotective against selective paraquat-mediated dopaminergic neuron death in the substantial nigra: implications for Parkinson disease. *J Biol Chem* 280: 29194-29198

Perfeito R, Cunha-Oliveira T, Rego AC (2012) Revisiting oxidative stress and mitochondrial dysfunction in the pathogenesis of Parkinson disease--resemblance to the effect of amphetamine drugs of abuse. *Free Radic Biol Med* 53: 1791-1806

Perry JJ, Hearn AS, Cabelli DE, Nick HS, Tainer JA, Silverman DN (2009) Contribution of human manganese superoxide dismutase tyrosine 34 to structure and catalysis. *Biochemistry* 48: 3417-3424

Perry JJ, Shin DS, Getzoff ED, Tainer JA (2010) The structural biochemistry of the superoxide dismutases. *Biochim Biophys Acta* 1804: 245-262

Pesah Y, Pham T, Burgess H, Middlebrooks B, Verstreken P, Zhou Y, Harding M, Bellen H, Mardon G (2004) Drosophila parkin mutants have decreased mass and cell size and increased sensitivity to oxygen radical stress. *Development* 131: 2183-2194

Petersen SV, Olsen DA, Kenney JM, Oury TD, Valnickova Z, Thogersen IB, Crapo JD, Enghild JJ (2005) The high concentration of Arg213-->Gly extracellular superoxide dismutase (EC-SOD) in plasma is caused by a reduction of both heparin and collagen affinities. *Biochem J* 385: 427-432

Pezzoli G, Cereda E (2013) Exposure to pesticides or solvents and risk of Parkinson disease. *Neurology* 80: 2035-2041

Pfeiffer S, Schrammel A, Koesling D, Schmidt K, Mayer B (1998) Molecular actions of a Mn(III)Porphyrin superoxide dismutase mimetic and peroxynitrite scavenger: reaction with nitric oxide and direct inhibition of NO synthase and soluble guanylyl cyclase. *Mol Pharmacol* 53: 795-800

Pilsl A, Winklhofer KF (2012) Parkin, PINK1 and mitochondrial integrity: emerging concepts of mitochondrial dysfunction in Parkinson's disease. *Acta Neuropathol* 123: 173-188

Pletjushkina OY, Lyamzaev KG, Popova EN, Nepryakhina OK, Ivanova OY, Domnina LV, Chernyak BV, Skulachev VP (2006) Effect of oxidative stress on dynamics of mitochondrial reticulum. *Biochim Biophys Acta* 1757: 518-524

Poewe W (2008) Non-motor symptoms in Parkinson's disease. *Eur J Neurol* 15 Suppl 1: 14-20

Poole AC, Thomas RE, Andrews LA, McBride HM, Whitworth AJ, Pallanck LJ (2008) The PINK1/Parkin pathway regulates mitochondrial morphology. *Proc Natl Acad Sci U S A* 105: 1638-1643

Poole AC, Thomas RE, Yu S, Vincow ES, Pallanck L (2010) The mitochondrial fusion-promoting factor mitofusin is a substrate of the PINK1/parkin pathway. *PLoS One* 5: e10054

Prince JA, Oreland L (1997) Staurosporine differentiated human SH-SY5Y neuroblastoma cultures exhibit transient apoptosis and trophic factor independence. *Brain Res Bull* 43: 515-523

Priyadarshi A, Khuder SA, Schaub EA, Priyadarshi SS (2001) Environmental risk factors and Parkinson's disease: a metaanalysis. *Environ Res* 86: 122-127

Przedborski S, Kostic V, Jackson-Lewis V, Naini AB, Simonetti S, Fahn S, Carlson E, Epstein CJ, Cadet JL (1992) Transgenic mice with increased Cu/Zn-superoxide dismutase activity are resistant to N-methyl-4-phenyl-1,2,3,6-tetrahydropyridine-induced neurotoxicity. *J Neurosci* 12: 1658-1667

Purisai MG, McCormack AL, Cumine S, Li J, Isla MZ, Di Monte DA (2007) Microglial activation as a priming event leading to paraquat-induced dopaminergic cell degeneration. *Neurobiol Dis* 25: 392-400

Radio NM, Mundy WR (2008) Developmental neurotoxicity testing in vitro: models for assessing chemical effects on neurite outgrowth. *Neurotoxicology* 29: 361-376

Rappold PM, Cui M, Chesser AS, Tibbett J, Grima JC, Duan L, Sen N, Javitch JA, Tieu K (2011) Paraquat neurotoxicity is mediated by the dopamine transporter and organic cation transporter-3. *Proc Natl Acad Sci U S A* 108: 20766-20771

Rettig WJ, Spengler BA, Chesa PG, Old LJ, Biedler JL (1987) Coordinate changes in neuronal phenotype and surface antigen expression in human neuroblastoma cell variants. *Cancer Res* 47: 1383-1389

Richardson JR, Quan Y, Sherer TB, Greenamyre JT, Miller GW (2005) Paraquat neurotoxicity is distinct from that of MPTP and rotenone. *Toxicol Sci* 88: 193-201

Rodriguez-Rocha H, Garcia-Garcia A, Pickett C, Li S, Jones J, Chen H, Webb B, Choi J, Zhou Y, Zimmerman MC, Franco R (2013) Compartmentalized oxidative stress in dopaminergic cell death induced by pesticides and complex I inhibitors: distinct roles of superoxide anion and superoxide dismutases. *Free Radic Biol Med* 61: 370-383

Rosner IA, Goldberg VM, Getzy L, Moskowitz RW (1980) A trial of intraarticular orgotein, a superoxide dismutase, in experimentally-induced osteoarthritis. *J Rheumatol* 7: 24-29

Ross RA, Spengler BA, Biedler JL (1983) Coordinate morphological and biochemical interconversion of human neuroblastoma cells. *J Natl Cancer Inst* 71: 741-747

Rothfuss O, Fischer H, Hasegawa T, Maisel M, Leitner P, Miesel F, Sharma M, Bornemann A, Berg D, Gasser T, Patenge N (2009) Parkin protects mitochondrial genome integrity and supports mitochondrial DNA repair. *Hum Mol Genet* 18: 3832-3850

Rugarli EI, Langer T (2012) Mitochondrial quality control: a matter of life and death for neurons. *EMBO J* 31: 1336-1349

Runkel ED, Liu S, Baumeister R, Schulze E (2013) Surveillance-activated defenses block the ROS-induced mitochondrial unfolded protein response. *PLoS Genet* 9: e1003346

Saccon RA, Bunton-Stasyshyn RK, Fisher EM, Fratta P (2013) Is SOD1 loss of function involved in amyotrophic lateral sclerosis? *Brain* 136: 2342-2358

Salvemini D, Riley DP, Cuzzocrea S (2002) SOD mimetics are coming of age. *Nat Rev Drug Discov* 1: 367-374

Salvemini D, Wang ZQ, Zweier JL, Samouilov A, Macarthur H, Misko TP, Currie MG, Cuzzocrea S, Sikorski JA, Riley DP (1999) A nonpeptidyl mimic of superoxide dismutase with therapeutic activity in rats. *Science* 286: 304-306

Samai M, Sharpe MA, Gard PR, Chatterjee PK (2007) Comparison of the effects of the superoxide dismutase mimetics EUK-134 and tempol on paraquat-induced nephrotoxicity. *Free Radic Biol Med* 43: 528-534

Samaranch L, Lorenzo-Betancor O, Arbelo JM, Ferrer I, Lorenzo E, Irigoyen J, Pastor MA, Marrero C, Isla C, Herrera-Henriquez J, Pastor P (2010) PINK1-linked parkinsonism is associated with Lewy body pathology. *Brain* 133: 1128-1142

Scherz-Shouval R, Elazar Z (2011) Regulation of autophagy by ROS: physiology and pathology. *Trends Biochem Sci* 36: 30-38

Scorrano L (2013) Keeping mitochondria in shape: a matter of life and death. *Eur J Clin Invest* 43: 886-893

Seto NO, Hayashi S, Tener GM (1990) Overexpression of Cu-Zn superoxide dismutase in Drosophila does not affect life-span. *Proc Natl Acad Sci U S A* 87: 4270-4274

Shamoto-Nagai M, Maruyama W, Kato Y, Isobe K, Tanaka M, Naoi M, Osawa T (2003) An inhibitor of mitochondrial complex I, rotenone, inactivates proteasome by oxidative modification and induces aggregation of oxidized proteins in SH-SY5Y cells. *J Neurosci Res* 74: 589-597

Shiba-Fukushima K, Imai Y, Yoshida S, Ishihama Y, Kanao T, Sato S, Hattori N (2012) PINK1-mediated phosphorylation of the Parkin ubiquitin-like domain primes mitochondrial translocation of Parkin and regulates mitophagy. *Sci Rep* 2: 1002

Shimizu K, Ohtaki K, Matsubara K, Aoyama K, Uezono T, Saito O, Suno M, Ogawa K, Hayase N, Kimura K, Shiono H (2001) Carrier-mediated processes in blood--brain barrier penetration and neural uptake of paraquat. *Brain Res* 906: 135-142

Shimura H, Hattori N, Kubo S, Mizuno Y, Asakawa S, Minoshima S, Shimizu N, Iwai K, Chiba T, Tanaka K, Suzuki T (2000) Familial Parkinson disease gene product, parkin, is a ubiquitin-protein ligase. *Nat Genet* 25: 302-305

Silvestri L, Caputo V, Bellacchio E, Atorino L, Dallapiccola B, Valente EM, Casari G (2005) Mitochondrial import and enzymatic activity of PINK1 mutants associated to recessive parkinsonism. *Hum Mol Genet* 14: 3477-3492

Sofic E, Lange KW, Jellinger K, Riederer P (1992) Reduced and oxidized glutathione in the substantia nigra of patients with Parkinson's disease. *Neurosci Lett* 142: 128-130

Spinelli W, Sonnenfeld KH, Ishii DN (1982) Effects of phorbol ester tumor promoters and nerve growth factor on neurite outgrowth in cultured human neuroblastoma cells. *Cancer Res* 42: 5067-5073

Stern LF, Chapman NH, Wijsman EM, Altherr MR, Rosen DR (2003) Assignment of SOD3 to human chromosome band 4p15.3-->p15.1 with somatic cell and radiation hybrid mapping, linkage mapping, and fluorescent in-situ hybridization. *Cytogenet Genome Res* 101: 178

Su X, Maguire-Zeiss KA, Giuliano R, Prifti L, Venkatesh K, Federoff HJ (2008) Synuclein activates microglia in a model of Parkinson's disease. *Neurobiol Aging* 29: 1690-1701

Sulzer D, Bogulavsky J, Larsen KE, Behr G, Karatekin E, Kleinman MH, Turro N, Krantz D, Edwards RH, Greene LA, Zecca L (2000) Neuromelanin biosynthesis is driven by excess cytosolic catecholamines not accumulated by synaptic vesicles. *Proc Natl Acad Sci U S A* 97: 11869-11874

Surmeier DJ (2007) Calcium, ageing, and neuronal vulnerability in Parkinson's disease. *Lancet Neurol* 6: 933-938

Surmeier DJ, Guzman JN, Sanchez-Padilla J, Schumacker PT (2011) The role of calcium and mitochondrial oxidant stress in the loss of substantia nigra pars compacta dopaminergic neurons in Parkinson's disease. *Neuroscience* 198: 221-231

Tain LS, Mortiboys H, Tao RN, Ziviani E, Bandmann O, Whitworth AJ (2009) Rapamycin activation of 4E-BP prevents parkinsonian dopaminergic neuron loss. *Nat Neurosci* 12: 1129-1135

Taira T, Saito Y, Niki T, Iguchi-Ariga SM, Takahashi K, Ariga H (2004) DJ-1 has a role in antioxidative stress to prevent cell death. *EMBO Rep* 5: 213-218

Tansey MG, Goldberg MS (2010) Neuroinflammation in Parkinson's disease: its role in neuronal death and implications for therapeutic intervention. *Neurobiol Dis* 37: 510-518

Thenganatt MA, Jankovic J (2014) Parkinson disease subtypes. *JAMA Neurol* 71: 499-504

Thomas KJ, McCoy MK, Blackinton J, Beilina A, van der Brug M, Sandebring A, Miller D, Maric D, Cedazo-Minguez A, Cookson MR (2011) DJ-1 acts in parallel to the PINK1/parkin pathway to control mitochondrial function and autophagy. *Hum Mol Genet* 20: 40-50

Trachootham D, Alexandre J, Huang P (2009) Targeting cancer cells by ROS-mediated mechanisms: a radical therapeutic approach? *Nat Rev Drug Discov* 8: 579-591

Tse DC, McCreery RL, Adams RN (1976) Potential oxidative pathways of brain catecholamines. *J Med Chem* 19: 37-40

Twig G, Elorza A, Molina AJ, Mohamed H, Wikstrom JD, Walzer G, Stiles L, Haigh SE, Katz S, Las G, Alroy J, Wu M, Py BF, Yuan J, Deeney JT, Corkey BE, Shirihai OS (2008) Fission and selective fusion govern mitochondrial segregation and elimination by autophagy. *EMBO J* 27: 433-446

Uttara B, Singh AV, Zamboni P, Mahajan RT (2009) Oxidative stress and neurodegenerative diseases: a review of upstream and downstream antioxidant therapeutic options. *Curr Neuropharmacol* 7: 65-74

Uversky VN, Li J, Fink AL (2001) Metal-triggered structural transformations, aggregation, and fibrillation of human alpha-synuclein. A possible molecular NK between Parkinson's disease and heavy metal exposure. *J Biol Chem* 276: 44284-44296

Valente EM, Abou-Sleiman PM, Caputo V, Muqit MM, Harvey K, Gispert S, Ali Z, Del Turco D, Bentivoglio AR, Healy DG, Albanese A, Nussbaum R, Gonzalez-Maldonado R, Deller T, Salvi S, Cortelli P, Gilks WP, Latchman DS, Harvey RJ, Dallapiccola B, Auburger G, Wood NW (2004) Hereditary early-onset Parkinson's disease caused by mutations in PINK1. *Science* 304: 1158-1160

Valko M, Leibfritz D, Moncol J, Cronin MT, Mazur M, Telser J (2007) Free radicals and antioxidants in normal physiological functions and human disease. *Int J Biochem Cell Biol* 39: 44-84

Vina J, Borras C, Abdelaziz KM, Garcia-Valles R, Gomez-Cabrera MC (2013) The free radical theory of aging revisited: the cell signaling disruption theory of aging. *Antioxid Redox Signal* 19: 779-787

Wang D, Qian L, Xiong H, Liu J, Neckameyer WS, Oldham S, Xia K, Wang J, Bodmer R, Zhang Z (2006) Antioxidants protect PINK1-dependent dopaminergic neurons in Drosophila. *Proc Natl Acad Sci U S A* 103: 13520-13525

Wang X, Michaelis EK (2010) Selective neuronal vulnerability to oxidative stress in the brain. *Front Aging Neurosci* 2: 12

Wang X, Winter D, Ashrafi G, Schlehe J, Wong YL, Selkoe D, Rice S, Steen J, LaVoie MJ, Schwarz TL (2011) PINK1 and Parkin target Miro for phosphorylation and degradation to arrest mitochondrial motility. *Cell* 147: 893-906

Wang ZQ, Porreca F, Cuzzocrea S, Galen K, Lightfoot R, Masini E, Muscoli C, Mollace V, Ndengele M, Ischiropoulos H, Salvemini D (2004) A newly identified role for superoxide in inflammatory pain. *J Pharmacol Exp Ther* 309: 869-878

Weihofen A, Ostaszewski B, Minami Y, Selkoe DJ (2008) Pink1 Parkinson mutations, the Cdc37/Hsp90 chaperones and Parkin all influence the maturation or subcellular distribution of Pink1. *Hum Mol Genet* 17: 602-616

Weihofen A, Thomas KJ, Ostaszewski BL, Cookson MR, Selkoe DJ (2009) Pink1 forms a multiprotein complex with Miro and Milton, linking Pink1 function to mitochondrial trafficking. *Biochemistry* 48: 2045-2052

Weinreb O, Mandel S, Youdim MB, Amit T (2013) Targeting dysregulation of brain iron homeostasis in Parkinson's disease by iron chelators. *Free Radic Biol Med* 62: 52-64

White KE, Humphrey DM, Hirth F (2010) The dopaminergic system in the aging brain of Drosophila. *Front Neurosci* 4: 205

Whitworth AJ, Theodore DA, Greene JC, Benes H, Wes PD, Pallanck LJ (2005) Increased glutathione S-transferase activity rescues dopaminergic neuron loss in a Drosophila model of Parkinson's disease. *Proc Natl Acad Sci U S A* 102: 8024-8029

Whitworth AJ, Wes PD, Pallanck LJ (2006) Drosophila models pioneer a new approach to drug discovery for Parkinson's disease. *Drug Discov Today* 11: 119-126

Wicks S, Bain N, Duttaroy A, Hilliker AJ, Phillips JP (2009) Hypoxia rescues early mortality conferred by superoxide dismutase deficiency. *Free Radic Biol Med* 46: 176-181

Winklhofer KF (2014) Parkin and mitochondrial quality control: toward assembling the puzzle. *Trends Cell Biol* 24: 332-341

Wispe JR, Clark JC, Burhans MS, Kropp KE, Korfhagen TR, Whitsett JA (1989) Synthesis and processing of the precursor for human mangano-superoxide dismutase. *Biochim Biophys Acta* 994: 30-36

Wood-Kaczmar A, Gandhi S, Yao Z, Abramov AY, Miljan EA, Keen G, Stanyer L, Hargreaves I, Klupsch K, Deas E, Downward J, Mansfield L, Jat P, Taylor J, Heales S, Duchen MR, Latchman D, Tabrizi SJ, Wood NW (2008) PINK1 is necessary for long term survival and mitochondrial function in human dopaminergic neurons. *PLoS One* 3: e2455

Wu S, Zhou F, Zhang Z, Xing D (2011) Mitochondrial oxidative stress causes mitochondrial fragmentation via differential modulation of mitochondrial fission-fusion proteins. *FEBS J* 278: 941-954

Wu XF, Block ML, Zhang W, Qin L, Wilson B, Zhang WQ, Veronesi B, Hong JS (2005) The role of microglia in paraquat-induced dopaminergic neurotoxicity. *Antioxid Redox Signal* 7: 654-661

Xie HR, Hu LS, Li GY (2010) SH-SY5Y human neuroblastoma cell line: in vitro cell model of dopaminergic neurons in Parkinson's disease. *Chin Med J (Engl)* 123: 1086-1092

Yang W, Chen L, Ding Y, Zhuang X, Kang UJ (2007) Paraquat induces dopaminergic dysfunction and proteasome impairment in DJ-1-deficient mice. *Hum Mol Genet* 16: 2900-2910

Yang W, Tiffany-Castiglioni E (2007) The bipyridyl herbicide paraquat induces proteasome dysfunction in human neuroblastoma SH-SY5Y cells. *J Toxicol Environ Health A* 70: 1849-1857

Yang W, Tiffany-Castiglioni E (2008) Paraquat-induced apoptosis in human neuroblastoma SH-SY5Y cells: involvement of p53 and mitochondria. *J Toxicol Environ Health A* 71: 289-299

Yang W, Tiffany-Castiglioni E, Lee MY, Son IH (2010) Paraquat induces cyclooxygenase-2 (COX-2) implicated toxicity in human neuroblastoma SH-SY5Y cells. *Toxicol Lett* 199: 239-246

Yang Y, Gehrke S, Imai Y, Huang Z, Ouyang Y, Wang JW, Yang L, Beal MF, Vogel H, Lu B (2006) Mitochondrial pathology and muscle and dopaminergic neuron degeneration caused by inactivation of Drosophila Pink1 is rescued by Parkin. *Proc Natl Acad Sci U S A* 103: 10793-10798

Yokochi M (1997) Familial juvenile parkinsonism. *Eur Neurol* 38 Suppl 1: 29-33

Yoritaka A, Hattori N, Uchida K, Tanaka M, Stadtman ER, Mizuno Y (1996) Immunohistochemical detection of 4-hydroxynonenal protein adducts in Parkinson disease. *Proc Natl Acad Sci U S A* 93: 2696-2701

Youle RJ, Karbowski M (2005) Mitochondrial fission in apoptosis. *Nat Rev Mol Cell Biol* 6: 657-663

Young IS, Woodside JV (2001) Antioxidants in health and disease. *J Clin Pathol* 54: 176-186

Zahid M, Saeed M, Yang L, Beseler C, Rogan E, Cavalieri EL (2011) Formation of dopamine quinone-DNA adducts and their potential role in the etiology of Parkinson's disease. *IUBMB Life* 63: 1087-1093

Zecca L, Youdim MB, Riederer P, Connor JR, Crichton RR (2004) Iron, brain ageing and neurodegenerative disorders. *Nat Rev Neurosci* 5: 863-873

Zecca L, Zucca FA, Albertini A, Rizzio E, Fariello RG (2006) A proposed dual role of neuromelanin in the pathogenesis of Parkinson's disease. *Neurology* 67: S8-11

Zhang J, Perry G, Smith MA, Robertson D, Olson SJ, Graham DG, Montine TJ (1999) Parkinson's disease is associated with oxidative damage to cytoplasmic DNA and RNA in substantia nigra neurons. *Am J Pathol* 154: 1423-1429

Zhou C, Huang Y, Shao Y, May J, Prou D, Perier C, Dauer W, Schon EA, Przedborski S (2008) The kinase domain of mitochondrial PINK1 faces the cytoplasm. *Proc Natl Acad Sci U S A* 105: 12022-12027

Zhou ZD, Refai FS, Xie SP, Ng SH, Chan CH, Ho PG, Zhang XD, Lim TM, Tan EK (2014) Mutant PINK1 upregulates tyrosine hydroxylase and dopamine levels, leading to vulnerability of dopaminergic neurons. *Free Radic Biol Med* 68: 220-233

Zimmermann M, Gardoni F, Marcello E, Colciaghi F, Borroni B, Padovani A, Cattabeni F, Di Luca M (2004) Acetylcholinesterase inhibitors increase ADAM10 activity by promoting its trafficking in neuroblastoma cell lines. *J Neurochem* 90: 1489-1499

Ziviani E, Tao RN, Whitworth AJ (2010) Drosophila parkin requires PINK1 for mitochondrial translocation and ubiquitinates mitofusin. *Proc Natl Acad Sci U S A* 107: 5018-5023

Ziviani E, Whitworth AJ (2010) How could Parkin-mediated ubiquitination of mitofusin promote mitophagy? *Autophagy* 6: 660-662

Abbreviations

AADC aromatic L-amino acid decarboxylase

AAV adeno-associated virus

BBB blood brain barrier

Ca_v voltage-sensitive L-type calcium (Cav) channels

CCCP Carbonyl cyanide m-chlorophenyl hydrazone

CRISPR clustered regularly interspaced short palindromic repeats

DA dopamine

DAergic dopaminergic

DAQ dopamine quinone

DAT dopamine transporter

DBS deep brain stimulation

DTT Dithiothreitol

DβH dopamine β hydroxylase

ETC electron transport chain

FITC fluorescein isothiocyanate

GAPDH Glyceraldehyde 3-phosphate dehydrogenase

GSH glutathione

GSSG oxidized glutathione

HPLC high performance liquid chromatography

IFN-γ interferon-γ

IMM inner mitochondrial membrane

LB Lewy bodies

LN Lewy neurites

LPS lipopolysaccharide

MAO monoamine oxidase

Mfn mitofusin

MPTP 1-methyl-4-phenyl-1,2,3,6-tetrahydropyridine

mt-roGFP2 mitochondrila-redox sensor GFP2

NA noradrenaline

NAergic noradrenergic

OMM outer mitochondrial membrane

OXPHOS oxidative phosporilation

PAMPs pathogen-associated molecular patterns

PD Parkinson’s disease

PI propidium iodide

PKC Protein kinase C

PPR pattern recognition receptor

PQ paraquat

PTP permeability transition pore

qRT-PCR quantitative Reverse transcriptase-polymerase chain reaction

RA retinoic acid

RNS reactive nitrogen species

roGFP2 redox sensor GFP2

ROS reactive oxygen species

RPII RNA polymerase II

RT-PCR Reverse transcriptase-polymerase chain reaction

SN Substantia Nigra

SNpc Substantia Nigra pars compacta

Sod Drosophila homolog cytosolic SOD1

SOD1 human superoxide dismutase 1 (cytosolic Cu,Zn-SOD)

Sod2 Drosophila homolog mitochondrial SOD2

SOD2 human superoxide dismutase 2 (mitochondrial Mn-SOD)

SOD3 human superoxide dismutase 3 (extracellular Cu,Zn-SOD)

TH tyrosine hydroxylase

TPA 12-O-tetradecanoylphorbol-13-acetate

Ub ubiquitin

UCHL1 Ubiquitin carboxyl-terminal esterase L1

UPS ubiquitin proteasome system

VMAT2 vesicular monoamine transporter 2

α-syn α synuclein